N 70 42175

NASA CR-72780

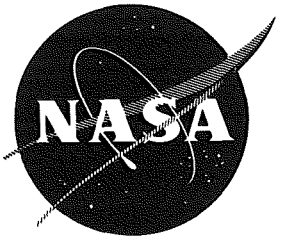

EXPERIMENTAL LIQUID METAL SLIP RING PROJECT

by

R. B. Clark

HUGHES AIRCRAFT COMPANY

prepared for

NATIONAL AERONAUTICS AND SPACE ADMINISTRATION

NASA Lewis Research Center

Contract NAS 3-11537

Robert R. Lovell, Project Manager

CASE FILE
COPY

NOTICE

This report was prepared as an account of Government-sponsored work. Neither the United States, nor the National Aeronautics and Space Administration (NASA), nor any person acting on behalf of NASA:

A.) Makes any warranty or representation, expressed or implied, with respect to the accuracy, completeness, or usefulness of the information contained in this report, or that the use of any information, apparatus, method, or process disclosed in this report may not infringe privately-owned rights; or

B.) Assumes any liabilities with respect to the use of, or for damages resulting from the use of, any information, apparatus, method or process disclosed in this report.

As used above, "person acting on behalf of NASA" includes any employee or contractor of NASA, or employee of such contractor, to the extent that such employee or contractor of NASA or employee of such contractor prepares, disseminates, or provides access to any information pursuant to his employment or contract with NASA, or his employment with such contractor.

Requests for copies of this report should be referred to

National Aeronautics and Space Administration
Scientific and Technical Information Facility
P. O. Box 33
College Park, Md. 20740

NASA CR-72780

FINAL REPORT

EXPERIMENTAL LIQUID METAL SLIP RING PROJECT

by

R. B. Clark

HUGHES AIRCRAFT COMPANY
Space Systems Division
Los Angeles, California 90009

prepared for

NATIONAL AERONAUTICS AND SPACE ADMINISTRATION

June 22, 1970

Contract NAS 3-11537

NASA Lewis Research Center
Cleveland, Ohio
Robert R. Lovell, Project Manager
Spacecraft Technology Division

FORWARD

The work described herein was done at the Space Systems Division of Hughes Aircraft Company under NASA Contract No. NAS 3-11537 with Mr. Robert R. Lovell, Spacecraft Technology Division, NASA-Lewis Research Center, as Project Manager.

TABLE OF CONTENTS

TABLE OF CONTENTS (continued)

LIST OF TABLES

LIST OF TABLES (continued)

LIST OF FIGURES

LIST OF FIGURES (continued)

LIST OF FIGURES (continued)

LIST OF FIGURES (continued)

ABSTRACT

Slip rings employing the liquid metal gallium to transfer electrical power across rotating joints were experimentally studied with respect to application in satellites. Candidate materials for electrodes, insulators and barrier films were tested. A ten ring assembly was operated in high vacuum for 60 days carrying 100 A. Data from electrical, physical, chemical and visual examination is presented. Contact resistance was less than one microhm cm^2 for nickel-plated electrodes wetted with gallium. Surface film on the gallium caused debris during rotation. Gallium was retained in the rings by surface tension.

SUMMARY

Liquid metal slip rings are sets of two concentric metal rings separated by a narrow annular gap, the gap being filled with a liquid metal. Electric current will flow from one ring to another with very low resistance, thus providing a means of transferring electrical power between two members of a machine which can rotate with respect to one another. Liquid metal slip rings may be expected to transfer electrical power and signals across rotating joints with extremely low power loss and electrical noise combined with long life, low mechanical friction and the elimination of the brush wear residue from conventional brush on ring assemblies. This program experimentally studied the feasibility of using the liquid metal gallium to transfer high power across rotating joints in satellites. Gallium was chosen primarily because of its very low rate of evaporation.

Candidate materials for slip ring electrodes, insulators and non-wetting barrier films for use with the very corrosive gallium were selected after a literature search. The approach selected was to use common engineering materials and wet the electrodes with the gallium to obtain the lowest electrical interface resistance. Exotic techniques were avoided, but stringent controls were exercised, including doing much of the work in an atmosphere of inert argon gas.

A screening test utilized 65 non-rotating material evaluation fixtures. Electrode samples in contact with gallium were subjected to various currents and temperatures for one month in an atmosphere of argon gas. All of the electrode samples were wetted with gallium by machining the active surface in a pool of liquid gallium. Electrical, physical, chemical and visual tests were used to choose nickel-plated copper and stainless steel as candidates for long-term vacuum tests. Beryllium and beryllium-copper were found to be unacceptably attacked by the gallium and tungsten was difficult to wet with gallium.

Thirty-five samples of insulation materials and barrier films were also tested. Epoxy-glass laminate and alumina ceramic resisted wetting by gallium. Teflon, polyethylene and polyimide were wetted by contact with gallium over a long period. Several organic coatings, including perfluorinated polymer, were tried as barrier films to prevent wetting of electrode surfaces by the gallium. None resisted wetting as well as the natural oxide films on the metals.

The long-term test included 105 days of elevated temperature operation in a high vacuum. After seven months of wetted contact, the gallium was corroding the copper under the nickel plate, causing small blisters of the nickel. The stainless steel was not significantly attacked.

An engineering test model liquid metal slip ring assembly was designed, fabricated and tested. The nickel-plated copper was used as an electrode material based on the screening test results that the interface

resistance to gallium is less than one microhm cm^2 and that the nickel surface is readily wetted with gallium.

Five slip rings of each of two different configurations were operated for 60 days in a vacuum chamber at less than 10^{-6} torr with currents of 0, 100, and 200 amperes, a temperature of 85°C, and with rotational rates of 1 and 20 revolutions per day to approximate service in a high power solar array orientation mechanism. The voltage drop and possible electrical noise across the rotating gallium interface were too small to be measured compared to the losses in the heavy copper bus bars employed. Resistance through the gallium is calculated to be less than one millionth of an ohm.

Rotation of the slip rings was found to generate debris resulting from atmospheric contamination of the gallium surface. The debris ceased to be generated after a few days in vacuum. X-ray diffraction and emission spectrograph studies did not positively identify the contaminating substance, but it is believed to be composed of amorphous oxides and hydroxides of gallium.

It was found that the gallium is readily retained by surface tension forces against acceleration forces due to one gravity, thus no rubbing seals are required. The retention was not affected by vacuum. The gallium has a freezing point of 29.78°C and a tendency to supercool. The gallium was frozen to permit retention during transportation of the engineering test model.

The project was intended to experimentally identify the problems which might be associated with the use of gallium slip rings for space applications. Several problems were identified and solutions were found for most. Some problems remain to be solved.

INTRODUCTION

Background

The transfer of electrical power across rotating interfaces in a spacecraft is typically accomplished with the well-known brush-on-ring assembly in which a spring-loaded, electrically-conductive brush on one member rides against a precious metal ring in the other member. Such systems are well developed and are being used with remarkable success. However, the brush-on-ring assembly has several drawbacks:

- High mechanical friction due to the rubbing contact
- Wear products are generated which can cause electrical breakdown and may contaminate bearings
- Life is limited due to the wear-out mode

- The interface resistance is appreciable, causing power loss when high currents are conducted
- Substantial electrical noise results from variations in contact resistance during rotation.

Purpose and Scope

The present work was initiated under NASA-LeRC Contract No. NAS 3-11537, in June 1969. This project is specifically directed to the use of gallium as the liquid metal. The application is transfer of electrical currents to a satellite from high power solar cell arrays. The basic concept is illustrated in Figure 1.

The contract was divided into three reporting categories (tasks):

1. Material Selection and Experiments
2. Engineering Test Model Design and Fabrication
3. Engineering Test Model Testing and Evaluation

A nine-month period of performance was specified.

Design Requirements

In brief summary, the experimental liquid metal slip rings were to demonstrate the feasibility of transferring power to the spacecraft from sun-tracking solar arrays to the main bodies of high power communications satellites. Rate of rotation to be one revolution per day with 20 revolutions per day slew rate. Ten rings were to be furnished, each capable of 100A normal and 200A maximum. Voltage between rings to be 30V to 3000V. The environment specified is 0°C to 80°C (273K to 353K) in a hard vacuum typical of space. Life: 5 to 10 years.

Design Approach

The following design problems were recognized for liquid metal slip rings:

- Retention of the liquid metal, particularly during launch
- Evaporation of the liquid metal

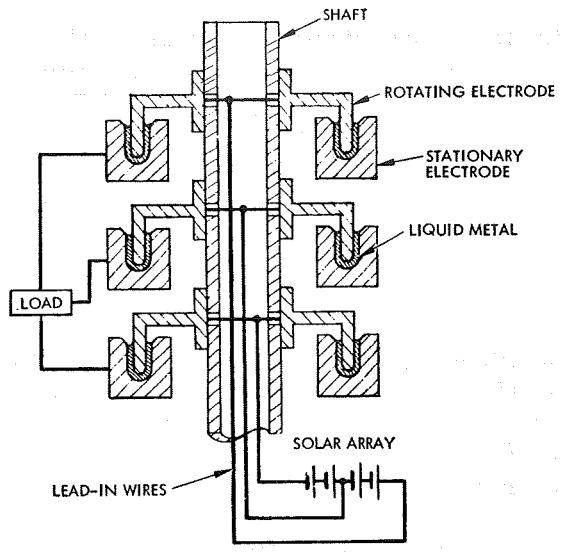

FIGURE 1. Liquid Metal Slip Rings

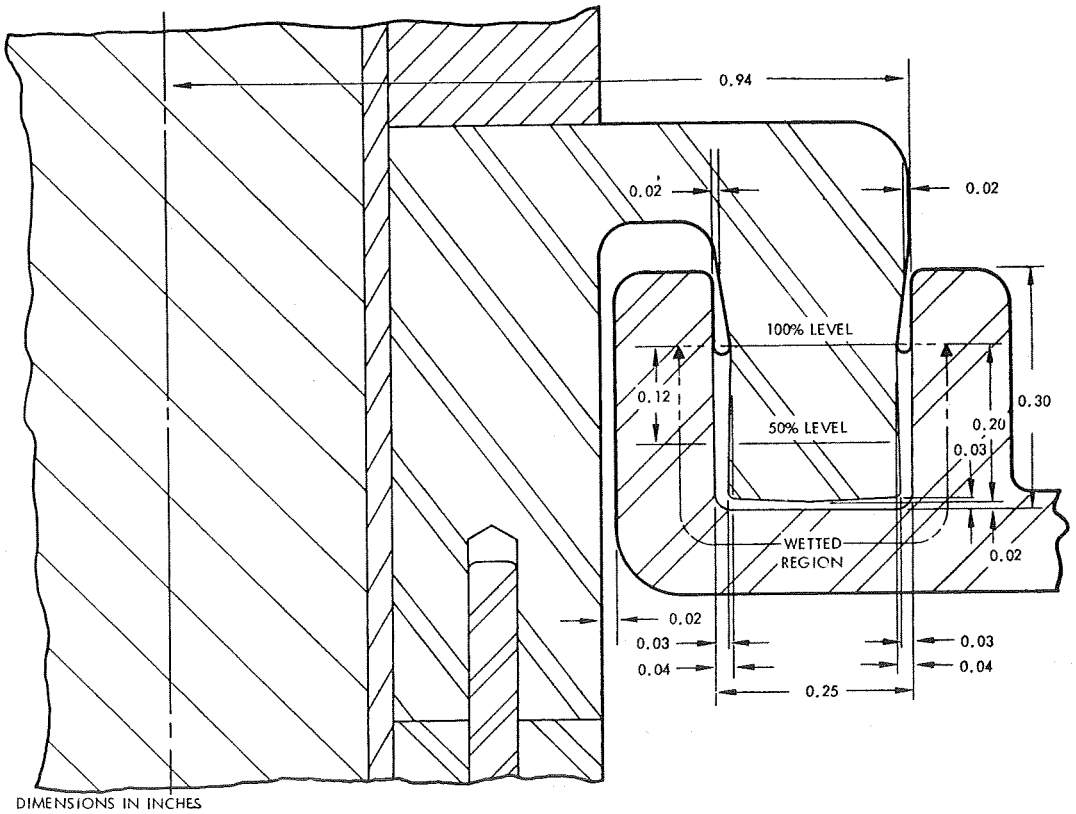

FIGURE 2. Electrode Configuration Proposed

- o Corrosion of electrodes
- o Deterioration of electrical properties

Retention of the gallium had to be accomplished without rubbing seals because the elimination of static friction is a major objective of this application. The surface tension of the liquid metal was used for containment, except for transportation and launch when the liquid metal was to be frozen.

A wetted electrode to liquid metal interface was selected by Hughes to obtain the lowest possible interface resistance. Non-wetting barrier films and insulators were proposed to aid in containment of the liquid metal during accelerations. Figure 2 shows the proposed electrode configuration.

The use of gallium as the liquid metal was expected to solve the problem of evaporation because of its very low vapor pressure, but gallium is very corrosive, resembling molten aluminum in its attack on other metals. Thus extensive screening tests were used to evaluate material combinations. The screening tests were sensitively instrumented to detect changes in electrical resistance. Physical and chemical tests were used to evaluate the effects of corrosion.

A project objective was to use common engineering materials and to avoid exotic techniques.

The engineering test model liquid metal slip ring assembly utilized an "open" design for the best possible visibility and accessibility and to provide high voltage insulation. Inner and outer rings were made independent and replaceable. The slip ring drive was dry lubricated to allow operation during the vacuum testing.

Conditions and Controls

The project work was accomplished in an engineering laboratory which is engaged in development of electromechanical equipment for space applications, including bearing and power transfer assemblies for spin-stabilized spacecraft and positioning mechanisms for antennas and solar arrays. The philosophy was that if the liquid metal slip rings could be successfully assembled and operated in this atmosphere, then the prospects were good for eventual assembly, testing and handling in a spacecraft production area.

From the beginning it was recognized that special care would have to be exercised to minimize contamination. One reason was to facilitate wetting of the electrode surfaces by the gallium. Another reason was to isolate variables so that the results of the experiments would be more meaningful. Also, it was noted that the reliability of electromechanical devices is dependent on the exclusion of contaminants.

Much of the work on the project was thus conducted under special conditions. The materials selection experiment was conducted in a glove box in an atmosphere of dry, filtered argon gas. Sample materials were final machined on specially cleaned machines, touched only with clean tongs or gloves, and stored in the dry argon atmosphere. Wetting of sample electrodes with the liquid gallium was accomplished by machining the electrode with the cutting tool submerged in liquid gallium. Wetted electrodes were immediately transferred to argon-flushed containers and moved into the glove box for storage and further processing. Clean gloves or tongs were always used so that the samples were never touched with bare hands.

The engineering test model liquid metal slip ring assembly (hereinafter referred to as the ETM) was assembled in a flow bench in a clean room with controlled temperature and humidity. Parts were fabricated and cleaned using best practice for spacecraft, and clean gloves were used for assembly. Particulate contamination was thus controlled. An inert gas environment was not used during assembly of the ETM.

Significance of the Work

The present work is believed to add much to the existing limited knowledge of the behavior of typical engineering materials in the presence of the liquid metal gallium. The characteristics of slip rings employing gallium are expected to be of great interest to those who have applications requiring transfer of large amounts of electrical power across rotating interfaces with minimum losses, as well as those requiring very low electrical noise or very low friction.

The task of ascertaining the feasibility of gallium slip rings for space applications is not complete. Most of the desirable features of the liquid metal slip rings are shown to be achievable.

MATERIALS SELECTION AND EXPERIMENTS

Literature Search

A search and study of pertinent available literature was used to aid in the selection of candidate materials for the liquid metal slip rings assembly. Ideas were also sought for the design and for processing, assembly and testing techniques.

Materials needed to be selected for four functions:

1. Liquid metal
2. Electrodes
3. Barrier films
4. Insulators

The studies were concentrated on:

- Properties of gallium and low melting point alloys of gallium.
- Compatibility of gallium with candidate materials for electrodes.
- Properties of materials for electrodes, barrier films and insulators.
- The physics of surfaces and interfaces with respect to containment of the gallium.
- Cleaning and treatment of surfaces with respect to wetting by the gallium.
- Electrical contacts utilizing liquid metals.

The following paragraphs give a short review of the pertinent information found in the literature. Appendix B lists the documents which were reviewed, primarily in the first month of the contract, and gives a subjective rating of the expected applicability to the liquid metal slip ring project of the information presented.

Liquid Metals

Gallium or alloys of gallium were specified by the contract. The reasons for the choice of gallium compared to the better known mercury are seen in Table 1.

TABLE 1. GALLIUM VERSUS MERCURY

Property	CUSTOMARY UNITS				SI UNITS			
	Temp.	Gallium	Mercury	Units	Temp.	Gallium	Mercury	Units
Density	30°C	6.095	13.6	g/cm^3	303K	6.095×10^3	1.36×10^4	$kg\ m^{-3}$
Surface tension	30°C	735	464	dyne/cm	303K	0.735	0.464	$N\ m^{-1}$
Viscosity	100°C	0.016	0.012	poise	373K	1.6×10^{-3}	1.2×10^{-3}	$N s m^{-2}$
Vapor pressure	80°C	10^{-33}	4×10^{-3}	torr	353K	1.3×10^{-31}	0.5	$N\ m^{-2}$
Boiling point	--	1983	357	°C	--	2256	630	K
Melting point	--	29.78	-39	°C	--	302.93	234	K
Resistivity	30°C	28	96	$\mu\ \Omega$ cm	--	28	96	$\mu\ \Omega$ cm
Toxicity		not toxic	poisonous			not toxic	poisonous	
Corrosivity		high	high			high	high	

The liquid metal must be contained without the use of rubbing seals because the major objective of the project is to develop a means of electrical power transfer with extremely low friction. High surface tension and low density are therefore desirable properties. The ratio of surface tension to density is 3.5 times higher for gallium than for mercury, indicating that containment of gallium by surface forces will be possible at accelerations 3.5 times greater than for mercury in a given design.

The slightly higher viscosity of the gallium will not be significant at the rotation rate of one revolution per day typical of application in a synchronous communications satellite. Combined with the lower density, it may be a slight advantage in the damping of any sloshing modes of the liquid metal.

The relatively high vapor pressure of mercury has proven to be a distinct problem in previous testing in a high vacuum. By contrast, the rate of evaporation and subsequent condensation of gallium can be considered to be insignificant. The vapor pressure of gallium listed in the table was extrapolated from data at much higher temperatures. The high boiling point of gallium gives it a liquid range of 1953K. Tin is the only other metal with such a broad liquid range.

The melting point of gallium is most authoritatively given as 29.78°C (85.60°F, 302.93K). This is a very convenient temperature to facilitate freezing for transportation and space vehicle launch but still permit passive control of temperature to keep the metal liquid during in-orbit operating conditions, with the possible exception of eclipse periods.

Lower resistivity is an obvious advantage, again in the ratio of about 3.5 to 1 in favor of gallium.

While mercury poisoning is well known, the Naval Medical Research Institute found a very low order of toxicity for gallium, of the order of that for aluminum.

Gallium is more aggressive in its attack on most solid metals than any other metal. This is a major obstacle to the use of liquid gallium as a high temperature coolant material.

Some other important characteristics of gallium are:

- Gallium and its alloys have a strong tendency to supercool.
- Gallium expands 3.2 percent by volume on freezing.
- The anisotropy of thermal and electrical properties of the orthorhombic gallium crystal is more pronounced than for any other metal.
- Liquid gallium wets many non-metals.

- o A thin surface film of oxide protects gallium from corrosion in air up to 400°C and in water to 100°C.

Gallium can now be obtained in pure form for $1.00 per gram and less. Very little liquid metal is required in a slip ring so that the cost of the gallium is not a major factor.

Gallium forms alloys with many metals. For use in liquid metal slip rings the choice was narrowed to the low melting point eutectic alloys listed in Table 2.

TABLE 2. LOW MELTING POINT ALLOYS OF GALLIUM

PERCENT BY WEIGHT				MELTING POINT	
Gallium	Indium	Tin	Zinc	°C	K
62.5	21.5	16.0	--	10.7	283.85
69.8	17.6	12.5	--	10.8	283.95
76	24	--	--	15.7	288.85
82	--	12.0	6.0	17	290

Alloys which are not eutectic have a temperature range in which the liquid and solid states are mixed, thus making thermal control more difficult.

Pure gallium was selected for the bulk of the experiment but an abbreviated evaluation was made of the 10.7°C melting point alloy. This alloy was chosen for its low melting point, low cost (because of the reduced quantity of gallium) and three alloy constituents which should provide a good contrast to gallium in chemical behavior.

Electrode Materials

Five materials were selected as candidates for the electrodes of the slip ring assembly. They were selected on the basis of low chemical attack by gallium at the operating temperatures, good potential wetting by gallium, good engineering properties and ease of fabrication. Table 3 presents the properties of the candidate materials intended for use in the materials evaluation experiments.

Beryllium was chosen despite its possible inclusion in the "exotic" class, because of its light weight, high thermal and electrical conductivity and reported good resistance to gallium attack even at high temperatures. Drawbacks were high cost, notch sensitivity in structural applications, and the toxicity of the oxide of beryllium, which might become important in attempts to displace the oxide film so that the gallium can wet the beryllium.

TABLE 3. CANDIDATE MATERIALS FOR ELECTRODES

Property	Beryllium	Beryllium-Copper	Nickel-Plated Copper		Stainless Steel	Tungsten	Gallium
			Copper	Nickel			
Material Specification	Berylco HP-20 98 % min. Be 2 % max. BeO_2	Berylco 25	QQ-C-502 CR, 1/2 hard	QQ-N-290 Class 2, 003" thick	AISI 304	Sylvania fine grain rod 99.95 % min. W	0.999999 pure
Density $g\ cm^{-3}$	1.85	8.25	8.9	8.9	8.0	19.3	6.1 liquid
Resistivity $\mu\ \Omega\ cm$	6.8	8.2	1.7	6.8	72	5.5	28 liquid
Thermal Expansion $10^{-6}\ K^{-1}$	12.2	16.7	17.7	13	17.8	4.3	18 liquid
Thermal Conductivity $J\ s^{-1} m^{-1} K^{-1}$	5.7×10^5	--	14.1×10^5	2.8×10^5	0.6×10^5	4.6×10^5	--
Surface Energy $N\ m^{-1}$ at (temperature)	1.1 (1773 K)	--	1.27 (1356 K)	1.83 (1523 K)	--	2.9 (2000 K) 6.43 (293 K)	0.735 (304 K) liquid
Tolerance to Gallium	773 K	--	<373 K	573 K	573 K	1073 K	n.a.

Copper was expected to be marginal in resistance to attack by gallium at 80°C (353K). The effect of the addition of a small amount of beryllium to make beryllium-copper was unknown insofar as resistance to attack by gallium was concerned, but the producibility of high precision parts of beryllium-copper having good electrical properties made the choice appealing.

Nickel is included because it is a popular material for plating of other materials, as well as being a strong, corrosion-resistant, highly conductive material electrically in bulk form. It was originally planned to use solid nickel, 0.9997 pure, but a nickel shortage due to a labor dispute caused a change in plans to use nickel as a heavy plating over copper. This combination could be expected to have the excellent thermal and electrical properties of copper with the corrosion resistance of nickel. Electroplated nickel was used in favor of electroless nickel because of the 5 to 10 percent phosphorous content of the latter.

Stainless steel (18 % Ni, 8 % Cr) was reported to be resistant to attack by gallium up to the same temperature as nickel, 300°C (573K). A.I.S.I. type 304 was chosen over the more popular type 303 because of the lower contents of sulphur and phosphorous. Sulfur (or selenium) and phosphorous are added to promote free machining but these elements were known to make compounds with gallium. Stainless steel has good mechanical properties but its thermal and electrical conductivity are poor.

Tungsten was reported to be the most resistant to attack by gallium of all the metals. Its thermal and electrical conductivity are excellent but its weight and poor machinability are drawbacks.

All the materials considered have a high enough surface energy that they were expected to be readily wetted by the gallium and a low contact angle formed if the oxide surface of the electrode was removed.

Some of the other materials considered are listed in Table 4.

Barrier Films

The converging surfaces shown above the level of the liquid gallium in Figure 2 are not to be wetted by the gallium. A stop-flow coating of a very low surface energy material was desired to aid in containment and to provide additional electrical insulation. The barrier film candidates should have the following properties:

- Resistance to wetting by the liquid metal
- Resistance to attack by the liquid metal
- Low outgassing properties and low vapor pressure
- Practical means of application to electrode materials
- Durability of film under anticipated handling and processing.

TABLE 4. OTHER MATERIALS CONSIDERED FOR ELECTRODES

Material	Density $g\ cm^{-3}$	Resistivity micro-ohm-cm	Remarks
Chromium	7.2	13	Popular material for plating. Good corrosion resistance. More porous than nickel.
Copper	9.0	1.673	Conductivity exceeded only by silver. Corrosion feared at $80^{\circ}C$.
Molybdenum	10.2	5.17	Not well known as other than an alloy constituent.
Palladium	12.0	10.8	Reasonable properties, available, readily fabricated, corrosion-resistant, somewhat expensive.
Platinum	21.5	9.83	Very corrosion resistant, may be difficult to wet with gallium, quite expensive, heavy.
Rhodium	12.4	4.5	Excellent material for plating electrical contacts.
Silver	10.5	1.59	Best conductivity Suspect poor resistance to corrosion by gallium.
Tantalum	16.6	12.4	Resistant to corrosion by gallium to $450^{\circ}C$. Somewhat expensive and heavy.
Titanium	4.5	47.8	Low weight, poor conductivity.
Vanadium	6.0	26	Conductivity approximately the same as liquid gallium.

Information on suitable materials for barrier films for use with liquid metals was not located. The materials in Table 6 were therefore chosen based on their better known engineering properties. They represent a wide range of chemical formulations and mechanical properties and are readily available.

TABLE 5. BARRIER FILM CANDIDATES

Item No.	Description	Specification*
1	Perfluorinated polymer	HP 7-27
2	Bonded teflon coating	HP 7-13, Type V
3	Parylene	HP 16-144
4	Silicone resin coating	DC 644
5	Epoxy conformal coating	HP 16-66, Type 1, Class 1

* HP means Hughes Process specification.

The perfluorinated polymer was selected because of its known resistance to wetting by lubricating oils. Such coatings have been used to retain lubricant in instrument ball bearings. The coating is very thin and must be handled with great care.

The particular bonded teflon coating tested is a solid lubricant variety which is not easily rubbed off by handling, will not evaporate or outgas, and is useful over a wide temperature range. The cured coating has a thickness of about 0.0005 inch (13×10^{-6} m).

Parylene is an electrically insulating coating which is deposited from a vapor and which polymerizes as it is deposited so that a uniform thickness builds up on irregularly shaped surfaces such as circuit boards with mounted components and exposed wiring.

The DC 644 silicone resin is a high purity single component resin normally used as high temperature electrical insulation. Silicone is known for its resistance to wetting and to chemical attack and for its wide temperature range. The film cures at 150°C to 200°C (423K to 473K). Film thickness is approximately 0.002 inch (50×10^{-6} m).

The epoxy conformal coating is normally used to prevent contamination of etched or welded circuitry and provides protection from mechanical damage. Film thickness is about 0.005 inch (130×10^{-6} m) on flat surfaces with a tendency to form fillets. Epoxy is known for toughness and adhesion but is brittle at cryogenic temperatures.

Insulation Materials

The criteria for the selection of insulating materials to separate components of the slip ring assembly include:

- o Resistance to wetting by the liquid metal.
- o Resistance to attack by the liquid metal.
- o Low outgassing properties in a high vacuum.
- o High dielectric strength and insulation resistance.
- o Good mechanical properties and dimensional stability,
- o Ease of fabrication.

The above criteria are to be judged in the anticipated temperature range of $0^{o}C$ to less than $100^{o}C$ (273K to <373 K).

If the insulating material is wetted by gallium or its alloys, creeping of the liquid will make it difficult or impossible to maintain required minimum surface insulation distances.

The information on compatibility with gallium was meager. Polytetrafluoroethylene (teflon) was chosen as a candidate because of its very low surface energy, chemical inertness, low outgassing and good electrical properties despite reports that it was wetted by gallium under vibration. The surface energy of teflon is reported as 16 to 25 ergs/cm^2 (0.016 to 0.025 N m^{-1}) compared to 735 ergs/cm^2 (0.735 N m^{-1}) for gallium. This should mean that gallium would not wet teflon. Liquids may, however, adhere to a surface even if that surface is not wetted by the test of a contact angle less than 90 degrees.

The companies which supply pure gallium normally ship it in polyethylene containers with an argon atmosphere to protect the purity of the gallium. This was taken to mean that gallium would not attack and probably would not wet polyethylene. Polyethylene also has a low surface energy, reported as 31 to 55 ergs/cm^2 (0.031 to 0.055 N m^{-1}). It has excellent dielectric characteristics, low density and is non-toxic. Flexibility, toughness and stress crack resistance are achieved without use of a plasticizer. Its ease of fabrication is outstanding. High density polyethylene was chosen to maximize the physical properties.

The candidates for insulator materials are listed in Table 6. Since the first two choices were soft materials, the next choice was a material with excellent strength and dimensional stability to go with good electrical properties and ready fabrication. No information was available on compatibility of polyimide with liquid metals.

TABLE 6. INSULATOR MATERIAL CANDIDATES

Item No.	Description	Specification
1	Polytetrafluoroethylene (teflon)	AMS 3651
2	Polyethylene	High density
3	Polyimide	Dupont Vespel SP-1
4	Epoxy-glass fabric laminate	L-P-509, Type IV, Grade G-10
5	Alumina ceramic	96 percent

Gallium is known to wet glass. The wetting is believed due to the oxide film on the gallium and does not occur in a high vacuum. The usefulness of epoxy-glass fabric laminate material for structural insulation is so high that the risk was considered justified. The grade specified has been qualified for many spacecraft at Hughes.

Alumina and beryllia were reported as resistant to wetting by gallium. Alumina was chosen as a well-known representative of the ceramic class of insulation. The alumina was used unglazed to minimize internal stresses and avoid surface cracks.

The surface energy of alumina is quite high, 580 ergs/cm^2 at 2050°C (0.58 Nm^{-1} at 2323 K) when the material is molten. At lower temperatures it would be expected to be much higher. This would tend to predict wetting of the ceramic by the gallium.

Wetting, Contact Angle and Surface Tension

Wetting or not wetting is important to the design of the liquid metal slip rings for two reasons:

1. The liquid metal is to be contained by capillary forces,

2. The interface resistance is strongly dependent on whether or not the liquid metal wets the electrode.

A great deal of information is now available on the physics of surfaces and interfaces. It is known that a liquid wets a solid surface when the surface energy of the solid surface is considerably higher than that of the liquid. Solids with low surface energy, such as teflon, are not expected to be wetted by liquids with higher surface energy.

The angle at which the liquid-vapor interface touches the solid, see Figure 3, is known as the contact angle. For wetting contact, the contact angle approaches zero. Where the solid is not wetted, the angle approaches 180 degrees (π rad). An expression has been advanced, often called Young's equation, by which the contact angle may be calculated.

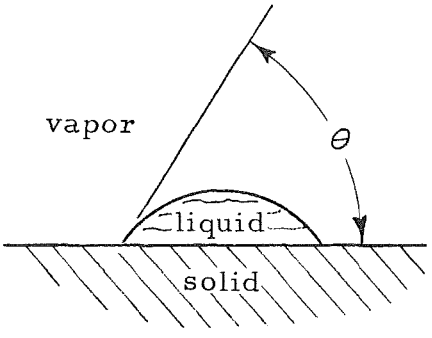

Figure 3. Contact Angle

Young's Equation:

$$\theta = \cos^{-1}\left(\frac{\sigma_{VS} - \sigma_{LS}}{\sigma_{VL}}\right)$$

where:

θ = contact angle

σ_{VS} = surface energy, vapor-solid interface

σ_{LS} = surface energy, liquid-solid interface

σ_{VL} = surface energy, vapor-liquid interface

The surface energy has been measured for a great many substances. The most extensive listing is in Reference 1, pages F-17 to F-30. Most commonly the surface energy is measured as the surface tension of the liquid phase. Surface tension is a monotonically decreasing function of temperature and vanishes at the critical point. Surface tension and surface energy are nearly analogous terms and are referred to interchangeably.

The customary units of surface energy are ergs/cm^2. The customary units for surface tension are dyne/cm. An erg is a dyne-cm so the units of surface energy and surface tension are the same.

Measurements of contact angle are extremely sensitive to contamination due to the changes in surface energy caused by the contamination. Reference 2 gives the following examples of the lowering of surface energies of solids by gaseous contaminants:

	σ_o		σ	
	ergs/cm^2	N m^{-1}	ergs/cm^2	N m^{-1}
Mica in air at 760 torr	4500	4.5	375	.375
Silver in oxygen at 150 torr	1140	1.14	350	.35
Copper in lead vapor at 0.1 torr	1800	1.8	780	.78

where σ_o is the basic surface energy of the clean surface in a vacuum and σ is the energy of the contaminated surface.

Low surface energy contaminants in mixtures migrate to the surface. An example is a trace amount of detergent in water. It lowers the surface energy and makes the water wet things. The surface is fully covered with the contaminant present in trace quantities. Adding detergent to make a 50 percent or greater mixture is not likely to further lower the surface energy.

The same could apply to solids. A small amount of gaseous contamination, for example, could diffuse to the surface of a solid and reside there more or less permanently.

Solids with high mechanical properties tend to have high surface energies and are often difficult to keep clean. Teflon with its low surface energy does not attract contaminants and is thus relatively easy to keep clean.

Capillary Pressure

The computation of of the forces available to contain the liquid metal against acceleration forces is dependent on the contact angle and the capillary pressure. The liquid-vapor interface begins and ends at a solid surface with a contact angle. The pressure difference across the liquid-vapor interface at any given point on the interface is given by the following expression, which is attributed to Laplace:

$$\Delta P = \sigma \left(\frac{1}{r_1} + \frac{1}{r_2} \right)$$

where σ is the surface tension and r_1 and r_2 are the principal radii of curvature at that point.

In the case of a wetted, low contact angle, attachment of the liquid metal to the electrodes as shown in Figure 2, the pressure is found to be lower in the liquid than in the vapor. If the vapor is a high vacuum, the liquid will actually be at a negative pressure; that is, it will be in tension.

Electrical Contacts Using Gallium

Several instances were found of the use of liquid gallium for electrical contacts. Experiments at NASA Lewis Research Center, Reference 3, demonstrated the low contact resistance and electrical noise of a beryllium contact lubricated with gallium which had been applied by ion plating. A liquid gallium slip ring with copper electrodes was employed in this experiment as a low friction, low resistance means of transferring electrical current across a rotating interface. A great deal of unidentified residue was found in the gallium after the test.

Reference 4 describes an experiment in the USSR which is similar to our proposed material selection experiments. Low voltage drop values are reported for "steel 40 Kh" and "beryllium bronze" using a gallium-indium-tin alloy between electrodes. It was stated that these materials were not corrosion resistant to the liquid metal, but the materials which had higher corrosion resistance had higher contact resistance.

Wetting Electrode Surfaces with Gallium

The wetting of metal surfaces with a liquid requires the removal of the oxide film which protects most metals from further oxidation, and the immediate, intimate contact of the liquid with the metal before the oxide film can reform. When the liquid is also a metal the problem is complicated by the surface contamination of the liquid.

Experiments at NASA-Lewis have shown success in ion plating of gallium on beryllium. U.S. Patent 3,061,528 by F. D. Foley, assigned to Hughes Aircraft Company, describes a ". . . method whereby fine-grained lustrous deposits of metallic gallium may be plated electrolytically." Wetting of several metals by gallium had apparently been accomplished utilizing a variety of means before the present work was begun.

Experiments

The experiments consisted of a screening test and a long-term evaluation test for candidate liquid metals, electrodes, barrier films and insulators.

The screening test was a one-month exposure of all candidate materials in an argon atmosphere to various temperatures, current densities, and with different surface finishes. Measurements were made to determine any change

in electrical characteristics while passing current from one electrode through the liquid metal to another electrode. No relative motion was provided. Pre-test and post-test measurements were made to determine the effects of exposure on the materials. The selection of materials for the Engineering Model Liquid Metal Slip Ring Assembly (ETM) was then made. The best performing candidates were then continued in a long-term evaluation test in a high vacuum to verify the screening test results.

Screening Test Parameters

Figure 4 shows the input parameters intended for the electrode materials in the screening test. It will be noted that 60 of the test samples were tested with the pure gallium. The 30°C (303 K) temperature was a minimum ambient to assure that the gallium was molten. The 80°C (353 K) temperature was also a minimum ambient intended to be representative of the application.

The 10 A current was selected to provide a design value of 10 A cm^{-2} current density for the liquid metal slip rings. This value permits a 100 A current to be passed through an area of 10 cm^2 with a voltage drop of only 28 μV for a path length (gap between electrodes) of 0.1 cm through the gallium. The 10 cm^2 area is readily provided on a slip ring whose minimum diameter would be 5 cm.

Variation in surface finish was a test parameter because of the expected effect of surface roughness on the wetting of the electrodes with gallium. A 4 microinch rms (0.1 μm rms) polished finish was expected to be more easily wetted but more expensive to prepare than a typical machine finish of 63 microinch rms (1.6 μm rms).

Samples of each of the five candidate electrode materials were coated with each of the five candidate barrier films and exposed to pure gallium in the 80°C temperature. Two samples of each insulator material candidate were also exposed to pure gallium in the 80°C temperature.

Total samples for screening test:

Electrode material	65
Barrier film	25
Insulator material	10
Total	105 samples

Long-Term Evaluation Test Parameters

Five samples of each of the two "best" electrode materials from the screening test were selected as follows:

1. fine finish, zero current, pure gallium
2. rough finish, zero current, pure gallium
3. fine finish, 20 A, pure gallium

Liquid Metal	Gallium (0.999999 pure)												Ga-In-Sn*
Temperature	30°C (303K)						80°C (353K)						80°C
Current, Amperes	0		10		20		0		10		20		20
Surface Finish Microinch RMS	4	63	4	63	4	63	4	63	4	63	4	63	63
Electrode Material													
Beryllium	X	X	X	X	X	X	X	X	X	X	X	X	X
Beryllium-Copper	X	X	X	X	X	X	X	X	X	X	X	X	X
Nickel-Plated Copper	X	X	X	X	X	X	X	X	X	X	X	X	X
Stainless Steel	X	X	X	X	X	X	X	X	X	X	X	X	X
Tungsten	X	X	X	X	X	X	X	X	X	X	X	X	X

X indicates a material evaluation fixture. Total 65.

* 62.5 % gallium, 21.5 % indium and 16.0 % tin. 0.9999 pure

FIGURE 4. Matrix for Electrode Material Evaluation, Screening Test

4. rough finish, 20 A, pure gallium
5. rough finish, 20 A, Ga-In-Sn alloy

Four barrier film samples were selected as the best two films on each of the best two electrode materials. Two each of the best two insulators were also tested. Pure gallium was the liquid metal.

Total samples for long-term evaluation test:

Electrode material	10
Barrier film	4
Insulator material	4
Total	18 samples

The samples were to be run at 80°C (353K) in a vacuum of 10^{-6} torr or less (1.3×10^{-4} N m^{-2}) for 5 months. The total exposure of the samples to gallium was to be 6 months.

Measurements

All electrode samples were to have the following test measurements for both the screening test and the long-term evaluation test:

- Electrode weight loss or gain
- Voltage drop, current and temperature:

  Every hour during screening test
  Every day during long-term evaluation test
- Contact angle, visual estimate
- Spectrographic analysis of liquid metal
- Melting/freezing point of liquid metal
- Surface tension of liquid metal
- Microscopic visual examination
- Photographs

Material Evaluation Fixture

Each sample for electrode material evaluation is a material evaluation fixture (MEF) as shown in Figure 5. This fixture positions two electrodes with a gap between them of 1.0 millimeter. The fixture is designed to provide one square centimeter of conducting area when filled as shown in Detail A. It was calculated that gallium would be supported between the electrodes by capillary forces with accelerations up to 4 g (39 m s^{-2}) in any direction.

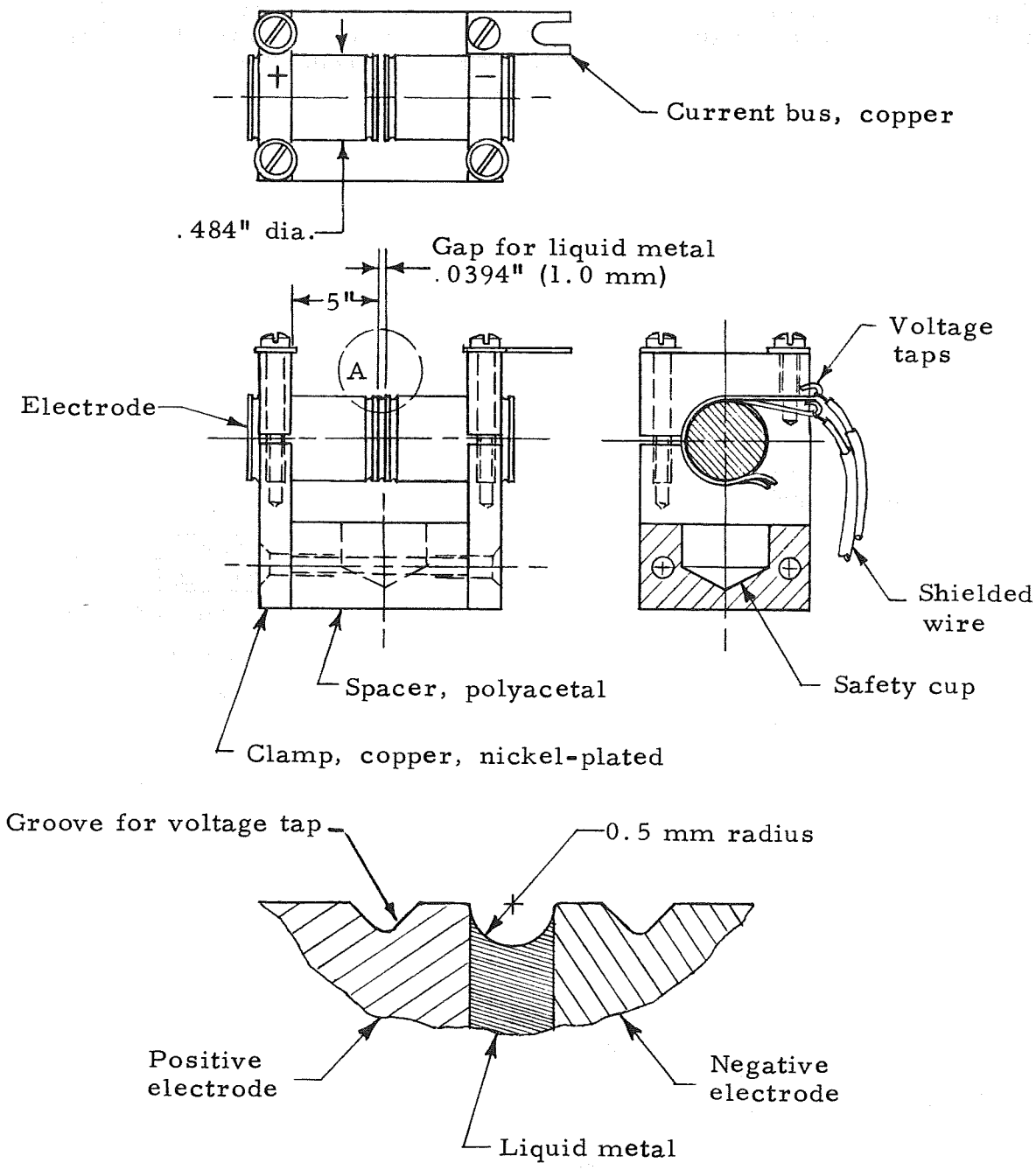

DETAIL A

FIGURE 5. Material Evaluation Fixture

The drawing used to procure the sample electrodes is shown in Figure 6. They are configured to promote an even current distribution through the liquid metal and have a voltage tap location close to the liquid metal to permit measurements of resistivity. The electrodes are made two-ended to provide a spare in the event of damage or an error in wetting with the liquid metal.

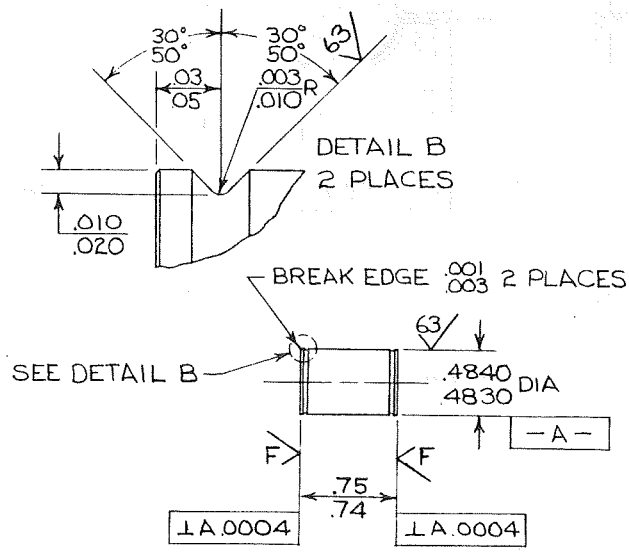

PART NO.	FINISH "F" μin rms 2 PLACES	MATERIAL
216706-1	F<4	BERYLLIUM BERYLCO HP 20 98% Min Be, 2% Max BeO_2
216706-2	32<F<125	
216706-3	F<4	BERYLLIUM-COPPER BERYLCO 25
216706-4	32<F<125	
216706-5	F<4	NICKEL Huntington Alloy Nickel 270 99.97% Min Ni
216706-6	32<F<125	
216706-7	F<4	STAINLESS STEEL AISI 304
216706-8	32<F<125	
216706-9	F<4	TUNGSTEN Sylvania, Fine Grain Rod 99.95% Min W
216706-10	32<F<125	

NOTES:

1. It is of utmost importance that these parts be made of pure materials and be scrupulously clean and free of oxides for use in a materials compatibility experiment.
2. Parts to be free of voids, pits and scratches.
3. Finish machine using clean holding tools and clean cutting tools. Package and seal in plastic bags with dry argon gas immediately on removal from machine. Handle parts only with clean forceps and use clean measuring tools.
4. Pack parts so as to protect them from abrasion during transportation. Storage time is to be minimized.

Rev. A, AISI 304 was AISI 302, 28 Aug 69

SAMPLE ELECTRODE				
R. B. Clarke	22 Aug '69	Bldg 366	M.S. A350	Phone 648-1173
HUGHES AIRCRAFT CO. CULVER CITY, CALIF.	SP 216706			

FIGURE 6. Drawing of Sample Electrode

The holes in the clamps for the electrodes were line-reamed to assure parallelism of the electrode faces which form the 1.0 mm gap. The gap was set at the operating temperature using a glass shim between the electrode faces. This avoided the need to compensate for differential expansion of the materials with temperature. The clamps are copper to aid in uniform current distribution and are nickel plated to avoid transfer of the soft copper to the electrodes during assembly.

Every clamp and insulator is permanently marked with an MEF identifying number. Each complete MEF with electrodes has been kept as a matched set.

The MEFs were tested with the liquid metal suspended in its gap in a vertical plane. It was intended that if the electrodes became non-wetting the liquid metal would fall into the safety cup. The connection would then be closed with a bus wire to allow the experiment to continue, since the MEFs were connected in series.

Barrier Film and Insulator Samples

The barrier film and insulator samples are small cylinders with a shallow spherical cavity in one end as shown in Figure 7.

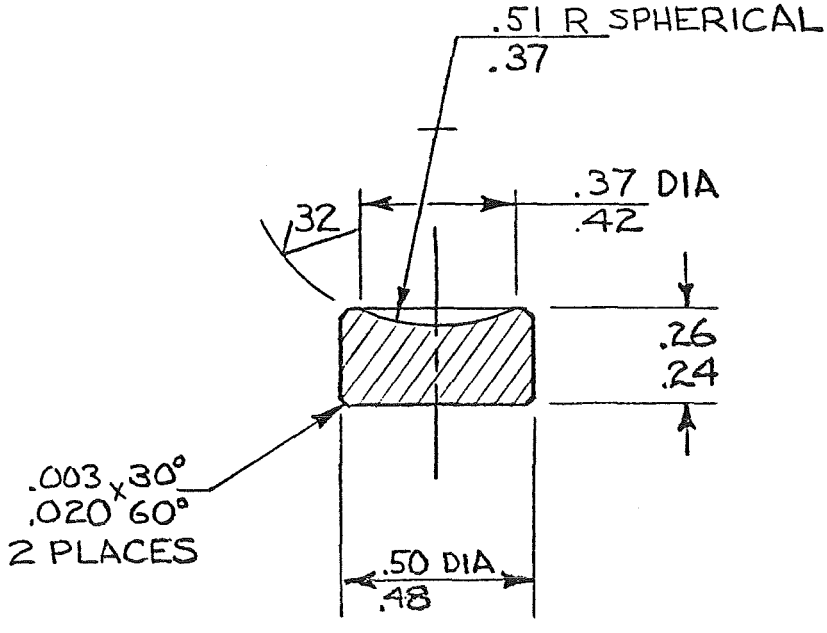

FIGURE 7. Barrier Film and Insulator Samples

Five samples of each candidate electrode material were made to these dimensions and using the same precautions to prevent contamination as are noted in Figure 6. Half of each cavity was then coated with a candidate barrier film per Figure 8. The samples were then stored in an argon atmosphere until use.

The insulator samples were also machined using clean holding tools and clean cutting tools. Chips and dust were removed with dry, filtered compressed air. The samples were then stored in argon gas.

Wetting with Gallium

Several methods were considered for the wetting of the end face of the electrodes with gallium. These were:

- Make a final machine cut under a bath of liquid gallium.
- Rub with a glass fabric impregnated with gallium.
- Rub gallium into the surface of the electrode with another electrode of the same material.
- Anodic cleaning followed by wetting while submerged in distilled deionized water.
- Gold plate the desired surface and allow the gallium to dissolve the gold.
- Blast with micro-size glass beads precoated with gallium.
- Ion plating.
- DC sputtering.

Machining in a bath of liquid gallium was selected for the first attempt.

Controls

All work possible was accomplished in the glove box in an atmosphere of pure dry filtered argon gas. All tools and equipment were carefully cleaned before being brought into the glovebox. The MEFs, minus the electrodes, were disassembled and ultrasonically cleaned, rinsed in xylene and ethyl alcohol, then reassembled in a flow bench using gloves before being brought into the glove box. Sample materials were final machined on machine tools which were cleaned by washing down the chucks, tools and work

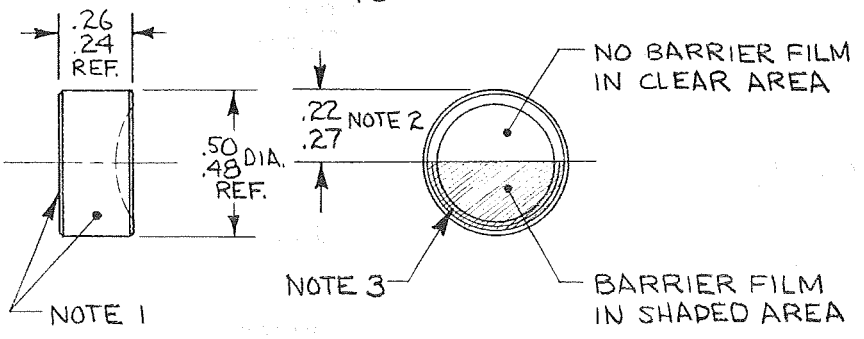

NOTES:

1. Barrier film optional on these surfaces, provided that dimensional tolerances are not exceeded.

2. Transition from complete barrier film to bare metal must occur within the tolerance indicated. A transition occurring in less than .010" is preferred but the need for good adhesion of the film at the transition is more important.

3. For films which are difficult to detect visually, a line is to be scratched into the rim as shown (before the film is applied) to indicate the extent of the film.

4. Thickness of film not to exceed .010".

5. "X" is the dash number of parts No. 216707 "SAMPLE MATERIALS" from which parts No. 216716 are to be made. Thus: Part No. 216716-2-5 is a beryllium-copper sample, part 216707-2, with an epoxy conformal coating as a barrier film.

6. Parts No. 216707 are to be furnished clean and sealed in plastic bags with dry argon gas. Handle parts only with clean forceps and seal in clean plastic bags immediately after film application is complete. Pack parts so as to protect them from abrasion during transportation.

PART NO. (See Note 5)	BARRIER FILM	SPECIFICATION
216716-X-1	PERFLUORINATED POLYMER	HP 7-27
216716-X-2	BONDED TEFLON COATING	HP7-13, TYPE V
216716-X-3	PARYLENE	HP 16-144
216716-X-4	SILICONE RESIN COATING	DC 644
216716-X-5	EPOXY CONFORMAL COATING	HP 16-66, TYPE 1, CL 1

PURPOSE					TITLE		
Liquid Metal Slip Ring Project					BARRIER FILM SAMPLES		
MATL. & SPEC.					SCALE	TOLERANCES ANGULAR ± —	LINEAR ± —	SKETCH PAD
as listed					2/1			
ORIGINATOR	APPR.	DATE	BLDG.	ROOM (STA)	PHONE	HUGHES AIRCRAFT CO. CULVER CITY, CALIF.		SP 216716
R.B.Clark		24 Sept 69	366	A 350	648-1173			

FIGURE 8. Application of Barrier Films

surfaces with a series of solvents: xylene, Freon PCA and ending with isopropyl alcohol. Only clean gloves, clean tools and clean plastic bags were allowed to touch these materials. Every reasonable effort was employed to minimize contamination of the samples and to minimize their exposure to air.

Electrode Material Selection

The electrode materials to be used on the ETM were selected from the screening test candidates on the basis of the following criteria:

1. Contact angle. Only wetting systems are to be considered. The effective contact angle must not exceed 45 degrees.

2. Surface tension should not change more than ±30 percent in 30 days, ±50 percent in 150 days.

3. Melting point should not change more than $\pm 5^{\circ}$C in 30 days, $\pm 10^{\circ}$C in 150 days.

4. Electrode weight loss (or gain) must not exceed a value equivalent to 0.0001 inch in 30 days or 0.0004 inch (.001 cm) in 180 days.

5. Electrical contact resistance should not vary more than ±20 percent in 30 days and ±30 percent in 150 days. Electrical noise shall not exceed 1.0 milliohm peak to peak when measured at 10 amps or 20 amps.

6. Visual appearance shall not show strong polarity or material degradation effects.

7. Spectrographic analysis is not to indicate more than 2.0 percent of any material except the original liquid metal after 30 days, or 5.0 percent after 150 days.

Apparatus and Procedures

Working Area

A restricted entry working area was set up in a clean room for exclusive use by the liquid metal slip rings project. The clean room air is controlled to $72^{\circ} \pm 5^{\circ}$F (295.4 ±2.8K) and 65 percent maximum relative humidity. The room contains two laminar flow benches certified to Class 10,000 but capable of Class 100, Federal Standard 209. Smocks and caps are required on going through the air lock into this room and only authorized persons are admitted. The technicians who work in this room

have been specially trained for work on materials and mechanisms suited to high vacuum and the special reliability required of spacecraft. The restricted area for liquid metal slip rings contains a workbench topped with black Formica, wall-mounted metal storage cabinets and a glove-entry box.

Glove Box

All work on the screening test, except fabrication and wetting of samples, was accomplished in the glove box in an atmosphere of pure argon gas.

The glove box measures 35 inches (0.89 m) wide by 25 inches (.636 m) deep by 27 inches (.685 m) high. It has two arm length rubber gloves in the lower front, a sloped view glass, and a pass-through on the side. The inside finish is epoxy. A removable panel in the back was adapted for the multiple electrical connections and the whole box was carefully reworked to be as gas-tight as possible.

The gas supply to the glove box is shown in Figure 9. The argon gas is supplied by AIRCO to a purity of 99.997 percent. The Robbins Purifier Model RAF6B "dehydrates to dewpoints less than -105°F (197 K) and simultaneously removes hydrocarbons to less than 1 PPM/w (hexane equivalent), and oil vapor and most noxious gases to less than 1 PPM/w" using an RAF-BCD13X desiccant cartridge. The particle filter is a five micron Millipore type.

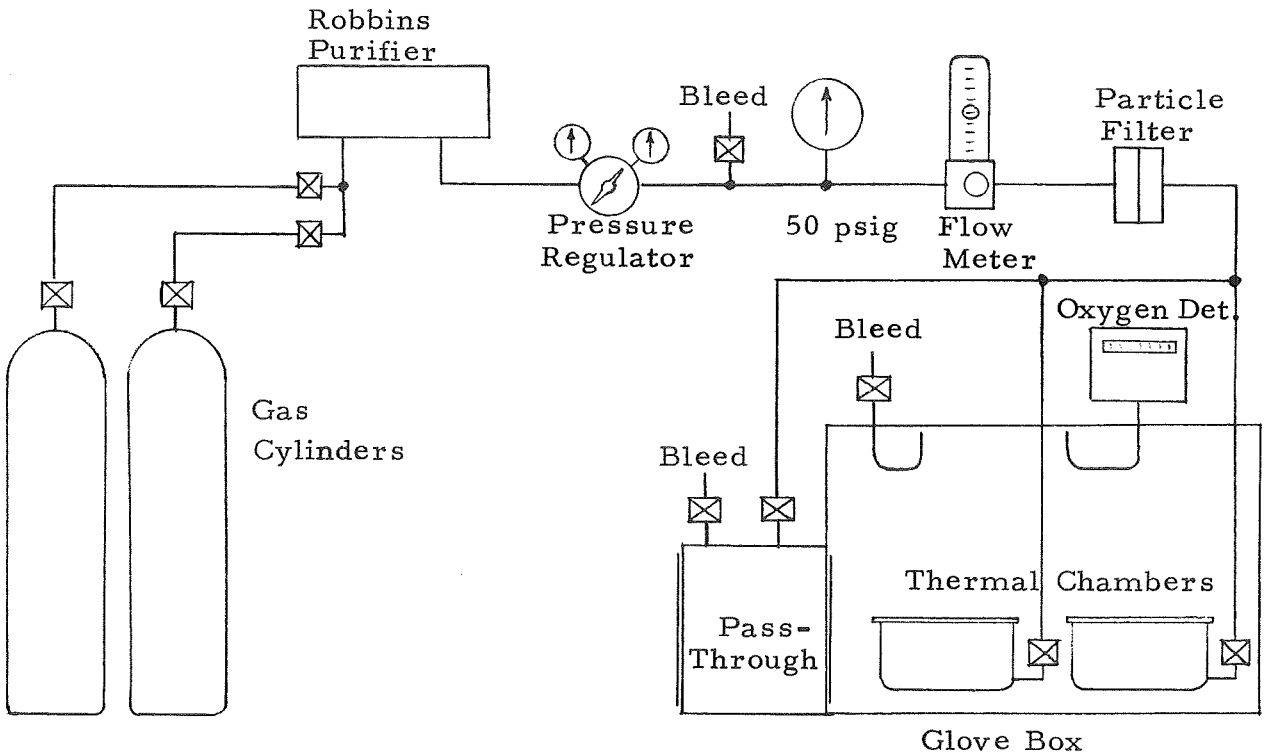

FIGURE 9. Argon Supply to Glove Box

The oxygen meter is a Beckman Model D2 with a full scale of 25 percent (190 mm) and a readability of 0.1 percent (about 1 mm). The meter is used to establish when an adequate flow rate of argon is established, as controlled by a needle valve on the flow meter. The flow meter is a Victor Model V-0158 with a range from 4 to 50 CFH (3.15×10^{-7} to 3.93×10^{-8} $m^3 s^{-1}$). With a flow rate of 50 CFH and the top bleed open, the oxygen content of the glove box could be reduced from 22 percent to less than 0.2 percent in one hour. Note that oxygen content is measured at the top of the glove box when using argon, because argon is more dense than oxygen.

Manipulation of tools and samples in the glove box requires that the arms move in and out. This often causes underpressure and small amounts of air are drawn in. A third arm-length glove, located on the pass-through, was used as a diaphragm to reduce the magnitude of underpressure. The glove, normally inflated, would collapse when an arm was withdrawn. This was more satisfactory than the use of high flow rates of argon. The high flow rates caused overpressure which restricted motion and interferred with the accuracy of instrumentation such as the analytical balance, which was used inside the glove box.

The oxygen content was found to be less than 0.1 percent after an hour of non-use with argon supplied at 4 CFH. In use at 10 CFH the oxygen content was normally under 0.2 percent. Operations were discontinued when the oxygen content exceeded 0.5 percent. All samples were normally stored in the thermal chambers where the oxygen content was too low for measurement.

It was found necessary to reduce the flow rate to 4 CFH to obtain repeatability in weighing. Weighing operations therefore required very careful movements by the operator.

Wetting of Electrodes with Gallium

Wetting of all electrode samples was accomplished by doing the final machining cut with the tool bit and the end of the electrode submerged in liquid gallium. The initial setup is shown in Figure 10.

It was soon found that the gallium would partially wet the cylindrical sides of the electrodes where it was rubbed-in by the teflon block. A separate tight fitting sleeve of teflon was used around most of the electrodes during machining to avoid this problem.

Preliminary trials without the gallium established that a machining cut .001 to .003 inch (25 to 76 μm) deep with a feed of .001 inch (25 μm) per turn produced the best surface finish obtainable with this tooling, about 16 microinch (0.41 μm) rms. Changing the feed to .003 inch (76 μm) increased the roughness to about 64 microinch (1.63 μm) rms. These settings are hereinafter referred to as "fine" and "rough" finish respectively and were used on all sample electrodes. Turning was done at one revolution per second.

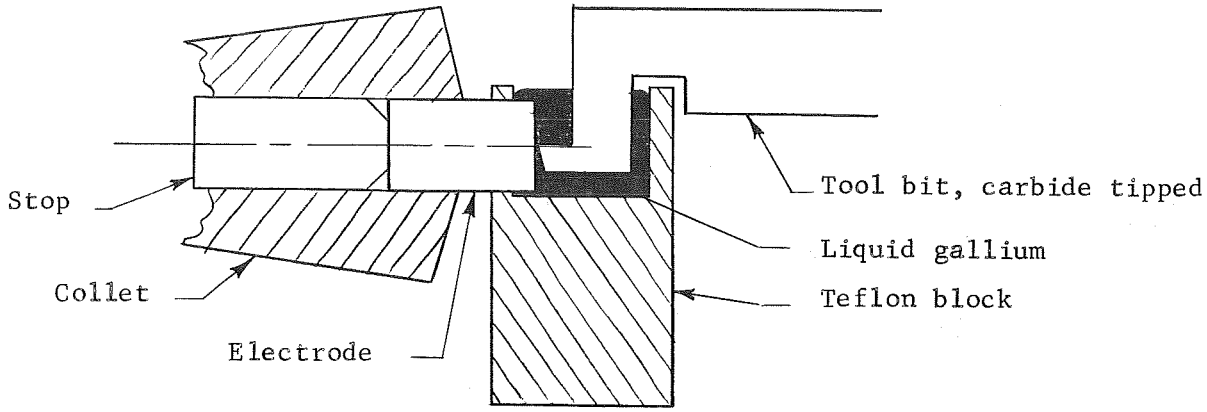

FIGURE 10. Setup for Machining Electrodes in Gallium

The gallium was kept liquid during machining by the proximity of the machinist's lamp.

The electrodes were put in plastic bags in argon-flushed containers as soon as they were removed from the specially cleaned lathe, and they were brought into the dry box no more than 4 hours after machining.

Initial wetting was achieved on all candidate electrode materials by the test that the gallium could be wiped off gently with a clean cloth and the gallium color would remain. When a small amount of fresh gallium was added it would readily spread over the initially wetted surface.

No difficulties were experienced with wetting of the nickel-plated copper or the beryllium-copper electrodes. The stainless steel and tungsten electrodes with the rough finish often failed to begin wetting for as much as 10 turns of the lathe leaving an unwet band of 0.03 inches (0.8 mm) at the periphery of the circular wetted area. Apparently the gallium was failing to get right behind the tool bit. The tool bit was carefully cleaned after each electrode. This problem was alleviated by hand-turning the lathe for the first few turns.

The most difficulty was experienced with the wetting of the beryllium electrodes. After initial wetting they were stored for several days sealed in plastic bags with argon gas. They were then found to be inadequately wetted and indeed corrosion appeared to have begun. They were all carefully cleaned off and wetted on the spare end with extreme precautions to minimize exposure to air. Weighing and assembly into MEFs was expedited. All beryllium electrodes were fine machined as this was found to produce the most reliable wetting.

Note that the beryllium chips were retained in the liquid gallium, thus providing a convenient means of control and disposal.

Fresh gallium, 99.9999 percent pure, was used for machining each different electrode material. The gallium which adhered to the wetted faces was allowed to remain until subsequent weighing in the glove box.

The first stainless steel samples were wetted with gallium on 20 October 1969 and have remained wetted to this writing. On 4 November 1969 the last of the recalcitrant beryllium electrodes was wetted and weighed and assembled in an MEF.

Weighing of Electrodes

The exact weight of each of the 130 electrodes was desired to permit determination of weight loss or gain due to the exposure to gallium. This was made difficult by the final machining under gallium. It was necessary to carefully wipe the gallium from each electrode face, weigh the electrode, then spread fresh gallium on the face. This also served the purpose of removing the gallium which was contaminated by air and by the machining chips. This work was done in the glove box.

The first attempts at wiping off the excess gallium utilized pads of unsized glass cloth. (Glass cloth normally is obtained with the fibers coated with a sizing that helps in the weaving and in wetting by adhesives.) The gallium was not absorbed by the glass cloth and repeated wiping still left excess gallium on the surface. A stretch nylon material used for gloves proved successful. The gloves had been approved for use in handling thermal finishes on spacecraft such as Surveyor.

The spreading technique used to encourage the gallium to cover the entire face of an electrode after wiping and weighing was to heat the electrode to about 40°C on a small hotplate in the dry box and apply a drop of gallium from a glass syringe. The gallium was extracted from below the surface film of the sample which was kept at 40°C to 60°C in a small glass container with a ground finish cover. Typically the drop did not spread by itself but needed to be encouraged by tapping the electrode on a nylon anvil. In this way no spreading tool was needed and difficulties in spreading were readily observed. This process is hereinafter referred to as "rewetting".

Retention of wetting characteristics by the faces of the electrodes was significantly inhibited by wiping pressure during cleaning. A few electrodes needed remachining under gallium as a result of heavy wiping. The contact angle became high and the gallium would "ball up" or refuse to spread evenly. The preferred wiping technique left slight streaks of gallium on the wetted face.

The repeatability of the wiping, weighing and rewetting process was demonstrated by the several trials shown in Table 7, then the weighing was reduced to once per electrode.

TABLE 7. REPEATABILITY OF ELECTRODE WEIGHTS

STAINLESS STEEL, CRES 304, ROUGH FINISH			
Electrode Number	First Weighing (grams)	Second Weighing (grams)	Third Weighing (grams)
First candidate	17.5286	17.5287[1]	17.5283[1]
9 negative	17.5504	17.5505	17.5508
9 positive	17.4956[2]	17.4941	17.4941
19 positive	17.4992	17.4990	
19 negative	17.4935	17.4938	
29 positive	17.5158	17.5158	
29 negative	17.5068	17.5066	
39 positive	17.5162	17.5165	
39 negative	17.4902	17.4906	
59 positive	17.4976	17.4980	
59 negative	17.4622	17.4626	
STAINLESS STEEL, CRES 304, FINE FINISH			
4 positive	17.5600	17.5603	
4 negative	17.5338	17.5341	
14 positive	17.5063	17.5064	
14 negative	17.5303	17.5302	

(1) Electrode face would not properly rewet after cleaning and weighing.

(2) Zero of analytical balance was off during this reading due to change of argon flow rate from 10 CFH to 4 CFH.

Assembly of Material Evaluation Fixtures

After each electrode was weighed it was placed in a numbered MEF and has since been identified by that number plus a positive or negative identification. The wetted faces of the positive and negative electrodes were placed close enough together that the gallium filled the gap between them. This was to avoid oxidation of partially drained surfaces by residual oxygen or if air should enter the glove box by accident.

Assembled MEFs were placed in the two thermal chambers. When all electrodes were weighed and the 65 MEFs were assembled, the thermal chambers were heated using built-in electric light bulbs.

Gap Setting

The setting of the one millimeter gaps was accomplished per the experiment plan. One MEF at a time was removed from the thermal chamber, which was approximately 5°C above operating temperature. One clamp was loosened and the electrode moved back enough to allow insertion of a glass microscope slide which was measured to be between .03933 and .03941 inch thick. The electrode was then pushed back against the slide and the clamp tightened. The slide was checked for fit as it was withdrawn.

The above was accomplished quickly such that the temperature drop was not expected to exceed 5°C at the time of gap setting. This took some experimentation and practice, particularly on the 80°C samples. A nylon glove was worn over the rubber glove in the dry box to reduce discomfort and possible damage to the rubber gloves when handling MEFs at up to 90°C.

Filling with Gallium

The weight of gallium required was numerically added to the measured weight of the particular electrodes and support assemblies which make up an MEF. Gallium was then added to the MEF until the total weight was within the required tolerance. It proved impractical to hold the amount of gallium to 0.630 to 0.636 gram. The tolerance adopted was .605 to .635 gram which was generally achieved on the third weighing of the filled MEF.

Most of the beryllium and some of the tungsten electrodes refused to accept the minimum amount of gallium. In the case of the tungsten, it was due to the typical .010 inch or more non-wetted edges aggravated by the shrinking of the gap when the 80°C MEFs cooled. In the case of beryllium, there was a distinct tendency for irregular areas around the edges of the electrodes to drain and discolor and refuse to wet. This tendency increased with time and temperature. The 80°C MEFs were filled first which tended to equalize the degradation of the beryllium electrodes between the two chambers. The poorest fill was MEF 41, because of the extra exposure involved in taking pictures. MEF 41 would accept only 0.4195 gram of gallium-indium-tin alloy, any additional added would run out if the MEF was disturbed, such as by tapping.

Thermal Chambers

The thermal chambers are two aluminum boxes, each 11 inches (28 cm) square by 6 inches (15 cm) deep with 1/4 inch (.635 cm) thick glass covers and coated inside and out with epoxy to protect the aluminum from gallium. Each chamber is fitted with a valved argon gas inlet and with electrical connectors for: power, thermocouples, current supply to the MEFs and two voltage taps for each MEF. Each MEF has a perforated copper table with insulating rails to support the MEFs. Electric light bulbs are mounted under the racks to provide heat, and thermocouples are provided to sample the temperature at:

1. Argon gas near inlet
2. The perforated metal table at its center
3. The perforated metal table at an edge
4. Zero current beryllium electrodes near a corner (for lowest temperature rise)
5. 10 A nickel on copper electrode (typical)
6. 20A stainless steel (for highest temperature rise)
7. Argon gas at the level of the electrodes

The test samples were protected from air in the thermal chambers whenever it was necessary to open the glove box to move large equipment in and out.

After the gaps were set and filled with gallium the electrical connections were made and the formal exposure begun. Figures 11 and 12 show the completed thermal chambers with all samples installed. The barrier film and insulator samples are in a tray at the rear in the 80°C chamber, Figure 12.

The photographs of Figures 11 and 12 were taken through the view glass of the glove box, demonstrating the visibility of all screening test samples.

The screening test was underway on 16 November 1969. The 30°C thermal chamber could not be controlled to stay within the planned 30°C (303K) to 40°C (313K) because of the proximity of the 80°C chamber and the dissipation in the 10A and 20A circuits. The dissipation in each thermal chamber was 20W due to the high currents in the connecting wires. The temperature of the argon in the glove box during the screening test was an average of 34°C (307K) with the heaters to the 30°C chamber off and the heaters to the 80°C chamber adjusted for a minimum MEF temperature of 80°C (353K). The average temperature of the MEFs in the 30°C chamber was 43°C (316K) and that in the 80°C chamber was 84°C (357K).

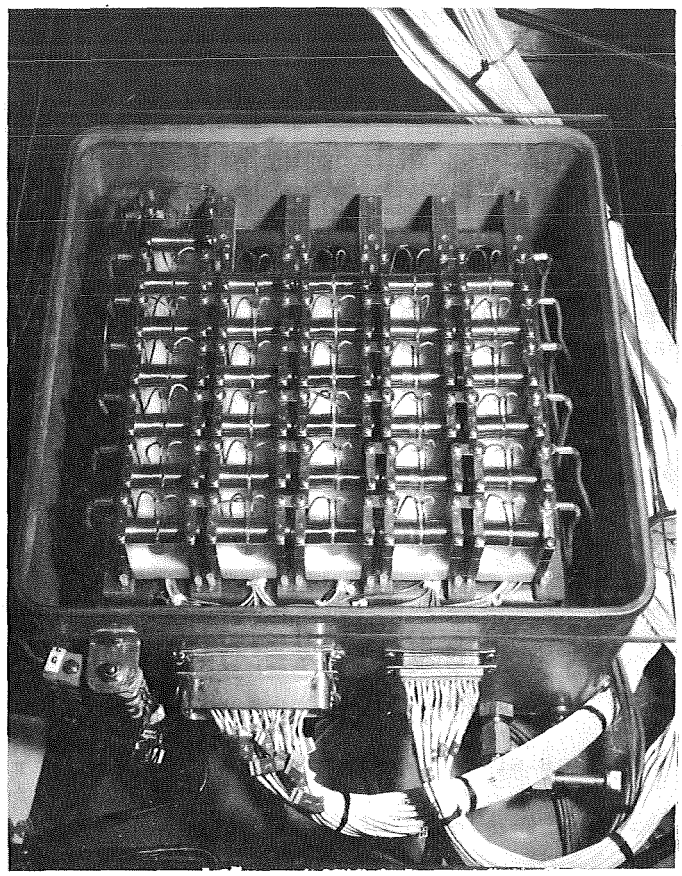

FIGURE 11. Thermal Chamber, 43°C

The argon flow rate to the glove box through the thermal chambers was 4 CFH (3.15 m^3 s^{-1}) for the duration of the screening test and the oxygen content in the glove box was less than 0.1 percent. The oxygen content in the thermal chambers was thus presumed to be less than 0.01 percent (0.1 mm).

Figure 13 shows the identification number and location of each MEF in the thermal chambers and gives typical temperature data.

Barrier Film and Insulator Samples

The samples of insulator materials and the electrode material samples with the partial coating of barrier film were allowed to degas for several days in the glove box before adding 0.1 cm^3 drops of pure gallium using a stainless steel hypodermic needle with a glass syringe. In the case of the barrier film samples, the gallium rested across the transition from bare electrode materal to coated. No attempt was made to wet the surfaces under the drops. The samples are seen to the rear in Figure 12.

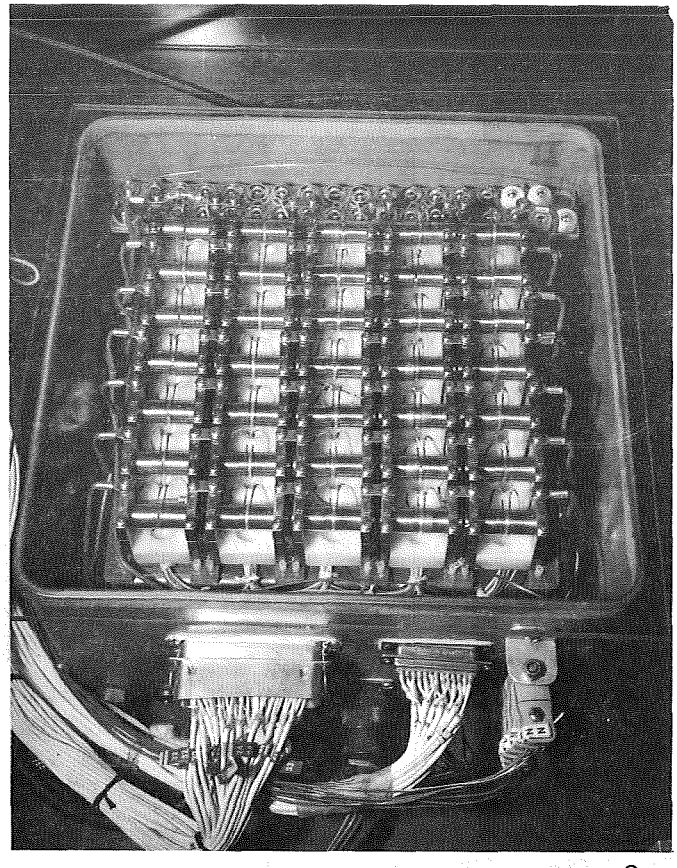

FIGURE 12. Thermal Chamber, 84°C

Electrical Measurements

Three test current circuits were provided. The "zero current" MEFs normally were open-circuited, but had 1.0 A direct current applied at infrequent intervals for measurements of resistivity. The 10 A and 20 A direct current samples were supplied continuously during the 30-day test.

Each MEF was provided with a voltage tap one millimeter from the liquid metal gap on both electrodes. Each of these leads was shielded. The voltage drop from positive to negative electrode of the 10 A and 20 A MEFs was recorded every hour during most of the screening test on a digital data recording system. Internal electrical noise considerations limited the sensitivity of this automatic data recording to approximating 300 μV. The use of an external digital voltmeter permitted measurements to a least count of one microvolt.

An oscilloscope with a vertical gain of 1 mV/cm was used at intervals to monitor electrical noise from the MEFs. To the rear in Figure 11 and in Figure 13 a) will be seen the "zero noise" electrode, a solid bar of copper mounted in an MEF clamp with voltage taps spaced the same as the sample electrodes, but with continuous copper in place of the gallium. The zero noise electrode was in the 10 A circuit and served as a measurement of background noise in the instrumentation.

50 Copper "zero noise" 10A				
56(41°C) Beryllium fine,0A Ga	57 Berylco 25 rough, 0A Ga	58 Nickel on Cu rough, 0A Ga	59 CRES 304 rough, 0A Ga	60 Tungsten rough, 0A Ga
51 Beryllium fine,0A Ga	52 Berylco 25 fine,0A Ga	53 Nickel on Cu fine, 0A Ga	54 CRES 304 fine, 0A Ga	55 Tungsten fine, 0A Ga
16 Beryllium fine, 10A Ga	17 Berylco 25 rough, 10A Ga	18(42°C) Nickel on Cu rough, 10A Ga	19 CRES 304 rough, 10A Ga	20 Tungsten rough,10A Ga
11 Beryllium fine, 10A Ga	12 Berylco 25 fine, 10A Ga	13 Nickel on Cu fine, 10A Ga	14 CRES 304 fine, 10A Ga	15 Tungsten fine,10A Ga
6 Beryllium fine,20A Ga	7(44°C) Berylco 25 rough,20A Ga	8 Nickel on Cu rough,20A Ga	9(45°C) CRES 304 rough,20A Ga	10 Tungsten rough,20A Ga
1 Beryllium fine, 20A Ga	2 Berylco 25 fine,20A Ga	3 Nickel on Cu fine,20A Ga	4 CRES 304 fine,20A Ga	5 Tungsten fine,20A Ga

a) 30°C Chamber

FIGURE 13. Identification and Map of Material Evaluation Fixtures

41 Beryllium fine, 20A Ga-In-St	42 Berylco 25 rough, 20A Ga-In-St	43 Nickel on Cu rough, 20A Ga-In-St	44 CRES 304 rough, 20A Ga-In-St	45 Tungsten rough, 20A Ga-In-St
66(81°C) Beryllium fine, 0A Ga	67 Berylco 25 rough, 0A Ga	68 Nickel on Cu rough, 0A Ga	69 CRES 304 rough, 0A Ga	70 Tungsten rough, 0A Ga
61 Beryllium fine, 0A Ga	62 Berylco 25 fine, 0A Ga	63 Nickel on Cu fine, 0A Ga	64 CRES 304 fine, 0A Ga	65 Tungsten fine, 0A Ga
36 Beryllium fine, 10A Ga	37 Berylco 25 rough, 10A Ga	38(85°C) Nickel on Cu rough, 10A Ga	39 CRES 304 rough, 10A Ga	40 Tungsten rough, 10A Ga
31 Beryllium fine, 10A Ga	32 Berylco 25 fine, 10A Ga	33 Nickel on Cu fine, 10A Ga	34 CRES 304 fine, 10A Ga	35 Tungsten fine, 10A Ga
26 Beryllium fine, 20A Ga	27(86°C) Berylco 25 rough, 20A Ga	28 Nickel on Cu rough, 20A Ga	29(84°C) CRES 304 rough, 20A Ga	30 Tungsten rough, 20A Ga
21 Beryllium fine, 20A Ga	22 Berylco 25 fine, 20A Ga	23 Nickel on Cu fine, 20A Ga	24 CRES 304 fine, 20A Ga	25 Tungsten fine, 20A Ga

b) 80°C Chamber

FIGURE 13. Concluded.

Fifty channels were scanned by the digital data recording system as follows:

Channels	Description
1 through 50	Voltage taps of MEFs 1 through 50
46	Voltage taps of the current measuring resistor in the 20A circuit, 0.010 ohms
47	Voltage taps of the current measuring resistor in the 10A circuit, 0.010 ohms
48	Thermocouple in the 30°C chamber, MEF 7
49	Thermocouple in the 80°C chamber, MEF 27
50	Voltage taps of the "zero noise" electrode

Spectroscopic Analysis

At the conclusion of the screening test and at the conclusion of the long-term evaluation test, a sample of the gallium in each MEF was carefully gathered and tested for dissolved elements using an Applied Research Model 2100 2-meter emission spectrograph. This equipment is capable of determining the amounts of dissolved electrode material to within 1 to 10 parts per million (ppm) by calibrating the spectral line intensity.

The samples were acquired in the glove box using a plastic eye dropper tipped with an unused piece of plastic tubing for each sample.

The spectrograph is not capable of detecting small amounts of atmospheric elements such as oxygen or nitrogen since the test takes place in air.

Determination of Freezing and Melting Temperatures

The determination of the effect of dissolved electrode materials on the melting point of the gallium was complicated by the tendency of the gallium to supercool and by the small size of the samples. This measurement was attempted on each MEF following the screening and long-term evaluation tests.

The melting and freezing points were determined by tapping a sample electrode until a small drop, usually about 3 mm diameter, fell into a tiny 1 cm^3 glass beaker. A small thermocouple supported in a neoprene stopper was placed in the gallium as shown in Figure 14. The beaker was placed in a close fitting hole in a copper block on a cold plate maintained near 0°C (273K). After supercooling for several degrees the sample might suddenly begin to freeze, causing the sample to warm until crystallization was complete, then the cooling would continue. Upon warming, the temperature would pause for a few seconds at the melting point.

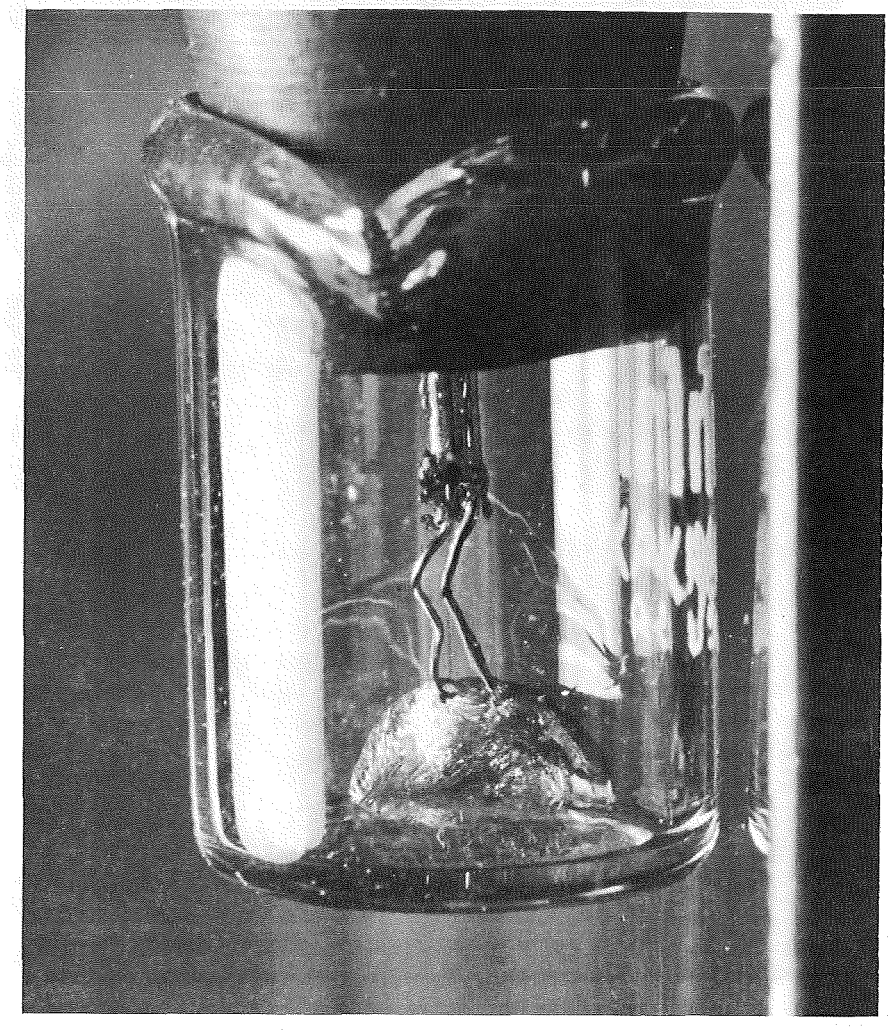

FIGURE 14. Enlarged View, Melting/Freezing Determination

The thermocouple output was monitored on a strip chart recorder. The recorder was calibrated with a thermocouple bridge for scale factor. Pure gallium was used as the temperature reference.

It was commonly necessary to condition a sample of gallium by dropping it directly onto the cold plate to force it to freeze. Once it had been frozen, it was more likely to repeat the performance in the beaker with the thermocouple. Readings could not be taken directly on the cold plate because the sample would freeze before the thermocouple could be inserted. Many samples refused to freeze in the beaker. The gallium-indium-tin alloy samples, with a published freezing point of 10.7°C, were never induced to freeze.

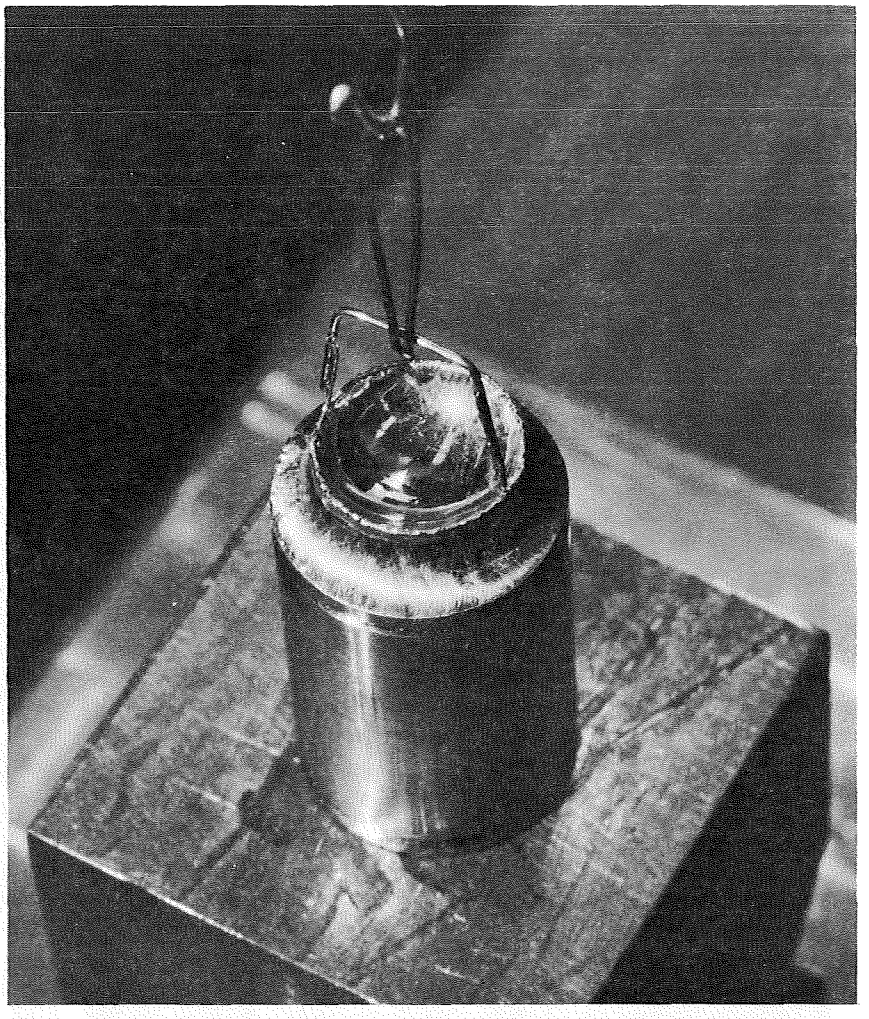

FIGURE 15. Measurement of Surface Tension by Ring Removal

Measurement of Surface Tension

A special tensiometer was constructed to suit the small size of the samples and the high surface tension of the gallium. The standard DuNony type tensiometers were designed for use with liquids having surface tensions an order of magnitude lower than the .735 $N\,m^{-1}$ expected for gallium, and the platinum rings were too large for our samples. The sessile drop measurement was not attempted because of difficulties in handling the two axis micrometer stage and microscope in the glove box. The horizontally oriented microscope would require a special external horizontal cross hair.

The ring removal tensiometer which was constructed utilized 0.010 inch (0.25 mm) diameter platinum wire formed in a ring with a 0.346 inch (8.78 mm) outside diameter. This was fastened to a sensitive force gage and

supported on a vertically moving stage driven at a low rate by an electric motor and lead screw. The output of the force gage was observed on a strip chart recorder. The peak force required to pull the ring out of the liquid metal is a direct measure of the surface tension. The tensiometer was calibrated with precision weights and is believed to have an accuracy of 2 percent. Comparison with pure gallium was the major objective. The comparison should be accurate to better than 1 percent.

Measurement of the surface tension was made for all MEFs on which adequate liquid metal remained after the samples were taken for spectrographic analysis and melting freezing point determination. This test was last because only one ring was employed, and though it was carefully cleaned between samples, there was a possibility of cross contamination.

A test is started by sliding the ring under the surface film from the edge, then lifting vertically. The peak force of about 4000 dynes (0.04 N) occurs when the film is nearly vertical as in Figure 15. The film then necks down and shortly thereafter tears. These readings proved repeatable within 2 percent.

Visual Data and Photographs

All pertinent data were recorded in laboratory notebooks, including sketches of the gallium to electrode interfaces which were made under a microscope. Direct reproductions of this data have been presented in the Monthly Technical Progress Narratives for the contract. Close-up photographs were taken of interesting samples, many of them in color.

Screening Test Data

The 30-day screening test exposure was complete on 16 December 1969. The electrode data from the screening test is compiled in Tables 8 through 12, and Table 13 lists the averages for all 13 MEFs of a given material.

Interface Resistance

The voltage measured across the voltage taps of each MEF for the 30-day period was remarkably consistent. Only four MEFs had changes larger than 10 microvolts, and a good part of the 10 microvolts is attributable to the instrumentation. The four changes were:

1. MEF 41, beryllium, changed from a rather high 0.5 millivolts on 17 November to 40 millivolts on 19 November when a shunt was applied to avoid disruption of the 20 A circuit if it should become completely open. The average voltage for the other four 20 A beryllium samples was 135 microvolts. At the completion of the test on 15 December the shunt was removed and the voltage was 59 millivolts. MEF 41 was the

TABLE 8. SCREENING TEST DATA,
BERYLLIUM ELECTRODES

MEF No.	Current amps	Temp. °C	Surface Finish	Microvolts Drop		Interface Resistance μΩ	Gallium grams	Weight Change (grams)	
				Ave.	Change			Positive Electrode	Negative Electrode
1	20.0	43	Fine	115	-5	1.1	.5629	+.0010	-0.0006
6	20.0	43	fine	122	-1	1.4	.5545	+.0008	+.0018
21	20.0	84	fine	179	-3	3.0	.4269	-.0024	-.0013
26	20.0	84	fine	223	-5	6.1	.4117	-.0087	+.0052
41	20.0	84	fine	.036 volts	.059 volts	18 to 2948	.3900	-.0036	-.0028
11	10.5	43	fine	89	-2	2.5	.4032	-.0025	-.0011
16	10.5	43	fine	129	0	5.4	.3491	+.0018	+.0010
31	10.5	84	fine	78	-2	1.5	.4289	-.0020	-.0017
36	10.5	84	fine	75	-2	-0.3	.4239	-.0030	-.0018
51	1.0	43	fine	16	-2	8	.2963	+.0011	.0000
56	1.0	43	fine	15	-1	6	.2554	-.0005	-.0013
61	1.0	84	fine	10	-4	3	.3575	-.0027	-.0013
66	1.0	84	fine	7	-5	2	.5859	-.0026	-.0036

TABLE 8 (concluded)

Melting Point (°F) °C Ave.	Surface Tension dyne/cm	Contaminants		Appearance and Remarks
		Element	Percent	
not neasured (N. M.)	629	Be Cu In Sn	.00004 .00003 .012 .020	Poor wetting typical of beryllium electrodes. Surface discolors to grey where previously wetted. Contaminated by G-In-Sn alloy
(85.45) 29.7	N. M.	Cu In Sn	.00002 .0034 .0037	Contaminated by Ga-In-Sn alloy
(85.75) 29.85	N. M.	Be Cu	.0028 .00003	Poor wetting accentuated by higher temperature and length of exposure
N. M.	N. M.	Cu	.00002	
N. M.	N. M.	Be	.00008 .0007	Large areas not wetted. Ga-In-Sn alloy. Rapid resistance change. Shunted after 3 days
N. M.	N. M.	Cu In Sn	.00003 .0016 .0020	Large areas not wetted. Contaminated by Ga-In-Sn alloy.
(85.55) 29.75	N. M.	Cu In	.00004 .0009	Contaminated by Ga-In-Sn alloy.
N. M.	N. M.	-	--	
N. M.	N. M.	Be	.0005	
(85.3) 29.6	N. M.	Be Cu In	.0049 .00006 .0004	Positive electrode look dry. Gallium dull. Contaminated by Ga-In-Sn alloy.
(85.25) 29.56	N. M.	Cu	.00003	Most gallium escaped during setup due to long exposure unfilled.
(85.75) 29.85	N. M.	Be	.0003	Note increased weight loss of electrodes at higher temperature.
(85.6) 29.80	N. M.	Be	.0013	All samples very poor wetting after test

TABLE 9. SCREENING TEST DATA, BERYLLIUM- COPPER ELECTRODES

MEF No.	Current amps	Temp. °C	Surface Finish	Microvolts Drop		Interface Resistance μΩ	Gallium grams	Weight Change (grams)	
				Ave.	Change			Positive Electrode	Negative Electrode
2	20.0	43	fine	136	-4	1.8	.6269	+.0362	+.0227
7	20.0	43	rough	152	-5	3.1	.6240	+.0309	+.0322
22	20.0	84	fine	103	-2	0.5	.6346	+.0677	+.0307
27	20.0	84	rough	108	-5	0.7	.6334	+.0728	+.0334
42	20.0	84	rough	150	-8	2.8	.6272	+.0458	+.0204
12	10.5	43	fine	86	0	3.7	.6309	+.0284	+.0257
17	10.5	43	rough	98	-3	4.9	.6349	+.0330	+.0269
32	10.5	84	fine	52	0	0.3	.6375	+.0620	+.0334
37	10.5	84	rough	59	+3	1.0	.6405	+.0570	+.0373
52	1.0	43	fine	6	-2	1.5	.6359	+.0231	+.0274
57	1.0	43	rough	9	-3	3.6	.5299	+.0216	+.0193
62	1.0	84	fine	6	-2	1.3	.6342	+.0343	+.0385
67	1.0	84	rough	2	-2	--	.6365	+.0472	+.0453

TABLE 9. (concluded)

Melting Point (°F) °C Ave.	Surface Tension dyne/cm	Contaminants		Appearance and Remarks
		Element	Percent	
(85.2) 29.55	681	Ag Cu	.00003 .0014	Electrode surface of all beryllium copper samples covered with tiny pimples where exposed to gallium.
(85.65)	668	Ag Cu	.00004 .0025	Drained areas at top of samples do not have pimples. 
N.M.	N.M.	Ag Cu	.00007 .0024	Note polarity effect on weight change. Compare to MEF 62.
N.M.	636	Ag Cu	.00006 .0020	
N.M.	543	Ag Cu	.00015 .0003	Ga-In-Sn alloy. Ag partly from Ga-In-Sn alloy
(85.3) 29.6	652	Ag Cu	.00003 .0021	
(85.6) 29.8	662	Ag Cu	.00004 .0028	
N.M.	625	Ag Cu	.00007 .0015	Note increase in silver with current and temperature.
N.M.	636	Ag Cu	.00007 .0016	
(85.6) 29.8	620	Cu	.0017	
(85.85) 29.9	697	Cu In	.0036 .0005	Some gallium lost during setup. Drained areas on electrodes dull, no pimples. 
(86.5) 29.8	662	Ag Cu	.00006 .0018	Melting point measurement uncertainty ±2°F.
N.M.	636	Ag Cu	.00005 .0013	All samples wet easily with gallium before and after test. Voltage tap probably open

TABLE 10. SCREENING TEST DATA,
NICKEL-PLATED COPPER ELECTRODES

MEF No.	Current amps	Temp. °C	Surface Finish	Microvolts Drop		Interface Resistance μΩ	Gallium grams	Weight Change (grams)	
				Ave.	Change			Positive Electrode	Negative Electrode
3	20.0	43	fine	73	-1	0.5	.6300	+.0039	+.0109
8	20.0	43	rough	74	-2	0.5	.6297	+.0017	+.0068
23	20.0	84	fine	58	-2	-.03	.6168	0	+.0038
28	20.0	84	rough	61	-2	-.01	.6398	-.0011	+.0156
43	20.0	84	rough	77	-3	0.8	.6459	+.0026	+.0076
13	10.5	43	fine	43	-1	0.8	.6193	+.0155	+.0121
18	10.5	43	rough	44	0	0.9	.6154	+.0040	+.0037
33	10.5	84	fine	34	-1	0.0	.6392	+.0013	+.0152
38	10.5	84	rough	37	-1	0.4	.6416	-.0012	+.0036
53	1.0	43	fine	4	-2	0.6	.6231	+.0076	+.0030
58	1.0	43	rough	3	-1	-0.2	.6492	+.0144	+.0011
63	1.0	84	fine	7	-5	3.5	.6302	+.0067	+.0184
68	1.0	84	rough	5	-3	1.6	.6345	+.0026	+.0045

TABLE 10. (concluded)

Melting Point (°F) °C Ave.	Surface Tension dyne/cm	Contaminants		Appearance and Remarks
		Element	Percent	
(85.6) 29.8	680	Cu Ni	.0022 .0022	Most nickel-plated electrodes have tiny burrs all over electrode surfaces. Affects weighing.
(85.6) 29.8	646	Cu Ni	.0020 .0028	
(84.0) 28.9	585	Cu	.0034	Pos. electrode relatively smooth. Melting point measurement uncertainty ±2°F
N. M.	652	Cu	.0038	Gallium holds particularly well in gaps of high temp., Ni-plated MEFs. Top: ⌐M⌐ Bottom: ⌐M⌐
N. M.	505	Cu	.0012	Ga-In-Sn alloy.
(85.85) 29.9	674	Cu Ni	.0033 .0060	Gallium has tire-shaped bulge at bottom of gap: ⌐U⌐
(85.6) 29.8	708	Cu Ni	.0040 .0079	Small pendant drop at bottom, <.04" diameter.
N. M.	636	Cu	.0019	Surface tension lower for high temperature MEFs.
N. M.	662	Cu	.0039	
(85.1) 29.5	681	Cu Ni	.0022 .0023	Negative electrode free of burrs.
(85.5) 29.7	697	Cu Ni	.0020 .0065	
N. M.	611	Cu	.0022	Note absence of Ni in high temperature MEFs.
N. M.	636	Cu	.0022	All samples wet readily with gallium before and after test exposure

TABLE 11. SCREENING TEST DATA
STAINLESS STEEL ELECTRODES

MEF No.	Current amps	Temp. °C	Surface Finish	Microvolts Drop		Interface Resistance μΩ	Gallium grams	Weight Change (grams)	
				Ave.	Change			Positive Electrode	Negative Electrode
4	20.0	43	fine	387	-5	2.4	.6387	-.0006	-.0006
9	20.0	43	rough	513	-2	8.5	.6281	-.0024	-.0006
24	20.0	84	fine	319	+13	-1.6	.6324	+.0014	+.0002
29	20.0	84	rough	446	0	4.7	.6308	+.0029	+.0030
44	20.0	84	rough	344	+98	-0.2	.6413	+.0004	+.0005
14	10.5	43	fine	234	-18	5.4	.6384	-.0001	-.0010
19	10.5	43	rough	295	+1	12.3	.6261	-.0035	-.0008
34	10.5	84	fine	196	-3	1.2	.6365	+.0014	+.0012
39	10.5	84	rough	172	-3	-1.2	.6330	+.0024	+.0029
54	1.0	43	fine	25	-4	7.6	.6343	-.0019	-.0018
59	1.0	43	rough	26	-2	8.7	.6181	-.0011	+.0004
64	1.0	84	fine	17	-5	-0.5	.6347	+.0016	+.0026
69	1.0	84	rough	22	-3	4.3	.6219	+.0018	+.0023

TABLE 11. (continued)

Melting Point (°F) °C Ave.	Surface Tension dyne/cm	Contaminants		Appearance and Remarks
		Element	Percent	
(85.6) 29.8	670	Cu	.00003	All samples clean appearing before and after test. Initial wetting slightly difficult, easier after test.
(85.65) 29.8	704	Cu	.00002	
(84.0) 28.9	594	Cu	.00001	
N. M.	697	Cu	.00001	
N. M.	531	Cu	.00014	Ga-In-Sn alloy. Looks normal, some sag. Large resistance change. Still wetted.
N. M.	668	Cu	.00070	
(85.5) 29.15	656	Cu	.00001	
N. M.	668	Cu	.00004	
(84.75) 29.3	644	--	--	
(85.95) 29.97	668	Cu	.00011	Pendant drop .07" diameter
N. M.	681	Cu	.00005	
(86.1) 30.06	643	--	--	
(85.75) 29.85	686	--	--	

TABLE 12. SCREENING TEST DATA, TUNGSTEN ELECTRODES

MEF No.	Current amps	Temp. °C	Surface Finish	Microvolts Drop		Interface Resistance μΩ	Gallium grams	Weight Change (grams)	
				Ave.	Change			Positive Electrode	Negative Electrode
5	20.0	43	fine	127	-.4	2.1	.6361	-.0021	-.0005
10	20.0	43	rough	123	-7	2.1	.6253	+.0016	-.0088
25	20.0	84	fine	132	+5	1.0	.4346	-.0004	-.0006
30	20.0	84	rough	87	-3	0.2	.6115	-.0006	-.0011
45	20.0	84	rough	103	-3	0.5	.5364	-.0009	+.0001
15	10.5	43	fine	87	-2	4.0	.5675	+.0012	+.0006
20	10.5	43	rough	66	-9	2.1	.6484	-.0039	-.0028
35	10.5	84	fine	44	+2	-0.1	.5879	-.0008	-.0003
40	10.5	84	rough	41	0	-0.2	.6183	-.0022	-.0008
55	1.0	43	fine	46	-4	42	.6269	+.0007	+.0001
60	1.0	43	rough	5	-2	1	.6276	-.0029	-.0022
65	1.0	84	fine	10	-3	4	.4289	-.0008	-.0002
70	1.0	84	rough	7	-1	3	.5426	-.0013	-.0011

TABLE 12. (concluded)

Melting Point (°F) °C Ave.	Surface Tension dyne/cm	Contaminants		Appearance and Remarks
		Element	Percent	
(85.65) 29.8	635	Cu	.00015	All samples clean appearing before & after test, wetting difficult before test, worse after. Pendant drop 0.1" dia. reduces conductive area.
(85.05) 29.45	668	Cu	.00160	Pendant drop 0.07" diameter.
(83.9) 28.85	N.M.	Ag Cu Pb Sn	.00025 .00003 .17 .20	Negative electrode poorly wetted. Gallium may be contaminated with solder.
(84.9) 29.4	618	Cu	.00003	Gallium film mostly taut.
N.M.	539	Cu	.00023	Ga-In-Sn alloy.
(85.7) 29.83	636	Cu	.00006	
(85.55) 29.75	626	Cu	.00004	Pendant drop 0.10" dia. Negative electrode not well wetted.
(85.05) 29.47	618	Cu	.00007	
N.M.	629	Cu	.00009	
(85.5) 29.73	611	--	--	Sags. Positive electrode poorly wetted. Not bright. High resistance.
(85.5) 29.73	656	Cu	.00005	Gallium surface not very bright
N.M.	596	Cu	.00002	Gallium bright. Edges poorly wetted all around.
(84.75) 29.3	641	--	--	

TABLE 13. SCREENING TEST DATA, AVERAGES

Electrode Material	Gallium Contained (gram)	Interface Resistance (micro-ohms)		Weight Change (milligrams)		Contaminants in Gallium (parts/million)
		Average	Worst Case	Positive Electrode	Negative Electrode	
Beryllium	.419	3.3*	2948	- 1.8	- 0.6	8.4
Beryllium-Copper	.625	2.1	4.9	+43.1	+30.3	20.1
Nickel-Plated Copper	.632	0.7	0.9	+ 4.5	+ 8.2	48.7
Stainless Steel	.632	4.0	12.3	+ 0.2	+ 0.6	0.9
Tungsten	.576	1.6*	42	- 1.0	- 1.4	1.8

* Worst case not included.

beryllium sample using the gallium-indium-tin alloy, and the positive electrode was exposed with the liquid metal wiped off for the longest period of any beryllium electrode. This exposure was for photographs and was in the glove box in the argon atmosphere. Estimated time of exposure: 5 minutes.

2. MEF 24, stainless steel, shows an increase of 13 microvolts, about 4 percent.

3. MEF 14, stainless steel, shows a decrease of 18 microvolts, about 8 percent. The changes in MEFs 24 and 14 may simply be the extremes of instrumentation error. MEF 14, however, shows the highest copper contamination, 7 parts per million, of any stainless steel sample.

4. MEF 44, stainless steel, shows increase in fairly linear fashion of 98 microvolts, about 33 percent. The liquid metal was again the gallium-indium-tin alloy and one electrode of this sample was exposed inside the dry box with excess liquid metal wiped off for a much longer time than the typical samples, during photography.

Tungsten MEF 55 showed a nearly constant voltage drop of 46 microvolts at 1A whenever it was measured. This was some 10 times higher than expected. On disassembly the positive electrode was found to be almost completely non-wetted.

The data on beryllium-copper MEF 67 indicates that one of the voltage taps was open. The sample was otherwise normal.

The interface resistance was calculated by subtracting the voltage drop through the liquid metal and through the end of the electrode material from the total voltage drop, then dividing by the current. The drop through the gallium was corrected for the amount of gallium in the gap. The resistance of the nickel plating was also accounted for.

Correction for the gap dimensions was also applied for the 44°C thermal chamber since it did not operate at the temperature for which the gaps were set. The resistance of the short length of electrode between the voltage tap and the liquid metal was corrected for the actual temperature based on published resistivity data.

The resulting interface resistance is for two interfaces, each of which has an area of approximately 1 cm^2. This value is subject to many errors, particularly for the stainless steel electrodes because of the high resistivity of stainless steel. The "worst case" figures in Table 13 exclude the values calculated for 1 amp, because of their reduced accuracy, but the one amp data is included in the averages.

The interface resistances calculated for the four nickel-plated copper electrode samples which were tested with pure gallium at 20 A are 0.45, 0.50, -0.32 and -0.06 microhm. This is the most accurate data of the test because of the high current and the low resistance of the copper electrodes. The average of these is 0.14 microhm. Since this is two resistances in series, the contact resistance for gallium on nickel is found to be 0.07 $\mu\Omega$ cm^2. This extremely low figure is considered one of the important findings of the project. The equivalent figure for each electrode material is in Table 14.

TABLE 14. Interface Resistance, Gallium to Candidate Electrode Materials (Calculated from data at 20A)

	$\mu\Omega$ cm^2	
	Mean Mean	Standard Deviation
Liquid Gallium to Beryllium:	1.06	0.70
Liquid Gallium to Beryllium-Copper:	0.78	0.59
Liquid Gallium to Nickel:	0.07	0.20
Liquid Gallium to Stainless Steel:	1.80	2.17
Liquid Gallium to Tungsten:	0.82	0.51

In Tables 8 through 12 there is apparent correlation of interface resistance with temperature. Much of this correlation may be due to uncertainties in the gap geometry and the material resistivities which were used in data reduction. The temperature coefficient of expansion of the polyacetal spacer of the MEF causes an error in the gap of approximately 0.2 percent per degree Kelvin. Though this seems small, it must be remembered that the interface resistance is the difference between two larger numbers, and is therefore very sensitive to errors in those numbers. The data at 84°C is considered more accurate than that at 43°C because the correction for the setting of the gaps is much smaller.

The apparent correlation of interface resistance with current is primarily due to the increased accuracy at the higher currents. Note that in the majority of cases the voltage drop reduced a few microvolts during the test. This is believed to be due to improvement in instrumentation.

There is a definite correlation between interface resistance and surface finish on the stainless steel MEFs. The correlation is also apparent for the beryllium-copper. Clearly a "fine" finish, better than 32 microinch rms, is superior, even when wetting in a pool of liquid gallium, although visual examination indicated nearly 100 percent wetting.

The most obvious correlation of input parameters with interface resistance is in the case of the gallium-indium-tin alloy in contact with

beryllium and stainless steel, where the result was dramatic increase in resistance during the 30-day screening test.

Electrical Noise

Electrical noise was so low as to be unmeasurable across the very low impedance gaps of the MEFs. The photographs shown in Figures 16 and 17 were taken on 20 November 1969. Unless otherwise noted the vertical scale factor is one millivolt per centimeter and the horizontal scale factor is five milliseconds per centimeter. The shutter was open for 0.10 s. The major grid lines are one centimeter apart on the oscilloscope. The photographs were taken with the cables removed from the digital data recording system so as to minimize noise pickup, except for Figures 17(f) and 17(g) which used the preamp with a gain of 10 and the oscilloscope with a vertical scale factor of 0.5 v/cm. The lower trace in each photograph is a zero input with the leads shorted.

In Figure 16 it will be noted that the spacing between the paired traces is the voltage across the gap, with some allowance for drift in vertical position. For Figure 16(a) the spacing represents 115 millivolts for beryllium at 20 amps while for Figure 16(i) the spacing represents 513 microvolts for a rough finish stainless steel MEF at 20 amps. No noise was seen at any sweep rate except for the slight ripple seen also on the lower trace which is characteristic of the oscilloscope at this high gain setting.

Each pair of traces is simply an attenuated version of the current waveform from the power supply which is seen in Figure 17(f) for the 20A circuit, and in (g) for the 10A circuit. Figure 17(h) is the solid copper electrode. Here the traces lie superimposed because the drop from voltage tap to voltage tap is only 5 microvolts.

The electrical noise is thus clearly seen to be less than 100 microvolts peak to peak and is probably less than 10 microvolts peak to peak for each MEF. This was also true of MEF 41, the beryllium sample which radically changed resistance, when it was examined with the shunt removed at the conclusion of the screening test. Any changes were too slow to be seen on the oscilloscope.

The very low electrical noise is not surprising in view of the very low interface resistances measured and considering that this was a static test with no relative motion of the electrodes.

Melting Point of Gallium

The first measurement made upon disassembly of an MEF was the freezing and melting points of the gallium. No significant change was found from pure gallium for any of the MEFs for which a reading could be obtained. The spread in the data in Tables 8 through 12 is primarily due to uncertainties in instrumentation and the small size of the sample. The figure listed is the average of the freezing and melting temperatures.

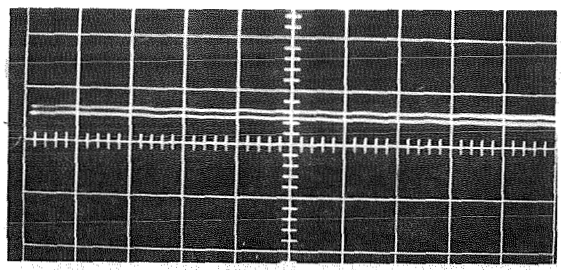

(a) MEF No. 1, Beryllium, fine

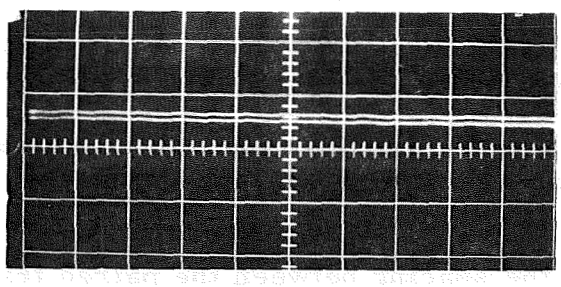

(b) MEF No. 2, Beryllium-copper, fine

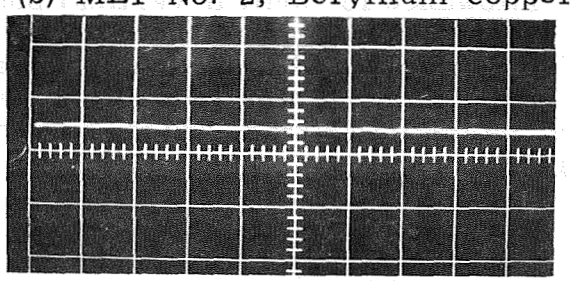

(c) MEF No. 3, Nickel on copper, fine

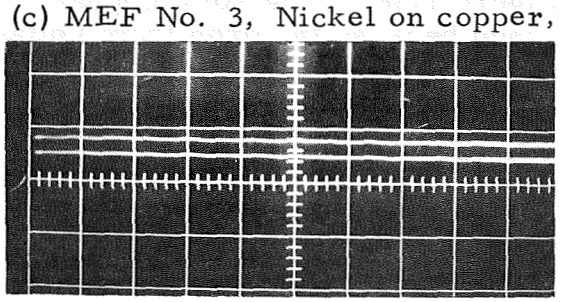

(d) MEF No. 4, Stainless steel, fine

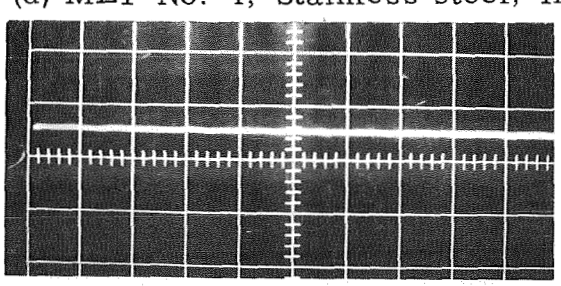

(e) MEF No. 5, Tungsten, fine

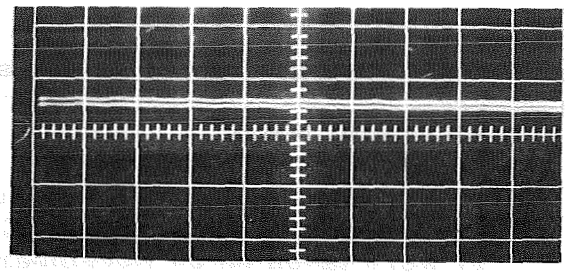

(f) MEF No. 6, Beryllium, fine

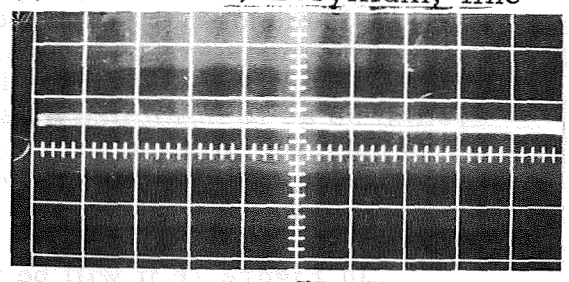

g) MEF No. 7, Be-Cu, coarse

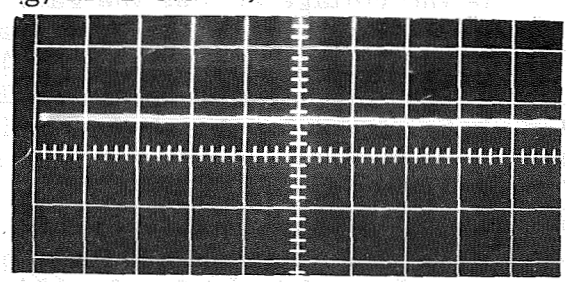

(h) MEF No. 8, Ni on Cu, coarse

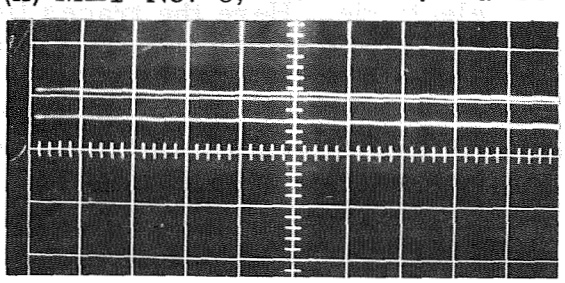

(i) MEF No. 9, SS, coarse

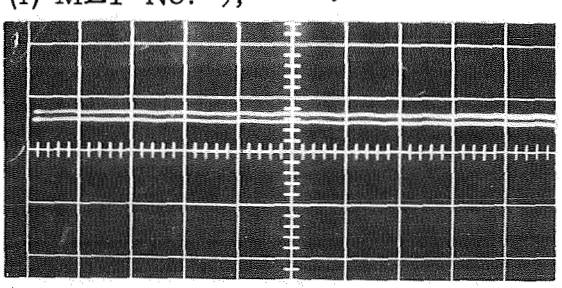

(j) MEF No. 10, Tungsten, coarse

FIGURE 16. Electrical Noise Photographs, 43°C Chamber, 20A.

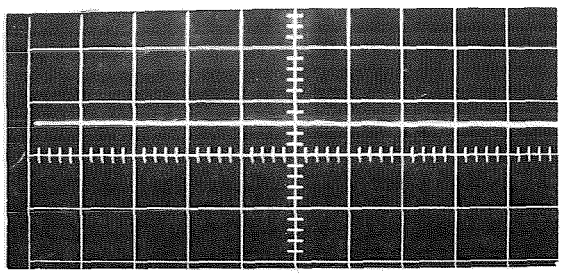

(a) MEF No. 21, Be, fine 84°C, 20A

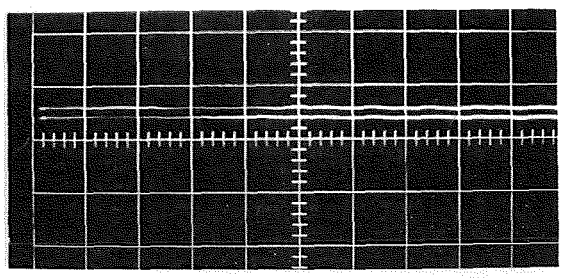

(b) MEF No. 22, Be-Cu, fine, 84°C, 20A

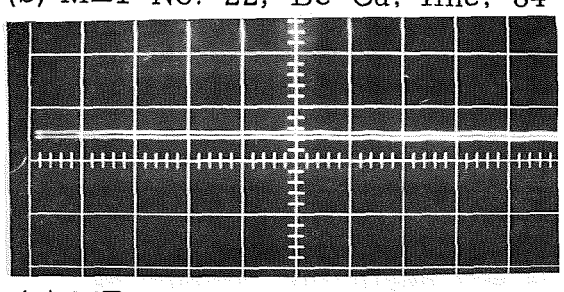

(c) MEF No. 23, Ni on Cu, fine, 84°C, 20A

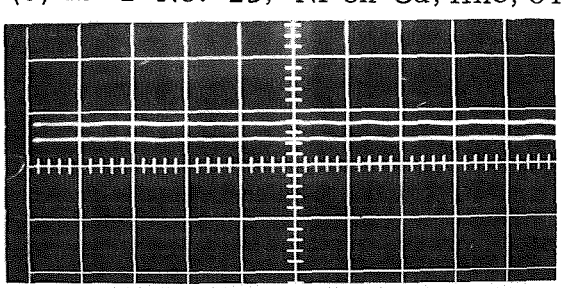

(d) MEF No. 24, SS, fine, 84°C, 20A

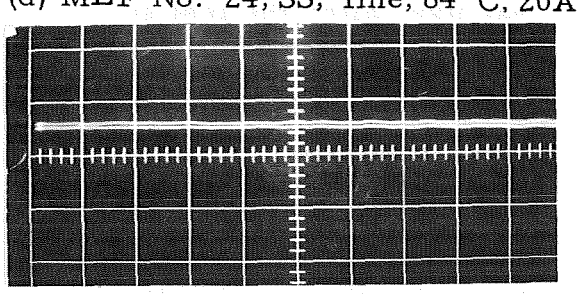

(e) MEF No. 25, W, fine, 84°C, 20A

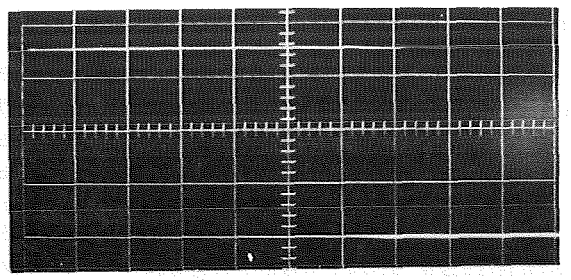

(f) Channel 46, 20.00A through a 0.010 ohm resistor.
Zero at -2.0 cm.
Vertical gain~50 mv/cm

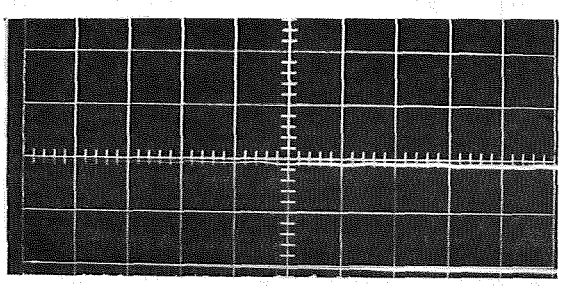

(g) Channel 47, 10.56A through a 0.010 ohm resistor.
Zero at -2.0 cm.
Vertical gain~50 mv/cm.

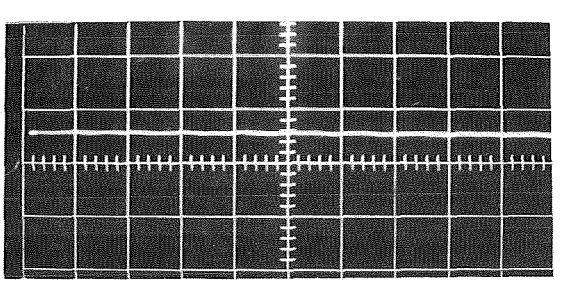

(h) Channel 50, "Zero Noise Electrode"

FIGURE 17. Electrical Noise Photographs, Screening Test

Surface Tension of Gallium

The surface tension measurements were all made at ambient temperature within the glove box in an argon atmosphere, approximately 35°C (308 K). There appears to be a trend towards lower surface tension in the 84°C samples than in those exposed at 43°C but there were no significant deviations from pure gallium and the total range of all gallium samples was only from 596 dynes/cm to 708 dynes/cm. Note that several of the stainless steel and tungsten samples can be considered pure gallium due to the absence of contaminants.

The surface tension of the gallium-indium-tin alloy samples varied only from 505 dynes/cm to 543 dynes/cm for the four samples which were large enough to be measured.

Gallium Retention

In Table 14, the figures for gallium contained are a good index to the ability of the electrode material to retain the gallium in the thin disc-shaped gap of the material evaluation fixtures (MEFs) with no edge preparation such as chamfers, barrier films or seals. The beryllium and the tungsten did poorly in this regard: the beryllium due to the growth of the non-wetting film during the time and handling between initial wetting and the beginning of the formal screening test exposure; the tungsten because of the poor initial wetting characteristics.

None of the 65 MEFs lost any gallium during the 30-day static exposure to elevated temperature and high current densities, and the change in appearance of the gallium in the gaps was negligible, amounting to a slight additional sag in some samples.

Electrode Weight Changes

The weight changes in Table 13 need some explanation. All electrodes were wetted by machining in a pool of liquid gallium, thus, it was necessary to wipe off the excess contaminated gallium in order to weigh the electrodes, then respread pure gallium over the desired conducting surface. If the wiping was too hard, the gallium would not respread after weighing, so some gallium residue remained. The same process of wiping, weighing and "rewetting" was used after the test so accuracy was reduced.

Beryllium and tungsten typically show loss of weight. This is believed to be due to two causes: First, both materials are sintered and may have lost moisture in the hot, dry argon atmosphere. Second, both materials became progressively less wet with gallium after each wiping, so there was less gallium residue during the post-test weighing.

The beryllium-copper grew tiny nodules under the liquid gallium. They grew larger at higher temperatures and higher currents and they became larger on the positive electrodes. This can be seen in Table 10. These nodules held the gallium during wiping and made the apparent weight

increase even larger. The nodules were noted in the initial photographs, taken 7 November 1969, 16 days after wetting. They grew much larger during the 30-day exposure and might eventually clog a slip ring.

The nickel-plated electrodes also have tiny nodules believed to be burrs thrown up during the machining under gallium. They did not change substantially during the screening test exposure, but they contributed strongly to the uncertainty in weighing. Also, some of the nickel electrodes were weighed by different people before and after the test. To check on this theory, the positive electrode of MEF 23 was reweighed post-test. This was a relatively smooth electrode and had been heavily wiped on 1 November 1969 to test its ability to "rewet" with gallium. A different person used a heavy wiping on 8 January 1970 and achieved the same weight to the nearest 0.0001 gram. This electrode was then rewet with no difficulty but some reluctance at the edges. MEF 23 filled to the edges when gapped and filled on 23 January 1970 for the long term evaluation test. The smooth negative electrode of MEF 53 was not singled out for heavy wiping and showed a weight gain of 3 milligrams.

The stainless steel electrodes were smooth and did not change except that they rewet somewhat better after the screening test. This may account for the slight increase in weight on the average. It is considered that the most meaningful weight loss or gain is that of the beryllium-copper electrodes, but it is accentuated by the gallium retained between the nodules.

After each electrode was weighed it was rewetted with pure gallium, reassembled in its MEF and retained in the argon atmosphere pending the results of material selection.

Spectrographic Analysis

The spectrographic analysis provided many suprises. The total contaminants in the gallium were much smaller than was expected. Evidently the gallium excludes most contaminants by pushing them to the surface film. Our samples were taken by probing to the inside of the drop with a fresh plastic tube for each sample.

The gallium-indium-tin alloy used in the 40-series MEFs had the following contamination in addition to the alloy constituents.

- o Silver 1.7 ppm (parts per million)
- o Lead 90 ppm
- o Bismuth 2.6 ppm

One case of contamination with solder was detected, Tungsten MEF 25, and several cases of contamination with the gallium-indium-tin alloy were noted, primarily in the beryllium electrodes whose gaps were set after the gapping of the 40 series MEFs, indicating that the alloy was carried by the glass shim despite cleaning after each use.

Copper contamination was widespread. This may be due to the copper trays in the thermal chambers or to the heated electrical wiring. The amount is small, however, typically less than one part per million.

The nickel-on-copper electrodes showed the most contamination, primarily nickel and copper. The worst case, MEF 18, had a total ot 0.0119 percent (119 ppm) nickel and copper in the gallium. This rate of contamination, if it continued linearly, would result in only 1.43 percent contaminants after 10 years.

Curiously, there was no nickel contamination found in the 80°C thermal chamber. Most likely the higher temperature caused the gallium to be more mobile and force the nickel to the surface. A sample of the gallium surface film from MEF 3 (exposed at 43°C) had 50 ppm copper and 120 ppm nickel contamination compared to 22 ppm copper and 22 ppm nickel in the liquid gallium.

Visual Inspection

Each electrode was carefully observed during wiping and rewetting before and after the screening test. Photographs were taken of the faces of representative electrodes of each material. The electrodes remained in the glove box and were photographed through the glass. The scale of Figures 18 through 23 is about 5 to 1. The electrodes are 0.484 inch (1.23 cm) diameter.

Figure 18(a) is of a beryllium electrode ready for weighing on 7 November 1969. This face of the electrode has been machined in a bath of liquid gallium and was wetted over its whole surface three days previously. It has been kept in an argon atmosphere with less than 0.1 percent oxygen during most of the intervening time. Just prior to this photograph the excess gallium was wiped away with a soft, clean, stretch nylon cloth. The discolored edge has no gallium adhering, the remainder appears to be 50 percent to 80 percent wetted. This electrode was fine machined, as were all beryllium electrodes.

Figure 18(b) shows the same electrode a few minutes later after the attempt to rewet with the gallium-indium-tin alloy by placing a drop on the surface and tapping as previously described. The appearance and wetting behavior of the eutectic alloy was almost identical to that of the pure gallium. Note that the gallium alloy is bridging much unwet area.

Figures 18(c) and (d) are equivalent to 18(a) and (b) respectively but taken on 20 January 1970 after the screening test exposure. Note in 18(d) that very little gallium will now adhere. This is the electrode that exhibited the rapid change in surface resistance and is the worst case in the experiment.

It was observed that the time and temperature of exposure of the beryllium electrodes, particularly with the gallium wiped off, made a

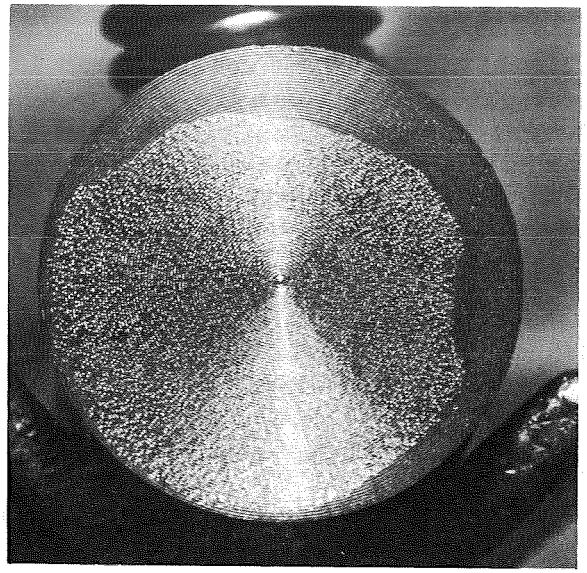

(a) Pre-test, wiped for weighing

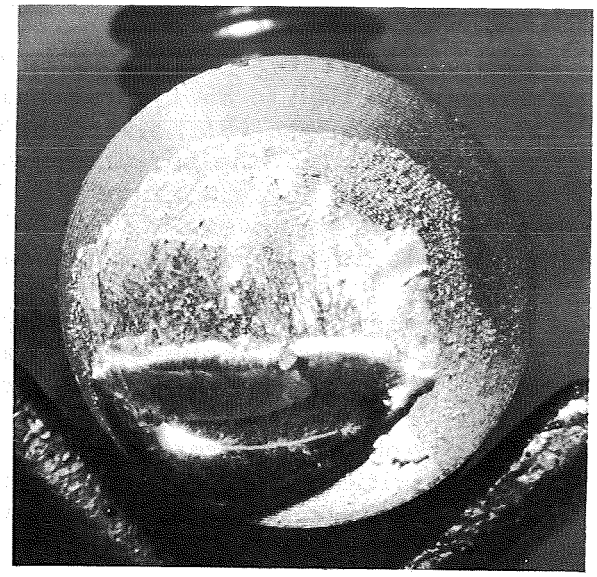

(b) Pre-test, rewetted

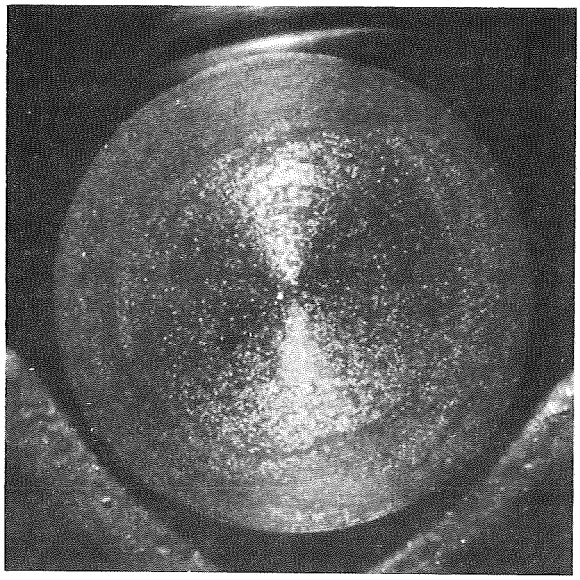

(c) Post-test, wiped for weighing

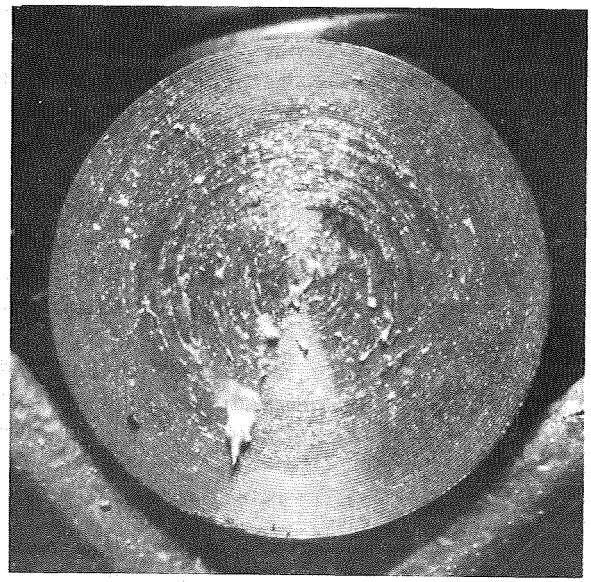

(d) Post-test, rewetted

FIGURE 18. Beryllium Electrode 41 Negative Before and After Screening Test

distinct difference in the wetting by the liquid metal. MEFs 41 through 45 had been heated to 85°C in preparation for gap setting when the pictures shown in Figures 18(a) and 18(b) were taken. Deterioration of the wetting characteristic of the beryllium was noticeable with each passing minute. MEFs 51 and 56 were among the last to have their gaps set. Note in Table 8 that they were able to hold the least gallium. The other electrode materials did not have this problem.

Figure 19 shows a beryllium-copper electrode, coarse machined, through the same sequence as the beryllium electrode of Figure 18. The photographs are typical of all beryllium-copper electrodes. Note in Figure 19 that some nodules are already forming. The lighting of the photographs in Figures 19(a) and 19(b) particularly accentuates any surface irregularities. The post-test views (c) and (d) show the crescent-shaped area where the liquid metal was drained from the surface by gravity during the screening test.

The liquid metal wetted all the beryllium-copper electrodes essentially to the edge of the machined face as is seen in Figures 19(b) and (d). The nodules had little effect on the wetting.

Figure 20 shows the characteristic burrs on the nickel surface which occurred during the machining under liquid gallium. The difference between Figure 20(b) pretest and 20(c) post-test is primarily in the lighting and the amount of gallium left on the surface. Figure 20(d) shows the positive electrode of MEF 23, one of two smooth nickel electrodes, after heavy wiping post-test. The weight of this electrode repeated to less than 0.0001 gram after 68 days of wetted exposure to liquid gallium including 30 days at 84°C and 20A. The only change was a deepening of the gray color of the wetted face.

The nickel was more difficult to wet than the beryllium-copper, but once wetted the gallium would cling tenaciously and rewetting after wiping was the most successful of all electrode materials.

Figure 21 shows the negative stainless steel electrode of MEF 44. The AISI 304 stainless steel electrodes would become almost shiny when wiped and were difficult to wet and keep wetted. Note the characteristic unwet edge. This edge was not permitted to exceed 0.020 inch (0.5 mm). Several stainless steel electrodes required remachining to meet this requirement.

In Figure 21(b) an unwet area may be seen near the center. This may have been the cause of the 33 percent increase in resistance of MEF 44 during the screening test, when it was filled with the gallium-indium-tin alloy. This area was looked for but not found post-test, as seen in Figure 21(c). Note in 21(c) the slight difference in the tone of the unwet edge. The stainless steel electrodes rewet more easily after the screening test exposure than before.

In Figure 21(d) an orthorhombic gallium crystal can be seen forming, characteristically from the center of bulk of the gallium. Often such a crystal

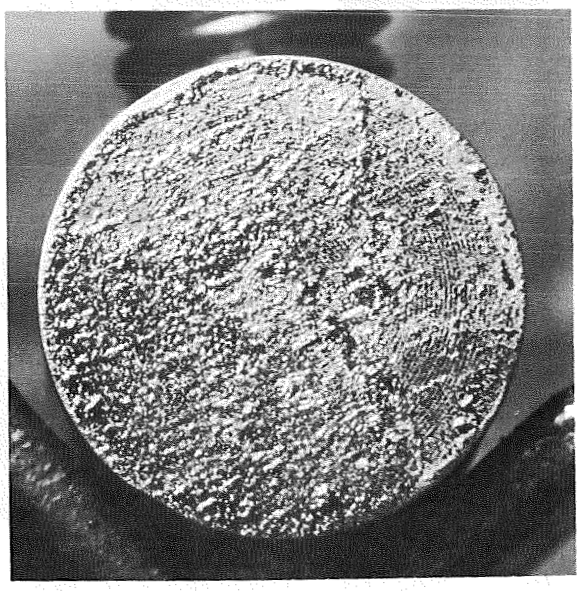

(a) Pre-test, wiped for weighing

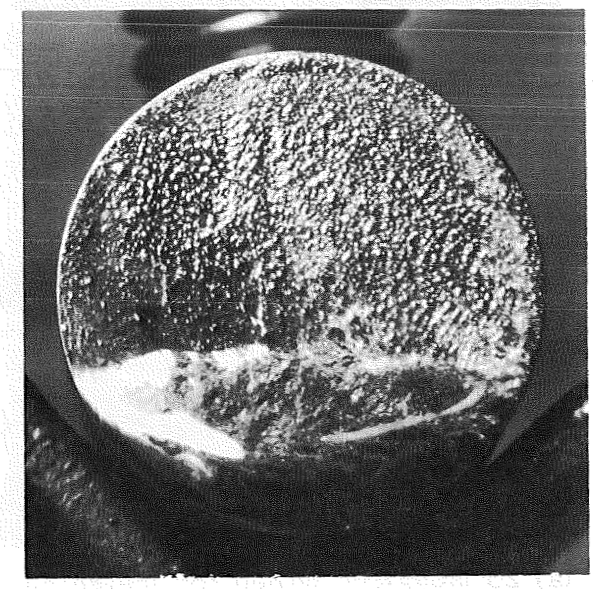

(b) Pre-test, rewetted

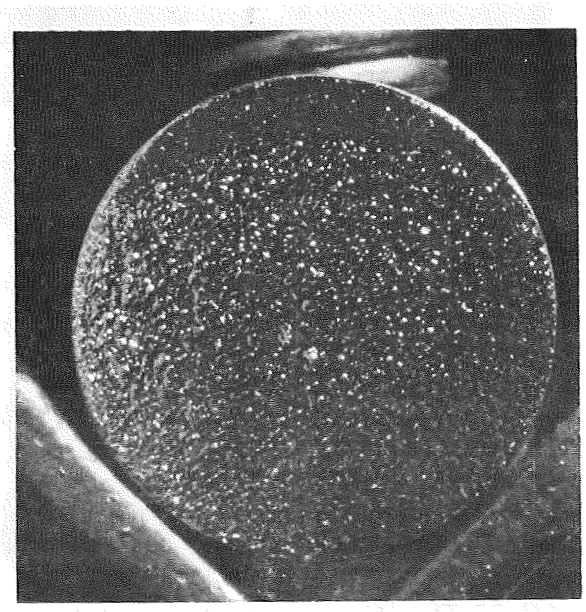

(c) Post-test, wiped for weighing

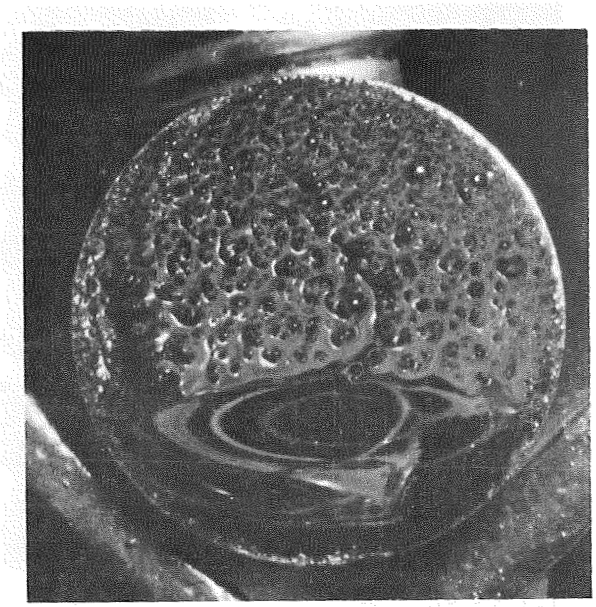

(d) Post-test, rewetted

FIGURE 19. Beryllium-Copper Electrode Before and After Screening Test

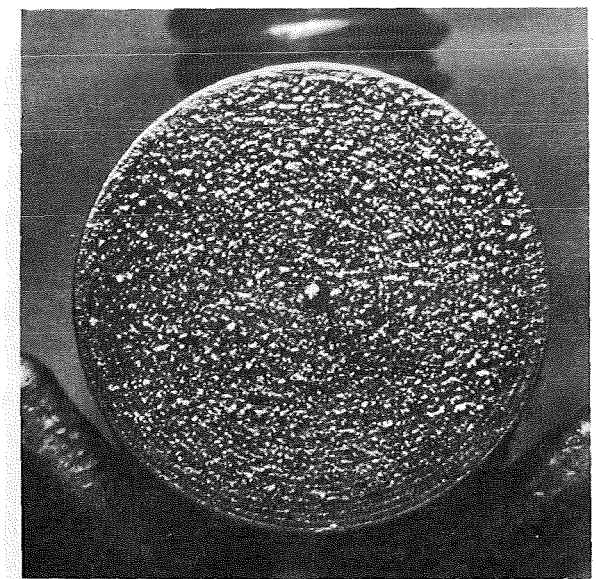

(a) 23 Negative wiped for weighing pre-test

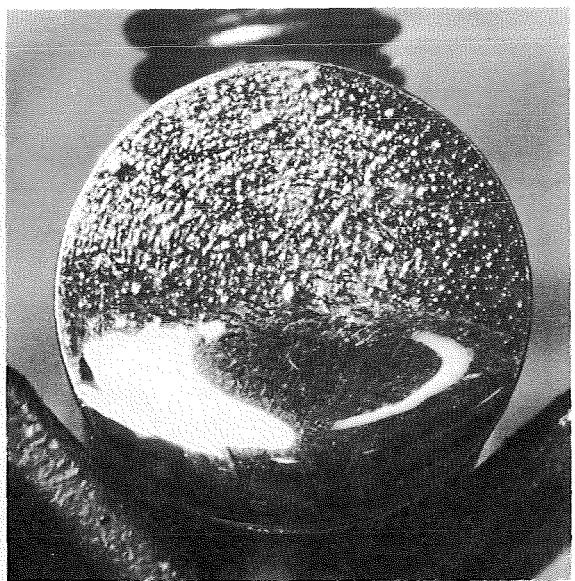

(b) 23 Negative rewetted pre-test

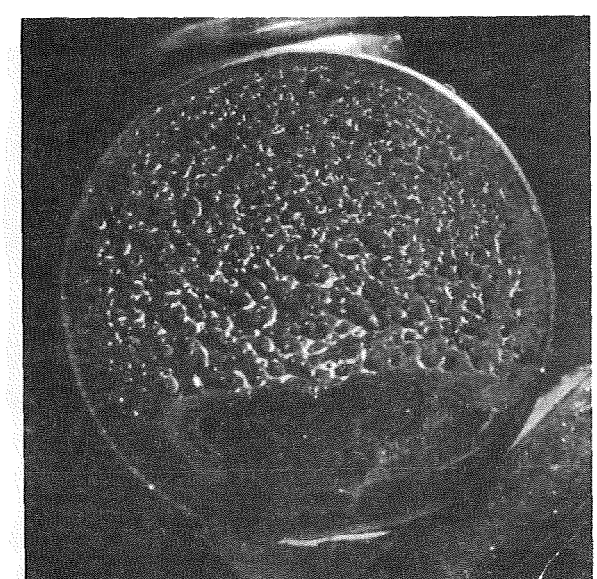

(c) 23 Negative rewetted post-test

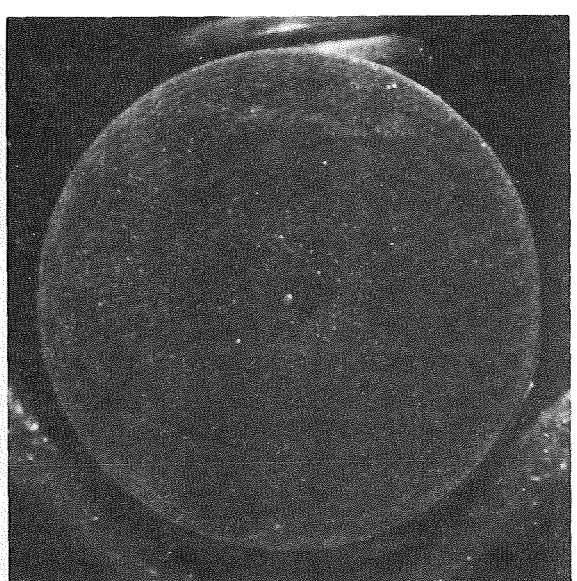

(d) 23 Positive wiped for weighing post-test

FIGURE 20. Nickel-Plated Copper Electrode Before and After Screening Test

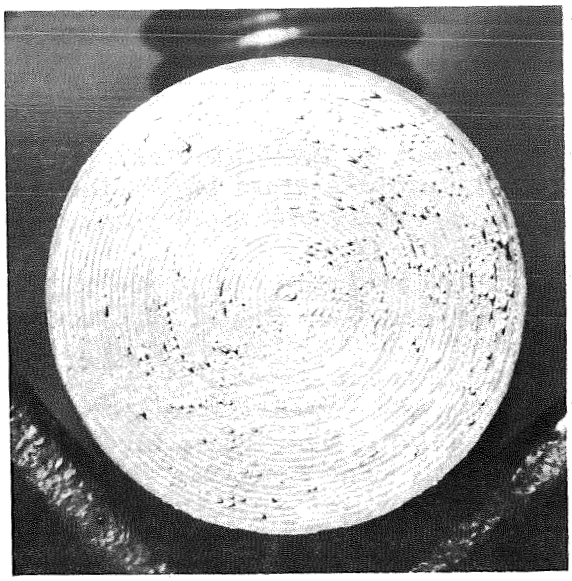

(a) Wiped for weighing, pre-test

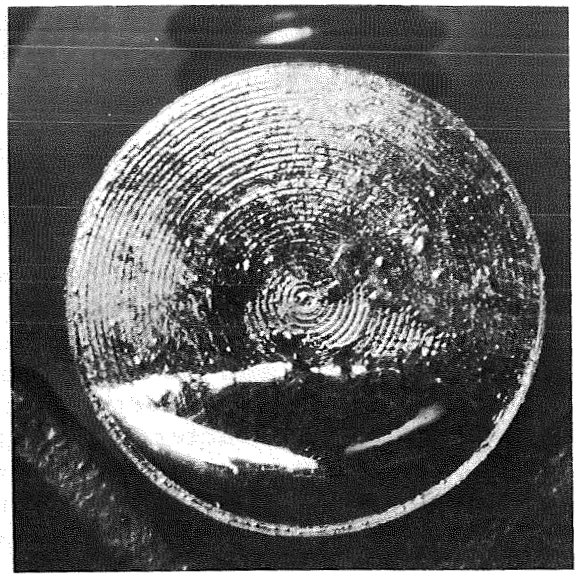

(b) Rewetted, pre-test, gallium-indium-tin alloy

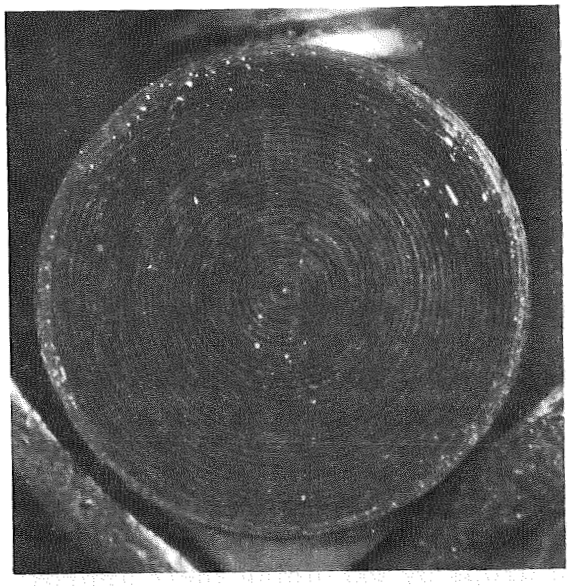

(c) Wiped for weighing, post-test

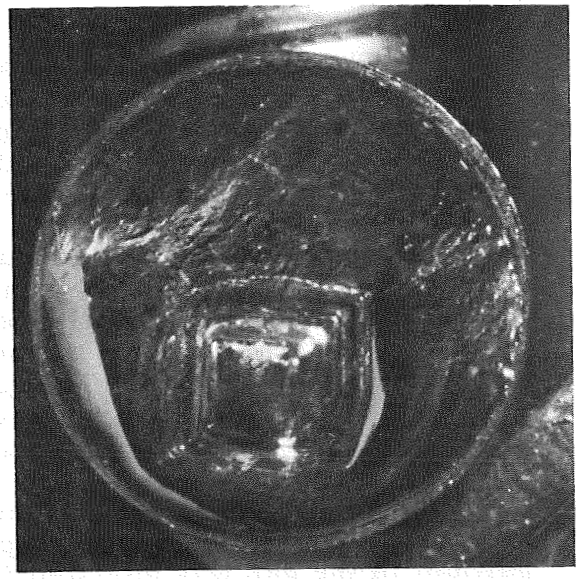

(d) Rewetted with pure gallium post-test. Note crystal forming.

FIGURE 21. Stainless Steel Electrode Before and After Screening Test

would be found in a glass container surrounded by supercooled gallium but not growing, presumably because its corners had touched the boundary of the liquid metal.

Note the shiny appearance of the gallium on the stainless steel compared to the other electrode materials. Stainless steel shows the least contamination of the gallium of all the candidate electrode materials.

In Figure 22 will be seen coarse finish tungsten electrode 45 negative. Figure 22(b) shows a drop of gallium-indium-tin alloy placed on the surface from a polyethylene eyedropper. The electrode face is nearly vertical and the liquid metal has drained from a small area leaving the area curiously reflective but demonstrating the approximately 0.25 rad contact angle characteristic of gallium on tungsten. The liquid metal was then spread by tapping the MEF on a nylon anvil. The result is shown in Figure 22(c). Note the appearance of the surface film. The lighting for Figures 22(a), (b) and (c) was identical.

Figure 22(d) shows the tungsten electrode after wiping, weighing and rewetting post-test. Additional non-wetted areas are apparent and there may be a great deal of bridging of unwet areas by the gallium.

Tungsten was second only to beryllium in difficult in wetting. In one instance, MEF 55, the resistance measurements indicated that an electrode was not properly wet. The condition found post-test is shown in Figure 23.

The appearance of the surface of the liquid metal in the gaps between the electrodes of completed MEFs was smooth and shiny and generally concave top and bottom for the nickel-plated copper and the stainless steel in the 80°C chamber. There was some sag in the 30°C chamber. The expansion of the gap during the rise in temperature appeared to center the gallium. The beryllium-copper displayed more sag, and the surface of the gallium was dull, even copper-tinted. The copper color may have been due to reflection of the shiny cylindrical sides of the electrodes off of the cover glasses of the thermal chambers. The gallium in the beryllium electrodes was typically grey and wrinkled and uneven. The gallium surface in the gaps of the tungsten electrodes was wrinkled and uneven where wetting was poor but in some places was smooth and taut and shiny.

Pendant drops of gallium were noted on a few MEFs, but none fell during the screening test exposure. The calculated resistance of the gallium in the gap was adjusted for such drops by excluding their approximate volume. These drops formed mostly during the handling necessary to attach the voltage and current taps and arrange the MEFs on the racks in the thermal chambers. It was noted that after such a drop had been formed for a few days, the MEF could be inverted and the liquid metal drained out of the drop, leaving a wrinkled empty sack. The excess liquid metal would be

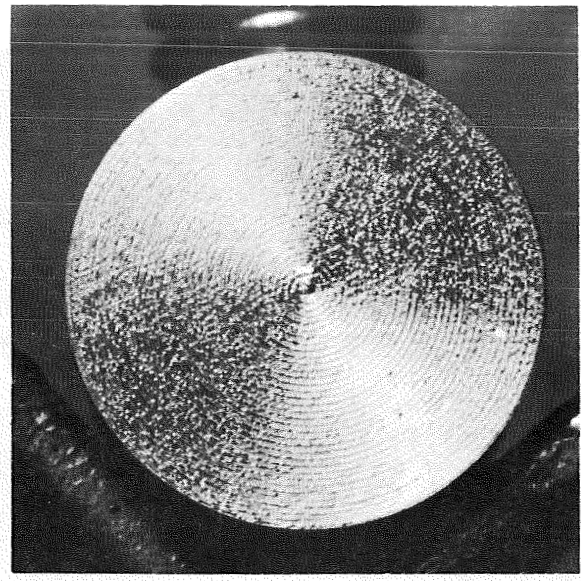

(a) Wiped for weighing, pre-test

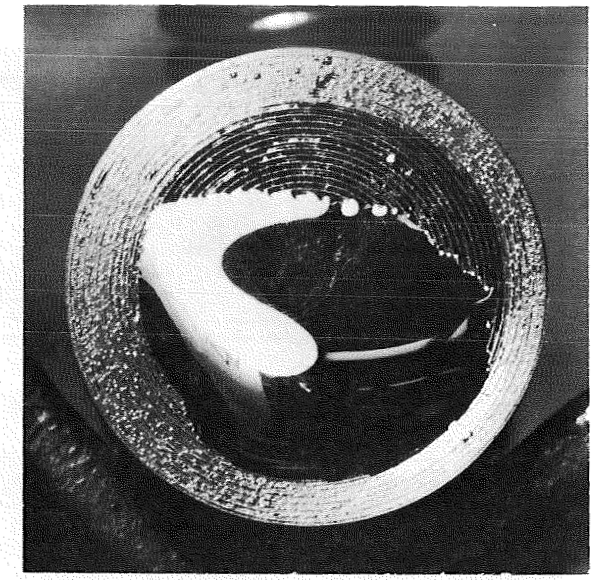

(b) Drop of liquid metal applied

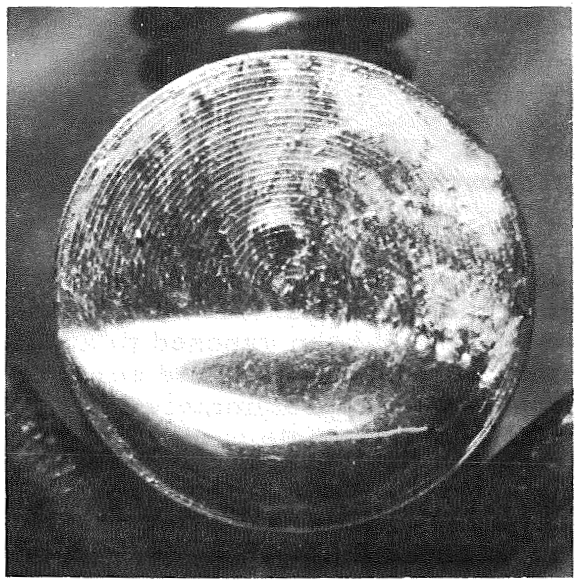

(c) Drop of liquid metal spread. Note surface film.

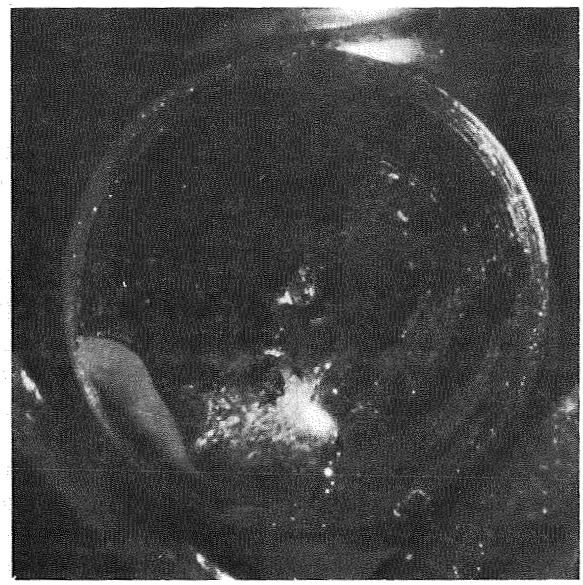

(d) Rewetted, post-test

FIGURE 22. Tungsten Electrode Before and After Screening Test

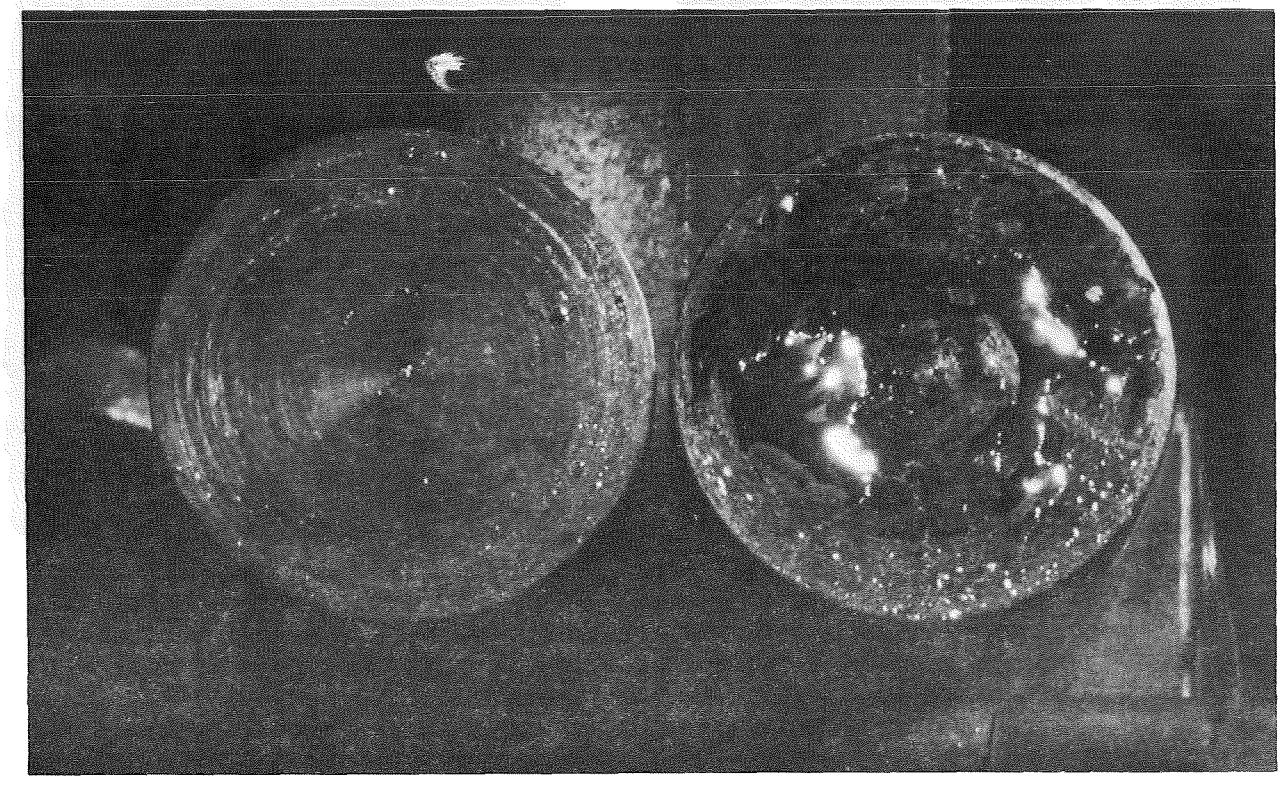

FIGURE 23. Electrodes of MEF 55 After the Screening Test

accommodated around the periphery of the gap. When the MEF was righted the gallium would flow back in, and the sack would become smooth, taut, and shiny again.

Contact angles of the gallium on the electrode materials were very dependent on previous history. The gallium did not wet any of the materials when placed for a short time on a surface which had been exposed to atmosphere. The contact angle on a freshly wetted surface approached zero for each material except the tungsten, for which it was approximately 15 degrees (0.25 radian). After wiping, the "advancing" contact angle during spreading might exceed 90 degrees ($\pi/2$ radian) on the beryllium, tungsten and stainless steel and up to 30 degrees (0.5 radian) on the beryllium-copper and nickel. A wetted beryllium or beryllium-copper surface drained by gravity would become a deeper gray and after a few days would not rewet without mechanical abrasion.

The boundary of a wetted area can sustain any contact angle from π radians to zero. In the case of the tungsten a slight shock will cause a "receding" contact angle which approaches zero to increase to 0.25 radian on a wetted surface.

The difference between a wetted and a non-wetted surface on the tungsten was not apparent to the naked eye. Each of the other materials became gray when wetted. Even the stainless steel became slightly gray after a long period as can be seen in Figure 21(c) by contrasting the unwetted edge to the central area.

Insulator Material Samples

The insulator samples are seen in Figure 24 subsequent to the screening test exposure for 30 days at 84°C. The row on edge has been allowed to retain the largest drop of gallium it can hold. The lower row has been tapped to remove all but tightly-adhered gallium. Remember that there had been no attempt to wet the virgin surfaces of the insulator. Only the 0.6 gram weight of the sample caused the contact.

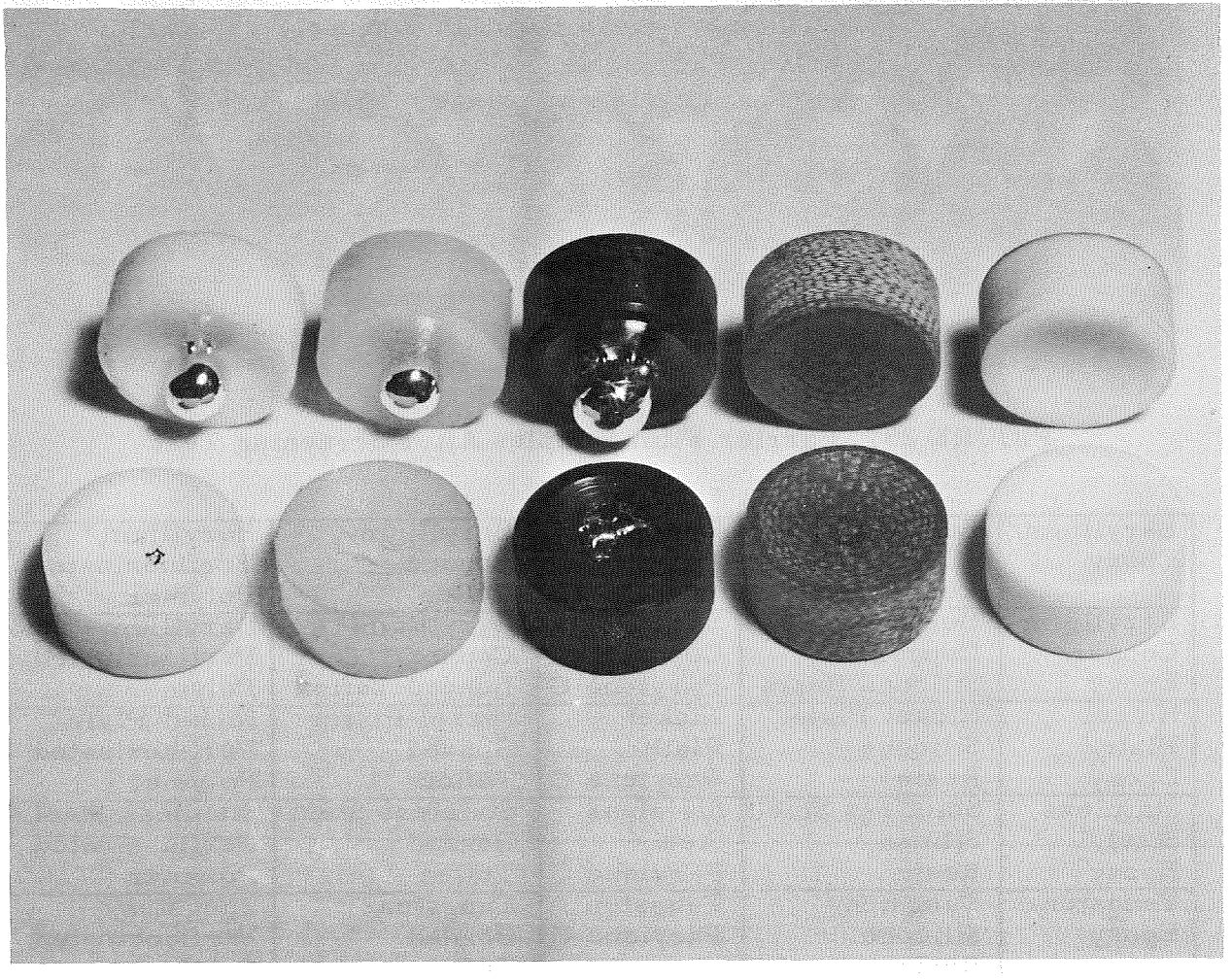

FIGURE 24. Insulator Samples After Screening Test

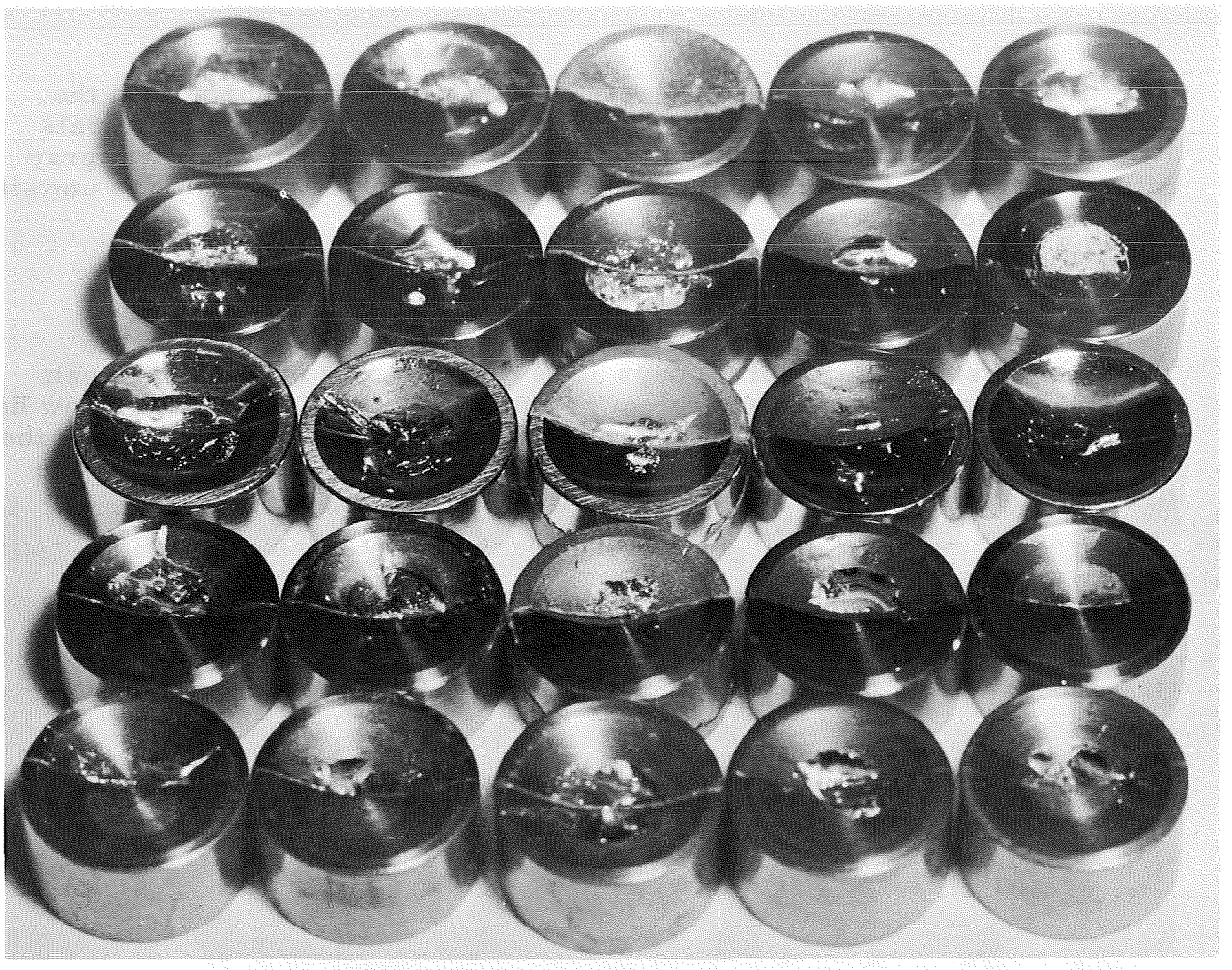

FIGURE 25. Barrier Film Samples After Screening Test

Beryllium/ Epoxy	Beryllium/ Silicone Resin	Beryllium/ Parylene C	Beryllium/ Bonded Teflon	Beryllium/ Perfluorinated Polymer
Beryllium-Copper/ Epoxy	Beryllium-Copper/ Silicone Resin	Beryllium-Copper/ Parylene C	Beryllium-Copper/ Bonded Teflon	Beryllium-Copper/ Perfluorinated Polymer
Nickel Plate/ Epoxy	Nickel Plate/ Silicone Resin	Nickel Plate/ Parylene C	Nickel Plate/ Bonded Teflon	Nickel Plate/ Perfluorinated Polymer
Stainless Steel/ Epoxy	Stainless Steel/ Silicon Resin	Stainless Steel/ Parylene C	Stainless Steel/ Bonded Teflon	Stainless Steel/ Perfluorinated Polymer
Tungsten/ Epoxy	Tungsten/ Silicone Resin	Tungsten/ Parylene C	Tungsten/ Bonded Teflon	Tungsten/ Perfluorinated Polymer

FIGURE 26. Location of Barrier Film-Electrode Material Samples in Figure 25

From left to right:

Teflon. The teflon was wetted in several small spots on both samples. The contact angle between these spots approached π radians.

Polyethylene. The gallium adheres to the polyethylene with a contact angle of from $\pi/2$ to π radians. A gallium drop of 0.03 cm^3 was suspended from an inverted sample. With slight tapping the gallium rolls off leaving the slight residue seen in the lower row.

Polyimide. The gallium adhered to both samples with about 25 percent of the contacting area becoming wetted.

Epoxy-Glass Laminate. The gallium did not adhere at all to this material although it did leave behind a slight greyish residue. The drops of gallium were so mobile in the spherical depression that one was inadvertently lost over the side during handling.

Alumina Ceramic. The gallium did not adhere at all to this material and the greyish residue was less than for any of the insulators tested.

The gallium was readily removed from all insulator samples by wiping with a cloth wetted with alcohol and there was no apparent trace of chemical attack.

Barrier Film Samples

The barrier film samples are shown in Figure 25 after they were tapped to remove all gallium that was not tightly adhered. The uncoated electrode material is in the foreground of each sample. Figure 26 can be used to locate the samples in Figure 25.

All 25 of the barrier film-electrode material combinations showed wetting or gallium residue on the barrier film. For the nickel-plated copper substrate material the least wetting of the barrier film occurred with the Braycote perfluorinated polymer, followed by the bonded teflon coating, although the bare nickel surface under the gallium was wetted to about the same extent. The bare stainless steel was almost free of gallium, but each barrier film was wetted except the perfluorinated polymer, to which the gallium adhered and left a thin residue. It is clear that the natural oxide film on the electrode materials is a better barrier film than any of the applied films insofar as resistance to wetting by gallium is concerned.

None of the barrier films was damaged by the gallium. The Parylene C coating failed to adhere to the bowl of the stainless steel sample. The Parylene C became markedly "frosted" on the beryllium sample. The gallium wetted and corroded the beryllium-copper/Parylene C sample on the bare metal. The beryllium-copper samples which had been heated to cure the coating resisted wetting by the gallium.

Selection of Materials

The conclusion of the screening test permitted selection of materials for the Long-Term Evaluation Test and for the Engineering Test Model Liquid Metal Slip Ring Assembly (ETM) which was then well advanced in design.

Electrode Materials

Table 15 compares the measured results with the criteria set forth on page 30 of this report. The nickel-plated copper was the only material to meet the contact angle criteria after a period of draining of the gallium by gravity. All materials failed to meet the weight change criteria because of the difficulties in removing the gallium without destroying the wetted characteristic. The beryllium and stainless steel failed to meet the criteria for stability of electrical resistance but tungsten passed despite one high resistance sample which did not change.

Table 16 was an attempt to provide an objective rating on the overall performance of the electrode materials. The ratings under each evaluation factor are simply stepped in order of performance. The workability factor is based on ease of wetting, wetting only where needed, and remaining wet despite heavy wiping. The visual appearance rating is based on apparent degradation in surface finish or wetting properties after the screening test. The cost ratings are approximations. All other ratings are based on the numerical data.

The following conclusions were reached based on the results of the screening test:

o Beryllium was considered eliminated from consideration due to the difficulty of obtaining and maintaining a wetted surface.

o Beryllium-copper was also considered unsuitable due to the observed growth of nodules on the wetted electrode surface, despite its second place numerical rating.

o Tungsten may be usable but it is difficult to work with. It is an improvement on the AISI 304 stainless steel only in better conductivity. The only failure (except for the unreliable weight loss or gain measurement) could have been caught and corrected by early measurement of contact resistance. See MEF 55 in Table 12.

o Stainless steel, AISI 304, was the best performer from the standpoint of degradation. It stayed clean and actually improved in wetting characteristics after the long exposure to gallium. Its high resistivity added uncertainty to calculations of contact (interface) resistance. Its one failure (other than weight loss or gain, in which it was the best performer) was a

gradually increasing contact resistance in MEF 44. This was using the gallium-indium-tin low melting point alloy. The cause of failure was not uncovered during post-test examination and both electrodes respread with gallium 100 percent after wiping for weighing and wiping for photographs.

o The best overall performer in the screening test was the nickel-plated copper. There was some concern over the amount of nickel and copper contaminants found, but the nickel was believed to be spurious and due to the tiny machining burrs observed. The copper may have dissolved into the gallium through cracks in the nickel due to the machining. It was thought that both of these concerns might be alleviated by eliminating machining of the nickel plating, which is possible because of the excellent wetting characteristics of the nickel.

It was, therefore, proposed that nickel-plated copper slip rings be used in the Engineering Test Model Liquid Metal Slip Ring Assembly (ETM). The nickel-plated copper was expected to be the least expensive to fabricate and to yield the best performance. More useful data would be compiled than if second place stainless steel was also used, because the high resistivity of the stainless steel masks the electrical performance of the gallium and the interface resistance.

The nickel-plated copper and the AISI 304 stainless steel were chosen for the Long Term Evaluation Test.

The gallium-indium-tin alloy was rejected for the Long Term Evaluation Test due to its poor performance in the screening test. Pure gallium was used in the samples slated for the alloy.

The type G-10 epoxy-glass laminate was confirmed for the ETM. The alumina ceramic was not used in the ETM because of its high cost but the epoxy-glass and alumina ceramic samples were chosen for the Long Term Evaluation Test.

For the ETM the perfluorinated polymer was chosen as film B and the bare, unwet nickel surface was used as film A. For the Long Term Evaluation Test the following four barrier film-electrode material combinations were used.

Part No. (See Figure 8)	Sample Material	Barrier Film
SP 216716-3-1	Nickel-plated copper	Perfluorinated Polymer
SP 216716-3-2	Nickel-plated copper	Bonded Teflon
SP 216716-4-1	Stainless Steel 304	Perfluorinated Polymer
SP 216716-4-2	Stainless Steel 304	Bonded Teflon

TABLE 15. Screening Test Results vs Selection Criteria, Electrode Materials

Property	Criteria	Beryllium
a) Contact Angle	45° ($\pi/4$ rad)	
Typical (after wetting)		0° to 180°
Worst case (after wetting)		180°
b) Surface tension (645 dyne/cm for pure gallium)	< 30 % change	-2.5 % one sample
c) Melting point (29.65°C for pure gallium)	$\pm 5^{\circ}$C	$+0.2^{\circ}$C -0.1°C
Number of samples		7
d) Equivalent electrode weight loss or gain, inches	±0.0001	+.00038 -.00187
e) Electrical contact resistance	±20 % change (10 and 20 amps)	+16400 % -4.4 %
f) Electrical noise, peak to peak	< .001 Ω (10 and 20 amps)	< .00001 Ω
g) Visual appearance	No strong polarity or degradation effects.	Grey film forms which is non-wetting
h) Spectrographic analysis	2 % dissolved	0.0049 %

TABLE 15. (concluded)

Beryllium Copper	Nickel-Plated Copper	Stainless Steel	Tungsten
0° 120°	0° 30°	0° 180°	20° 180°
+8.1 % -3.9	+9.8 % -9.3	+9.2 % -7.9	+3.6 % -7.6
+0.25° C -0.1° C 7	+0.25° C -0.75° C 7	+0.4° C -0.75° C 8	+0.2° C -0.8° C 10
+.0035 -.00093	+.00081 -.00005	+.00015 -.00017	+.00003 -.00018
+5.1 % -5.3 %	0 % -3.9 %	+33.6 % -7.4 %	+ 3.8 % -13.6 %
< .00001 Ω	< .00001 Ω	< .00001 Ω	< .00001 Ω
Hard modules growing, more on positive electrodes. Rewet easily.	Little change, rewet easily	Very little change. Rewet more easily than initially.	No visual change. Became even more difficult to wet
0.0036 %	0.0119 %	0.00070 %	0.0016 %

TABLE 16. Rating of Electrode Materials

Evaluation Factor	Points	ELECTRODE MATERIAL				
		Beryllium	Beryllium-Copper	Nickel on Copper	Stainless Steel	Tungsten
1. Compatibility with Gallium						
A. Wetting						
Contact angle	5	1*	4*	5	3*	2*
Gallium retention	10	2	6	10	8	4
Workability	10	2	8	10	6	4
Subtotal	25	5	18	25	17	10
B. Degradation (corrosion)						
Surface tension	5	5	3	1	2	4
Melting point	5	5	4	3	1	2
Weight loss or gain	5	1*	2*	3*	5*	4*
Contact resistance	10	2*	8	10	4*	6
Visual appearance	10	4	2*	8	10	6
Spectrographic analysis	5	2	3	1	5	4
Subtotal	40	19	22	26	27	26
2. Material Properties						
A. Weight	10	10	6	4	8	2
B. Conductivity	10	6	4	10	2	8
Subtotal	20	16	10	14	10	10
3. Cost						
A. Material	5	1	5	3	4	2
B. Fabrication	5	1	5	4	3	2
C. Wetting	5	1	5	4	3	2
Subtotal	15	3	15	11	10	6
TOTAL	100	43	65	76	64	52

* Failed to meet original criteria.

Long-Term Evaluation Test

Test Samples

Ten material evaluation fixtures (MEFs) were used in the Long Term Evaluation Test. These MEFs had been used in the Screening Test and were regapped and refilled for the long term test on 23 January 1970. They were chosen per the list on Page 22 of this report except that pure gallium was used in place of the gallium-indium-tin alloy. Electrode materials were nickel-plated copper and stainless steel, chosen as described above.

The two samples each of epoxy-glass laminate and alumina ceramic insulator materials were cleaned, dried, weighed, a small amount of gallium added and weighed again.

The four barrier film samples as listed above were prepared by wetting the bare metal of the bowl with gallium, leaving a band of unwet metal about 0.05 inch (1.3 mm) wide adjacent to the barrier film. When the gallium drop was added it lay across barrier film, unwetted metal and wetted metal surfaces in sequence.

The barrier film and insulator samples are seen in Figure 27. The nickel-plated copper and the alumina ceramic are in the top row and the stainless steel and the epoxy-glass laminate are in the bottom row. The perfluorinated polymer barrier film is on both samples in the left column, with the next column being the bonded teflon. This arrangement is common to the following figures of these samples.

Note that a crystal is forming in the lower right sample of gallium.

Test Set-Up

The samples were placed in an ion-pumped vacuum chamber as shown in Figure 28. The MEFs were electrically connected to permit 20A continuous current through six MEFs and 10A for short intervals for measurements of resistance. All 10 MEFs were supplied with voltage taps as in the screening test.

A thermocouple was attached to one MEF for temperature measurement and light bulbs were again used as heaters. The heaters were placed below the copper trays.

It was necessary to expose the samples to atmosphere for a few hours to effect the move from the glove box to the vacuum chamber. Vacuum pump-down started on 27 January 1970 but on 30 January it was apparent that the desired 80°C (353K) would not be obtained. The vacuum was shut down by back-filling with dry nitrogen and the chamber opened to permit improved insulation, foil heat reflectors and two more heating lamps to be installed. Pumpdown was again begun the same day.

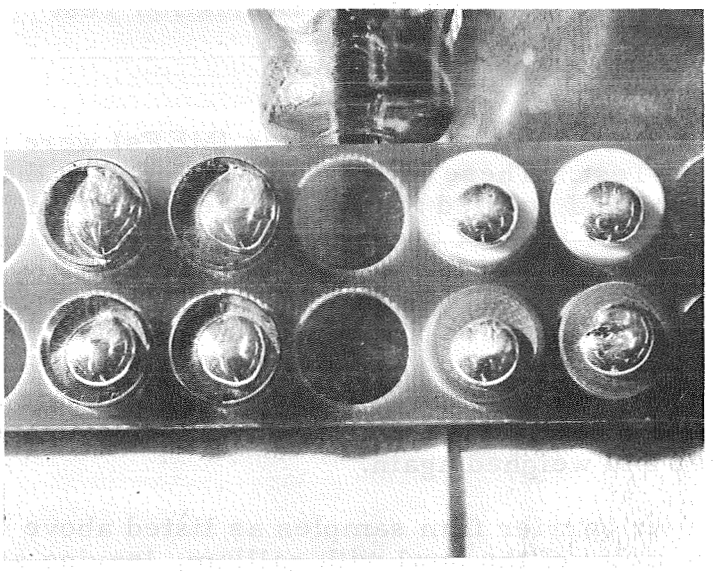

FIGURE 27. Barrier Film and Insulator Samples Before Long-Term Evaluation Test

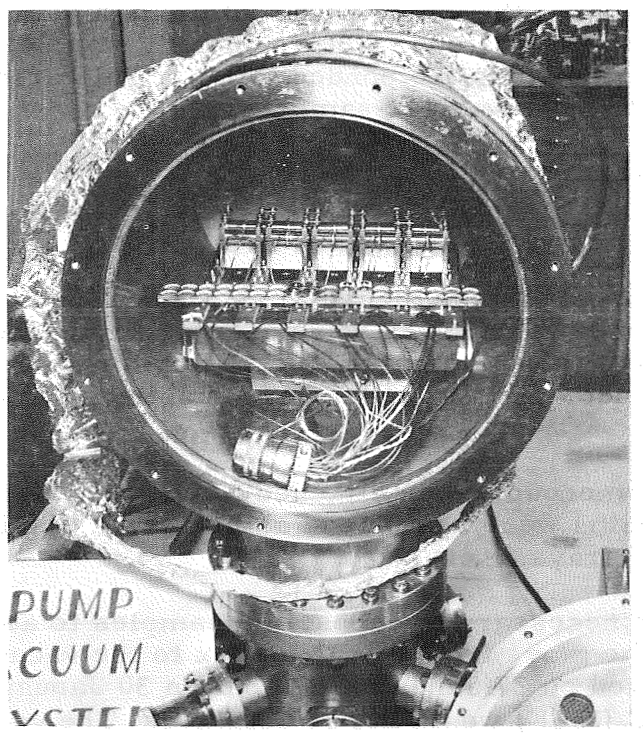

FIGURE 28. Samples in Vacuum Chamber for Long-Term Evaluation Test

On 31 January the 20 A current was again applied and the vacuum was 1.5×10^{-6} torr. On 4 February the chamber pressure was 1×10^{-6} torr and the MEF temperature had been adjusted to 81°C.

A viewing port in the top of the vacuum chamber, not visible in Figure 28, permitted visual monitoring of all samples.

The 10 A current was applied to the zero current samples for short periods to permit voltage drop measurements. Measurements of voltage drop were taken on each MEF every working day for three weeks, then reduced to once each week.

Gallium Retention

It was noted that the gallium remained near the top of the gap in all 10 MEFs during pumpdown but developed a wrinkled surface as sketched in Figure 29. The wrinkles were regular and were probably due to the removal of atmospheric pressure on the surface film of the gallium. The gallium surface remained concave.

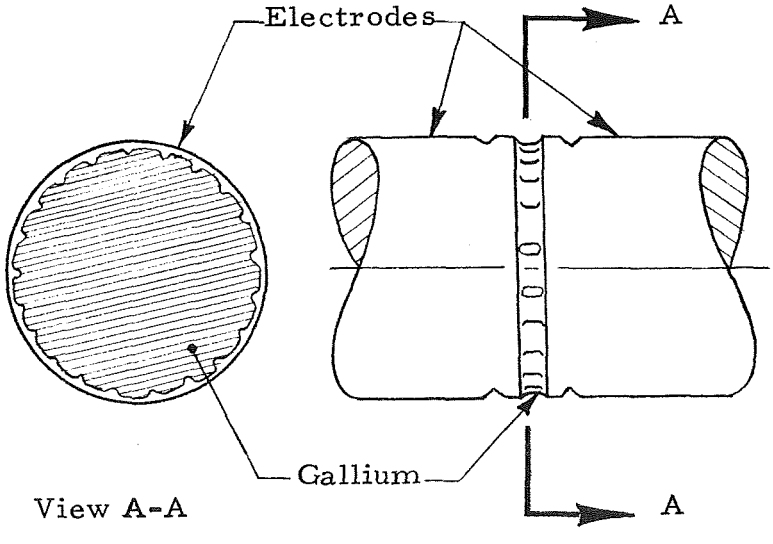

FIGURE 29. Gallium Wrinkles After Pumpdown

The samples were subjected to cooling and reheating twice during the month of April due to power outages. This caused the gaps in the MEFs to shrink noticeably then open up again. This flexing caused considerable smoothing of the wrinkles. The gallium surface in one nickel-plated copper MEF became quite smooth, similar to the screening test. The question arises whether the surface film on the gallium has partially evaporated or is it elastic enough to rearrange itself during the slow flexing at the gap?

Each of the MEFs retained all of its original fill of gallium despite cooloffs for installation in the vacuum chamber, the two cooloffs during the test and the cooloff after removal from the vacuum chamber. Pendant drops formed below most MEFs during the before and after cooloffs (where they could be observed) and presumably also in the vacuum chamber. The MEFs could be observed from above in the vacuum chamber and the gaps were noted to shrink to about 0.03 inch during cooldown, compared to 0.040 inch at 80°C. Subsequent heating and enlarging of the gap caused the pendant drops of gallium to pull back up into the gap against the force of gravity. All ten MEFs remained full to the top of the gap for the whole test and there were no drops in the overflow cups. This is in contrast to the sag which developed in many MEFs during the screening test.

Figure 30 shows the gallium in the gaps during the cooldown after removal from the vacuum chamber. The stainless steel electrodes are on the left. Note the bulging of the gallium.

Summary of Data

The long-term evaluation test was concluded on 15 May 1970. The samples had been in a high vacuum for 108 days and at rated current, temperature and vacuum for 100 days.

Electrical resistance data was quite constant during the test. Gallium-to-electrode interface resistances were found to be less than 0.4 microhm cm^2 for the nickel-plated copper and less than 4 microhm cm^2 for the stainless steel. True values for the nickel-plated copper are undoubtedly much smaller but are obscured by test uncertainties. The interface resistance for gallium to stainless steel is quite unpredictable and variable. One stainless steel MEF showed a tendency to increasing resistance, probably due to its exposure to a gallium-indium-tin alloy during the previous screening test.

All post-test data gathering was accomplished in the glove box, just as for the screening test.

Temperatures of melting and freezing for the gallium samples were not changed significantly by the exposure. Surface tension of the samples is approximately 5 percent higher than for pure unexposed gallium.

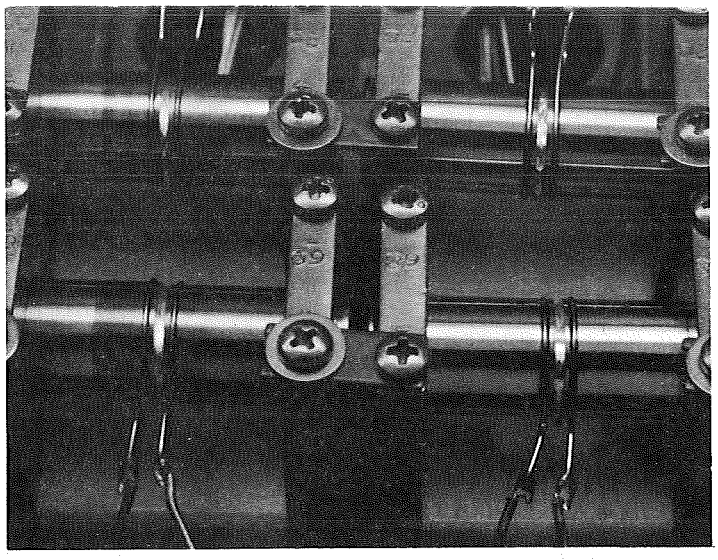

FIGURE 30. Stainless Steel and Nickel-Plated Copper Material Evaluation Fixtures after Long-Term Evaluation Test

MEF No.		MEF No.
44		43
63		29
64		28
68		24
69		23

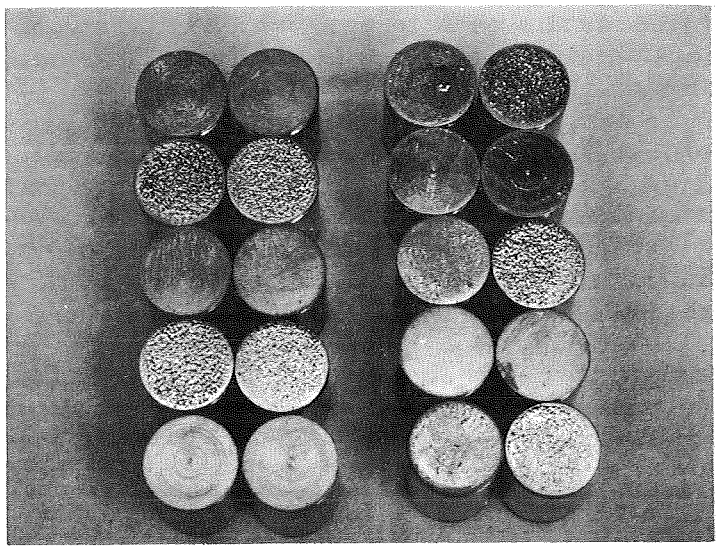

FIGURE 31. Stainless Steel and Nickel-Plated Copper Electrodes After Long-Term Evaluation Test

The alumina ceramic and epoxy-glass laminate insulator samples remain unwetted by the long exposure. The teflon and perfluorinated polymer (Braycoat) barrier film candidates were wetted by the gallium, as was a previously unwet nickel-plated surface. The only successful barrier film was a previously unwet surface of stainless steel.

The surface film on the gallium appeared slightly less bright after the vacuum exposure but there was no noticeable change in its behavior.

The major finding of the long-term evaluation test was that the nickel plating failed to provide adequate protection to the copper from the corrosive attack of the gallium. Small blisters were beginning to form on the surfaces of the positive nickel-plated copper electrodes which are exposed to gallium. No significant attack on the stainless steel electrodes was observed after almost seven months of continuous exposure to gallium.

Electrical Data

Table 17 is a compilation of results of data from the long-term evaluation test. A pressure of 1×10^{-6} torr and a temperature of 177.2°F (80.7°C) were reached on 4 February 1970. The test was terminated 100 days later on 15 May 1970. The average voltage drop in microvolts tabulated in Table 17 for each MEF was calculated from the voltage drop in the log for which the temperature of MEF 23 was between 175.8°F and 178.5°F and for those measurements for which the same instrumentation was used. The average temperature of MEF 23 for the times at which the data was taken was 176.9°F (80.5°C).

Mental averaging was used to discriminate against electrical noise of about 20 microvolts peak to peak which entered the digital voltmeter due to insufficient shielding of the voltage taps. This caused much of the spread in the data which is labeled "Max Δ" in Table 17.

A voltage tap to MEF 44 became open circuited after one month of testing, but up to this time its voltage drop had increased 10 percent in a relatively steady manner. MEFs 43 and 44 were filled with pure gallium during this test but had been filled with the gallium-indium-tin alloy during the screening test. It will be remembered that MEF 44 showed a ramp change in resistance during the screening test.

The cooling which occurred on 4 April and 20 April due to power interruptions appeared to cause some slight readjustments of voltage drops as well as smoothing the surface of the gallium in the gaps.

The interface resistance tabulated in Table 17 is calculated by subtracting the resistance predicted for the gallium and for the electrode material between the voltage taps. The wetted area on each electrode is 1.04 cm^2 so the resistance per unit area can be obtained by multiplying by 0.52. The uncertainties of the measurement are too high to permit this data to be meaningful beyond the establishment of an upper limit.

The true interface resistance is probably less than 0.1 microhm cm^2 on the nickel once it is properly wetted with gallium. The large variations in voltage drop from one stainless steel MEF to another makes it difficult to draw the same conclusion for the stainless steel, but the difficulty appears to be due to the high resistivity of the stainless steel and possibly some thermoelectric effects in the wiring and instrumentation. The voltage taps are nickel-plated.

Weight Changes and Appearance of Electrodes

The nickel-plated copper electrodes continued to gain weight. Perhaps the weight changes following the screening tests were not all due to differences in wiping techniques. The appearance of blisters in the positive electrode surfaces indicates that the gallium is attacking the copper substrate through openings in the nickel plate.

It should again be noted that the gallium-wetted surfaces of most of the nickel-plated copper electrodes are covered with tiny burrs which occurred during machining of the surface under a bath of liquid gallium. These burrs trap gallium and make it difficult to obtain repeatability of weighing.

Two trends are noted in the weight change data for the nickel-plated copper. First, the increase in weight for the positive electrodes is greater than for the negative electrodes. This corresponds to the appearance of blisters on the positive electrodes only. The screening test data indicated greater attack on the beryllium-copper on the positive electrodes. Second, the most significant weight changes occurred for the electrodes which carried currents only for short periods during measurement. This may be due to greater exposure of copper on these particular surfaces or simply due to difficulties in weighing on the rough surfaces.

The blisters were noted on the reasonably smooth surfaces of MEFs 23, 28 and 43 which did not show large weight gains compared to the negative electrodes. The weight change data is thus considered to have less significance than the visual examination and spectrographic analysis (see Figure 31).

The weight changes for the stainless steel are much smaller and appear to correspond mostly to the surface roughness. "Fine" means approximately 16 microinches rms and "rough" means approximately 64 microinches rms. The average weight change of 0.00027 gram is equivalent to a film of gallium 17 microinches (0.43 μm) thick.

Small areas that were not wetted with gallium were noted on the negative electrodes of MEFs 24 and 44 after the exposure. There was no visible evidence of corrosion.

Freezing and Melting Temperature

The freezing and melting temperatures of a small sample of gallium

TABLE 17. Long-Term Evaluation Test Data, Electrode Materials

MEF No.	Material	Surface Finish	Current (amps)	Microvolts Drop		Interface μΩ	Gallium (grams)
				Average	Max Δ		
23	Ni on Cu	fine	20.0	63.1	9	-0.10	.6260
28	Ni on Cu	rough	20.0	68.5	16	+0.17	.6351
43 (2)	Ni on Cu	rough	20.0	80.1	10	+0.75	.6194
63	Ni on Cu	fine	10.0 (1)	26.4	12	-0.62	.6390
68	Ni on Cu	rough	10.0 (1)	40.2	11	+0.76	.6297
24	SS 304	fine	20.0	256.0	10	-4.9	.6395
29	SS 304	rough	20.0	233.0	16	-6.0	.6243
44 (2)	SS 304	rough	20.0	186.4	29	-8.3	.6329
64	SS 304	fine	10.0 (1)	211.8	21	+3.5	.6290
69	SS 304	rough	10.0 (1)	172.0	8	-0.5	.6388

NOTES:

(1) 10.0 amp current used for measurement only. Current normally zero.

(2) MEFs 43 and 44 used Ga-In-Sn alloy during screening test; were filled with pure gallium for this test.

TABLE 17. (concluded)

Weight Change (grams)		Melting	Surface Tension	Contaminants		Appearance and Remarks
Positive Electrode	Negative Electrode	$\Delta^{o}C$	Δ %	Element	ppm	
+.0024	+.0064	-0.03	+5.5	Ag Cu Mg Ni	0.2 45 0.5 3	Small blisters on previously smooth positive electrode
+.0055	+.0040	-0.06	-0.8	Cu Mg Ni	52 0.3 3	Three blisters .03" dia. x .005 high on positive electrode.
+.0075	+.0065	-0.14	+5.5	Cu	91	Blister .04" dia. x .007 high on positive electrode.
+.0264	+.0191	+0.16	+5.4	Cu Mg	32 2	Both electrodes remain rough
+.0279	+.0111	0	+8.6	Cu	37	Both electrodes remain rough
-.0006	-.0014	-0.06	+7.0	Cu	0.2	Negative electrode has small dry spot.
+.0023	+.0011	-0.08	+5.5	-	-	No visible change.
+.0019	+.0019	0	+0.6	Ag Cu Mg	0.4 76 4	Negative electrode has small dry spot. Resistance steadily increasing.
-.0006	-.0009	+0.27	+4.8	Cu Mg	0.3 0.4	No visible change.
-.0012	+.0002	+0.50	+5.4	Cu	0.7	No visible change.

from each MEF was measured with a thermocouple as previously described. Several measurements were also made of pure, unexposed gallium. The differences between the exposed sample and the average for the pure gallium are given in Table 17. The differences are within the experimental error and are not considered to indicate significant change.

Surface Tension

The surface tension of the gallium in each MEF was measured as previously described. The changes compared to pure, unexposed gallium are given in Table 17. The samples show a typical increase of about 5 percent over the pure gallium. The change may be due to the elimination of dissolved gases after the long exposure to vacuum.

Spectroscopic Analysis

Each sample was tested for the elements to be found in the gallium using the Applied Research Model 2100 2-meter emission spectrograph. The contaminating elements found are listed in Tables 17 and 18 in parts per million.

The only significant contaminating element was copper. The slight amounts of magnesium and silver may have come from airborne dust during the transfer between the dry box and the vacuum chamber, during electrical connections in the vacuum chamber, and during transportation to the spectrograph. The copper is seen to be higher for the nickel-plated copper electrodes which had 20 amps current than for those with nominally zero current. Only traces of copper were found in the gallium from the stainless electrodes except MEF 44 with 76 ppm. MEFs 43 and 44 were tested with the gallium-indium-tin alloy during the screening test. The high corrosivity of the low melting point alloy would explain the high copper in the sample from MEF 43 but not in stainless steel MEF 44. Contamination from other sources is suspected.

Two samples of the "pure" gallium were included with the test samples. This material was transferred from the covered glass container into the graphite sample holders using the same technique as used for all test samples. A length of clean plastic tubing was inserted into the end of an eyedropper. The end of the tube is slid under the surface film of the gallium and the eyedropper is used to suck up a small sample. The sample is moved to the graphite sample holder and discharged. The operation is conducted in the glove box in an argon atmosphere. The tray of graphite sample holders is covered with a plastic lid before removal from the glove box. Despite these precautions, the two samples of pure gallium were found to have the following impurities:

Sample No.	Copper (ppm)	Magnesium (ppm)
1	0.9	1.0
7	2.4	5.0

TABLE 18. Spectroscopic Analysis of Long-Term Evaluation Test Samples

MEF[1] No.	Material	Finish	Current amps[2]	Contaminants, ppm			
				Cu	Ag	Mg	Ni
23	Ni on Cu	fine	20.0	45	0.2	0.5	3
28	Ni on Cu	rough	20.0	52	-	0.3	3
43[3]	Ni on Cu	rough	20.0	91	-	-	-
63	Ni on Cu	fine	0	32	-	2	-
68	Ni on Cu	rough	0	37	-	-	-
24	SS 304	fine	20.0	0.2	-	-	-
29	SS 304	rough	20.0	-	-	-	-
44[3]	SS 304	rough	20.0	76	0.4	4	-
64	SS 304	fine	0	0.3	-	0.4	-
69	SS 304	rough	0	0.7	-	-	-
Pure gallium				0.9	-	1	-
Pure gallium				2.4	-	5	-
Barrier Film Samples							
Substrate	Film						
Ni on Cu	Braycoat			16	-	0.8	-
Ni on Cu	Teflon			20	-	1	33
SS 304	Braycoat			-	-	1.4	-
SS 304	Teflon			-	-	-	-
Insulator Samples							
Alumina	Ceramic			0.3	-	13	-
Alumina	Ceramic			-	-	0.3	-
Epoxy-glass	G-10			0.2	-	0.7	-
Epoxy-glass	G-10			-	-	0.6	-

[1] Material evaluation fixture

[2] Zero current MEFs had infrequent currents

[3] Used with Ga-In-Sn alloy in screening test

The gallium was purchased to a requirement of one part per million maximum impurities. No impurities were detected in the gallium from stainless steel MEF 29 and in the gallium from a stainless steel/teflon barrier film sample.

Insulator and Barrier Film Samples

Figures 32 and 33 show the insulator and barrier film samples post-test with the gallium in place and with it removed by pouring and tapping.

The alumina ceramic and the epoxy-glass laminate successfully withstood wetting by the gallium for the 108-day vacuum test. A very slight residue remained on the epoxy-glass surface at the gas-gallium-insulator interface but there was no tendency for the gallium to stick. The gallium sample was rolled over the residue on one sample and the residue was absorbed.

The gallium rolled clear of the alumina ceramic with no sticking and no visible residue. It had been feared that the return of atmospheric pressure would push the gallium into the pores of the ceramic but this did not happen.

The barrier film samples repeated the performance of the screening test in that the gallium adhered to the perfluorinated polymer (Braycoat) film as well as to the bonded teflon coating. This was true for films on the nickel plated copper and on the stainless steel samples.

For the long-term evaluation tests the "bare" metal portion of the sample under the gallium was wetted by abrasion except for a band adjacent to the barrier film. The gallium lay across this band. At post-test examination of the nickel-plated copper samples the band was found to be wetted. The band was not wetted on the stainless steel samples. Thus one effective barrier film for gallium on metal surfaces has been verified. It is the natural oxide film on AISI 304 stainless steel.

Weighing data for the insulator and barrier film samples is given in Table 19. Note the absence of residue on the insulator samples. The change in weight of the gallium is of interest. On one alumina sample it did not change at all, confirming the low evaporation rate expected. The large change in gallium weight on the other sample must be the result of an accident which was undetected during test setup or teardown. The tip of a wire or tool might have moved rapidly through the gallium, flicking out a 36.7 milligram portion.

The other samples indicate a weight loss for gallium of up to 4 milligrams with an average weight loss of 1.77 milligrams (excluding the sample which lost 36.7 milligrams) out of 637 milligrams or 0.28 percent. Part of the weight loss is due to weighing errors and part to absorption in the sample but the possibility of measurable evaporation is indicated.

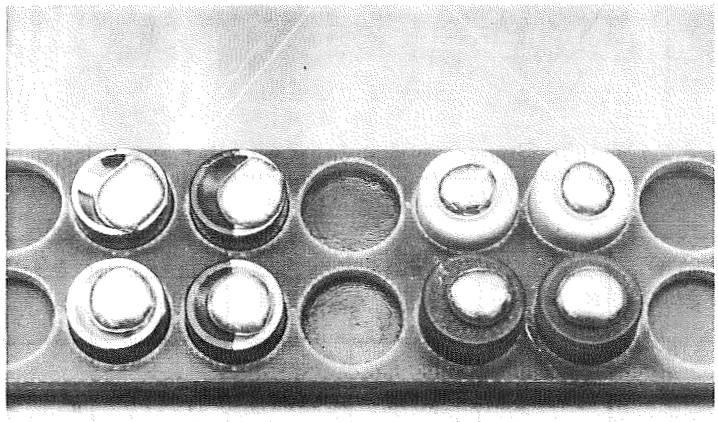

FIGURE 32. Barrier Film and Insulator Samples After Long-Term Evaluation Test

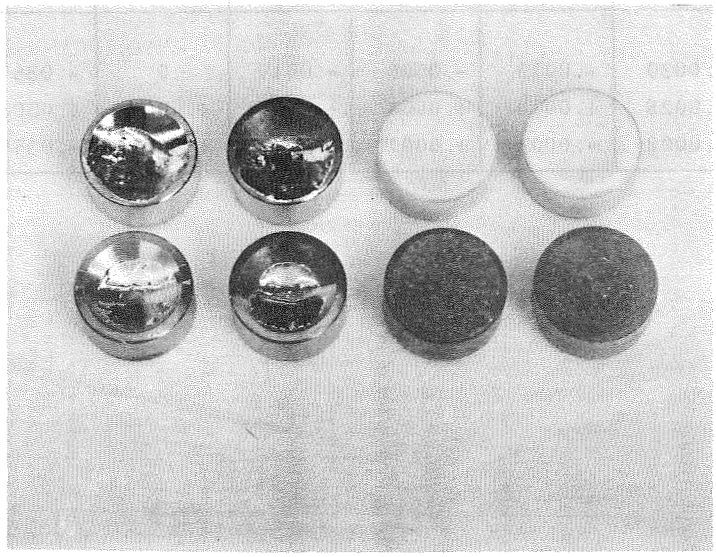

FIGURE 33. Barrier Film and Insulator Samples With Gallium "Poured" Off

TABLE 19. Weight Changes of Insulator and Barrier Film Samples During Long-Term Evaluation Test
(All data in grams)

Ref. No.	1	3	2	4	5	7	6	8
Material Film	Ni on Cu Braycoat	Ni on Cu Teflon	SS 304 Braycoat	SS 304 Teflon	Alumina	Alumina	Epoxy-Glass	Epoxy-Glass
Start 23 January								
Empty	6.1977	6.2263	5.5088	5.5207	2.7445	2.7990	1.3631	1.3809
Filled	6.8460	6.8897	6.1301	6.1213	3.4202	2.4268	1.9730	2.0179
Gallium	0.6483	0.6634	0.6213	0.6006	0.6757	0.6278	0.6099	0.6370
End 15-19 May								
Filled	6.8458	6.8894	6.1302	6.1199	3.4209	3.3909	1.9720	2.0143
Gallium poured off	6.2620	6.2768	5.5154	5.5692	2.7452	2.7998	1.3640	1.3813
Gallium cleaned off	6.2005	6.2273	5.5092	5.5212	2.7452	2.7998	1.3640	1.3813
Gallium residue	0.0615	0.0495	0.0062	0.0480	0	0	0	0
Gallium	0.6453	0.6621	0.6210	0.5987	0.6767	0.5911	0.6080	0.6330
Change								
Gallium	-.0030	-.0013	-.0003	-.0019	0	-.0367	-.0019	-.0040
Sample	+.0028	+.0010	+.0004	+.0005	+.0007	+.0008	+.0009	+.0004
Total	-.0002	-.0003	+.0001	-.0014	+.0007	-.0359	-.0010	0.0036

The contaminants in the gallium of the insulator and barrier film samples are shown in Table 19. The only significant amounts are the copper in the nickel-plated samples and the nickel in one nickel-plated sample. The copper must be due to corrosion by the gallium through openings in the nickel plating. The nickel may be due to residual particles from the abrasive wetting process. The magnesium is undoubtedly from atmospheric dust.

Note that there were no impurities found in the stainless steel barrier film sample with teflon despite the abrasive wetting process used. The gallium used for wetting was wiped off of each barrier film sample before placing the 0.1 cc test sample of pure gallium.

ENGINEERING TEST MODEL DESIGN AND FABRICATION

Design Objectives

The purpose of the engineering test model liquid metal slip ring assembly (ETM) is to provide a test bed to verify design concepts in an operating power transfer system. The design and fabrication of the ETM was Task 2 of the contract.

At the time that the requirements were prepared the decision had not been made between using high voltage, low current versus low voltage, high current solar arrays, so the ETM was to be capable of up to 3000 V between rings and each ring was to be capable of 100 A with 100 percent overload capability.

Ten rings were to be provided and they were to have differences in configuration. Rubbing seals were to be avoided because the major reason for using liquid metal was to reduce friction. Ball bearings were to be used on the ETM but provision for large compliances were to be part of the ring design so that a magnetic suspension or other exotic bearing with very low friction could be accommodated.

The design was to be capable of operating in the hard vacuum of a space environment with temperatures of $0^{\circ}C$ (273K) to $80^{\circ}C$ (353K) for 5 to 10 years.

Rotation rates of one revolution per day (rpd) and ±20 rpd were to be provided by a built-in torquer. Heaters were to be provided as well as provisions for instrumentation of

- bulk ring temperature
- noise generation
- inter-ring electrical coupling
- power loss

o between-ring dielectric strength under vacuum conditions

Current flow was to be maintained with up to 50 percent loss of the liquid metal in any ring. The liquid metal to be used was gallium.

One goal of early design work was to have a design suitable for flight testing. This was found to be quite difficult due to the combination of high current and high voltage requirements. Also it was desired to have ease of assembly and disassembly consistent with an engineering model, and open construction to permit visual observation of the slip rings to the greatest possible extent.

Calculations were to be performed to determine the maximum allowable radial and axial accelerations at which the liquid metal would be retained in the cavities (see Figures 1 and 2) by surface tension forces. Rotational forces were not to be relied upon to determine fluid position. It was assumed that the liquid metal would be frozen for launch and the design needed to permit the expansion of the gallium on freezing as well as normal expansion and contraction of the liquid.

Design Description

General Description

The completed ETM may be seen in Figures 34 and 35.

The slip ring assembly consists of ten pairs of electrically conductive outer and inner rings. Each outer ring is electrically connected to its corresponding inner ring by gallium in the gap between them. The ring material is nickel-plated copper as chosen in Task 1 from the screening test results.

The ten ring-pairs are electrically insulated from each other but adjacent inner rings can be connected by jumpers attached at the ends of the shaft. Adjacent outer rings can be connected by jumpers. For vacuum testing, the rings were jumpered to permit a test current from one source to flow through eight rings in series.

Voltage taps are provided on the inner rings for use during bench tests. Voltage taps for the outer rings were connected to the instrumentation outside of the vacuum chamber to permit measurement of voltage drops through two ring-pairs in series.

Current and voltage tap wiring is arranged in groups so that the top five rings may be operated at 3000 volts difference from rings six through ten.

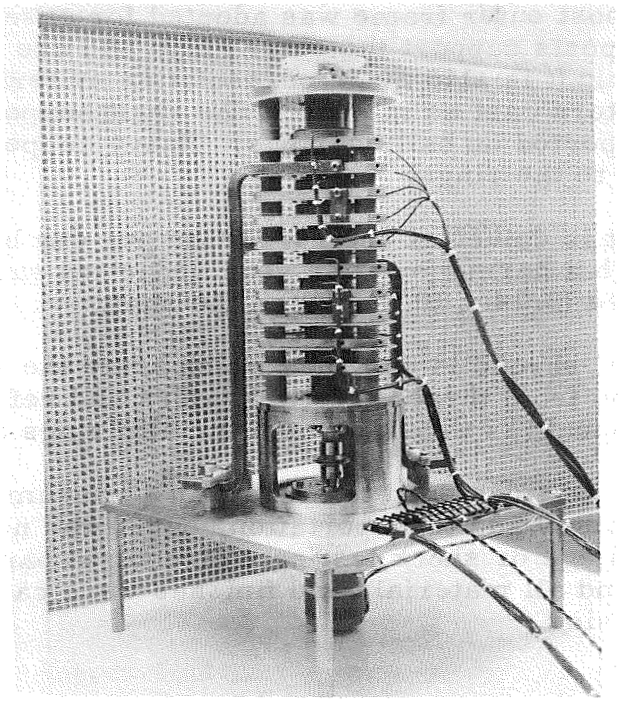

FIGURE 34. Engineering Test Model with Thermal Shroud Removed

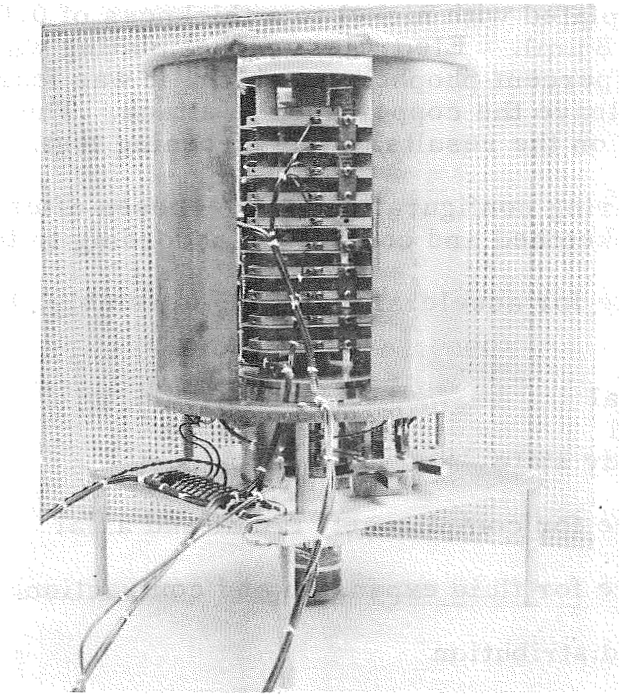

FIGURE 35. Engineering Test Model Liquid Metal Slip Ring Assembly

A three post outer frame was adopted for ease of assembly and visibility. The posts support the outer rings and are made of insulating material. The shaft is also made of insulating material with the current-carrying conductors cast as inserts. The shaft supports the inner rings and is itself supported on ball bearings. Heavy copper bus bars are provided to bring current to the rings.

The shaft is driven at one revolution per day by a stepper motor operating through a harmonic drive gear reduction such that each step is only 0.018 degree (3.14×10^{-4} rad) on the shaft.

A thermal shroud is provided which heats the slip ring assembly by thermal radiation from three electric heaters and reflectors but which provides large openings through which the slip rings can be viewed.

The ETM was designed to operate in a vacuum and to be readily handled for assembly and transportation, but it was not designed for vibration, centrifuge or shock testing. Structural parts are primarily stainless steel and all materials and finishes were carefully chosen to minimize outgassing.

Slip Rings

Two slip ring configurations were provided for the ETM. They are shown twice size in Figure 36. The gaps are dimensioned in Figures 37 and 38. The inner and outer rings were each made of solid copper and were electrolytically plated with nickel to a thickness of 0.0003 inch (7.6 μm) to 0.0007 inch (17.8 μm). Electroless nickel plating was not used because it contains 5 to 10 percent phophorous which, it was feared, would dissolve in the gallium and leave the copper open to attack. The selection of materials was made based on the results of the screening test.

The slip ring configurations were chosen after many other variations of design were sketched and considered according to the following criteria:

- Tolerance for acceleration during assembly, handling, launch, in orbit:

radial	slosh
axial	vibration
steady state	shock

- Tolerance for compliance: radial and axial
- Tolerance for fluid expansion and contraction, including freezing
- Current distribution

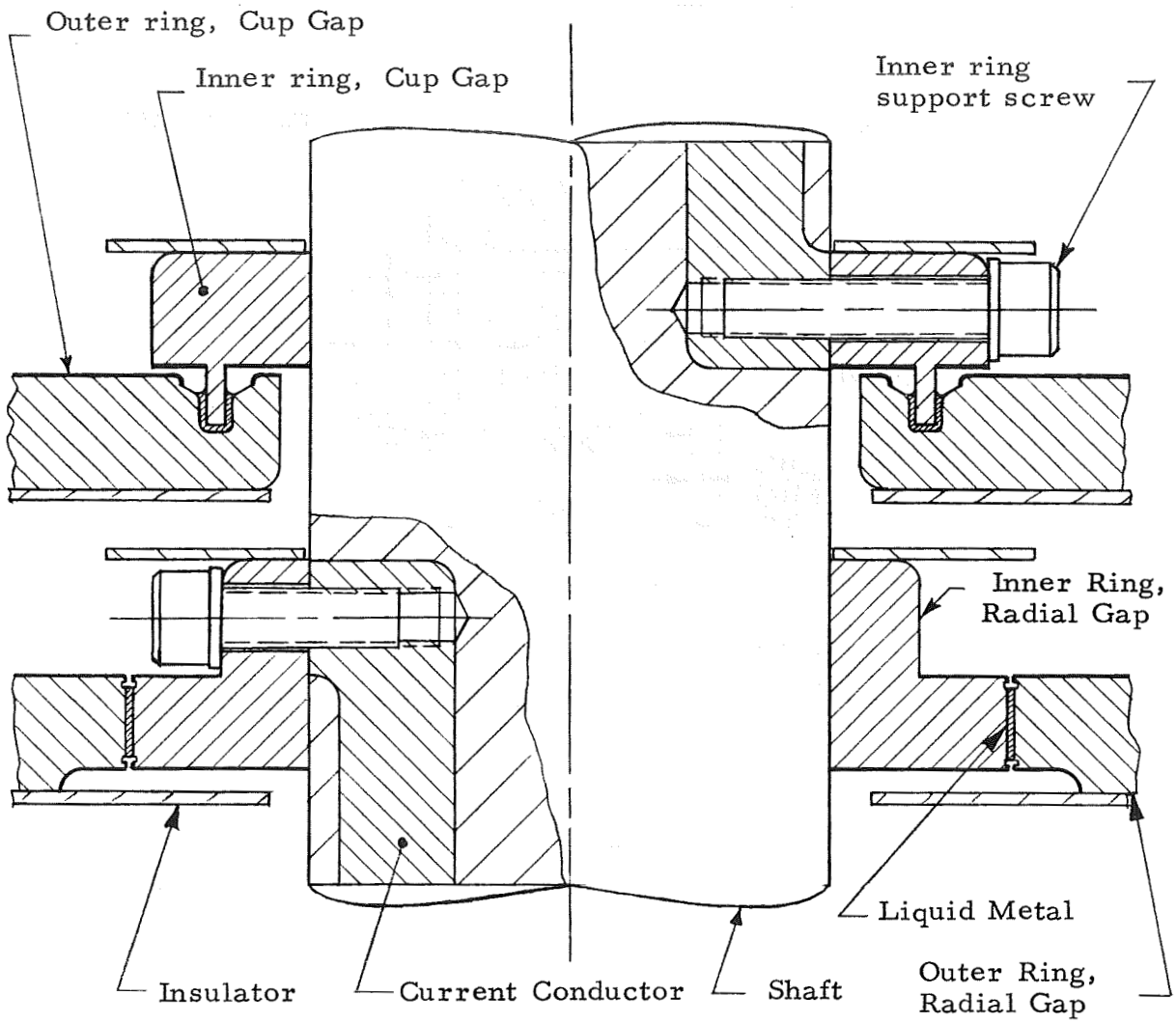

FIGURE 36. Slip Ring Configurations for ETM

- Cost:

  Complexity of machining
  Dimensional tolerances
  Barrier coating
  Wetting with liquid metal
  Assembly

- Fluid disposition during and after catastrophe

- Insulation: nominal, during catastrophe, after catastrophe

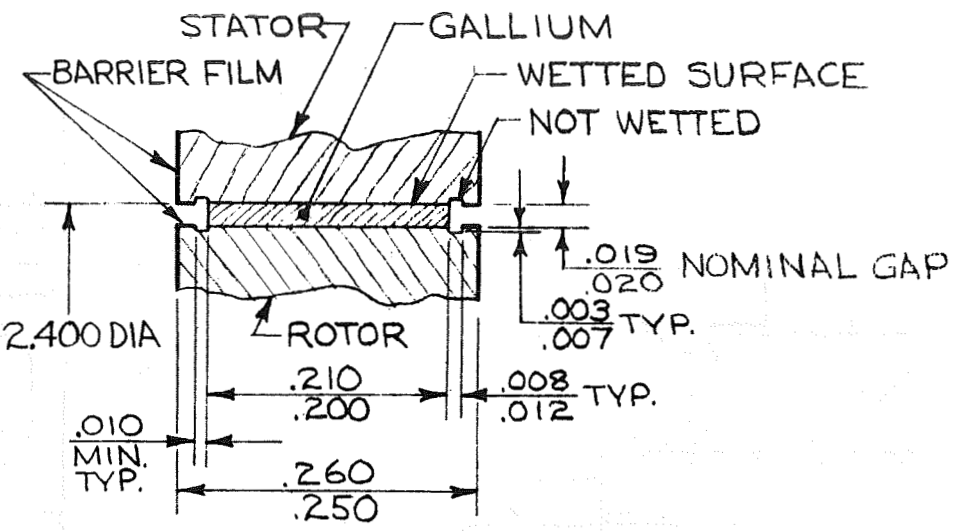

FIGURE 37. Dimensions of Radial Gap Ring

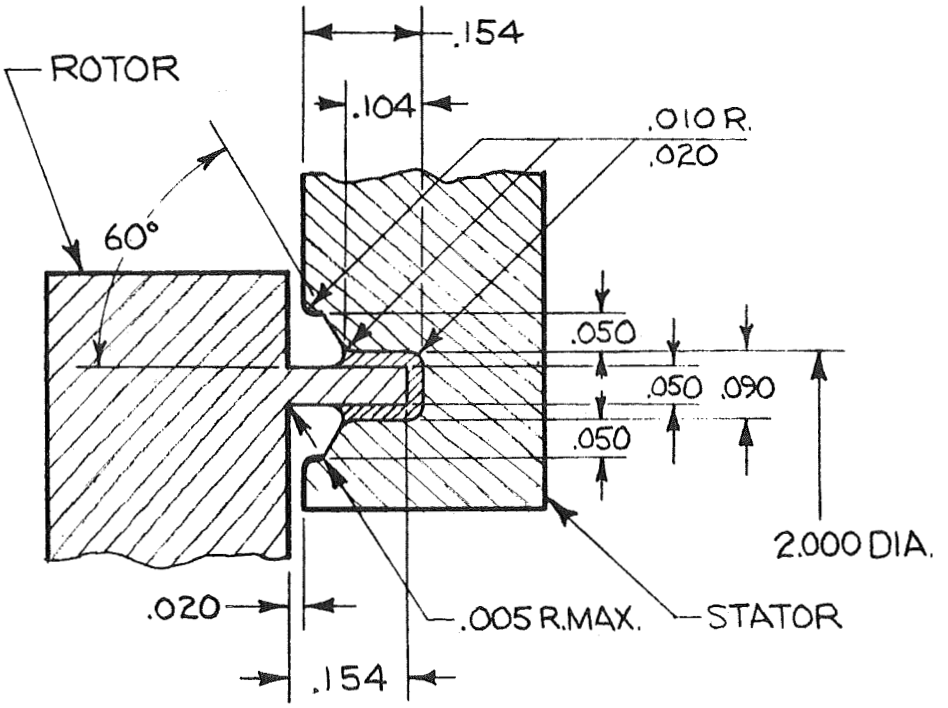

FIGURE 38. Dimensions of Cup Gap Ring

- Size: radial, axial, volume
- Ease of observation (not a strong consideration)

Axial gap configurations were discarded because of their sensitivity to axial displacement between the rings. The radial gap has very low sensitivity to axial displacement and has constant volume versus radial displacement, although the liquid is required to flow tangentially during radial displacement.

If the insulating baffles on the radial gap rings were removed, such a design could be assembled quite easily by slipping a completely assembled shaft and inner ring assembly into a completely assembled housing and outer ring assembly. The danger in such a design is that a sudden radial displacement could cause the liquid metal to squirt from between the inner and outer rings and bridge the space between adjacent rings, causing a momentary short circuit. The baffles are intended to prevent this and to aid in fluid retention and high voltage insulation.

A tendency to squirt has been observed for the liquid gallium. When ejected from a hypodermic needle with sufficient momentum, the gallium hangs together and lands on the bench top intact, like a silver thread. This tendency might be used to advantage in a design like the cup gap configuration, wherein a curved undercut in the inner ring portion of the circumferential expansion chambers might serve to recirculate "squirted" liquid back to the gap.

The cup gap configuration resembles the proposed configuration (see Figure 2) but is smaller, considerably easier to machine and contains less gallium. The smaller size was possible because of the very low interface resistance found in the screening test. A current density of 10 A/cm^2 at 100 A was used for both ring configurations, which is the same as that used in the screening test at 10 A.

The gap clearances used were 0.020 inch (0.5 mm) based on presumed high bearing compliances in a flight model which might permit displacements of 0.010 inch or more. Half of the slip rings were machined with an eccentricity of 0.010 inch (0.020 inch runout) to simulate this condition. The slight taper shown in the gap in Figure 2 was discarded because it requires more gallium, has a lower tolerance for acceleration and was expensive to machine. It had been intended that the taper would cause the remaining gallium to seek the bottom of cup in the event of a significant spill or evaporation.

The gap resistance is readily calculated.

$$R = K_1 h/A + 2 K_2/A$$

where

K_1 = 28 $\mu\Omega$ cm, the resistivity of gallium

h = 0.05 cm, the gap length

A = 10 cm^2, the gap area

K_2 = 0.1 $\mu\Omega$ cm^2, the interface resistance

Therefore,

R = 0.14 + 0.02 = 0.16 $\mu\Omega$ per ring.

At 200 amps the voltage drop through a full gap should be only 32 microvolts and the power loss only 6.4 milliwatts. For a ring which was only half-full these figures would increase by a factor of two or more but would still be extremely small compared to any other known method of rotary power transfer.

When the liquid metal moves out of the cup gap, it expands into a chamber where the wetted walls diverge with an included angle of 60 degrees (1.04 rad). This causes a large change in surface radius for a small displacement and therefore provides a stiff suspension. The opposite walls of the circumferential expansion chambers are coated with barrier film and the escape path beyond is through a 0.020 inch (0.5 mm) gap.

The acceleration tolerance of the liquid metal in the rings can be calculated using the expression for capillary pressure:

$$\Delta P = \sigma \left(\frac{1}{R_1} + \frac{1}{R_2} \right)$$

where σ = surface tension

and R_1 and R_2 are the principal radii of curvature of the liquid surface at the point being considered. For a simple radial gap the response to an axial acceleration can be seen in Figure 39.

In Figure 39

$$P_A - P_o = \sigma \left(\frac{1}{R_{1A}} + \frac{1}{R_{2A}} \right)$$

$$P_B - P_o = \sigma \left(\frac{1}{R_{1B}} + \frac{1}{R_{2B}} \right)$$

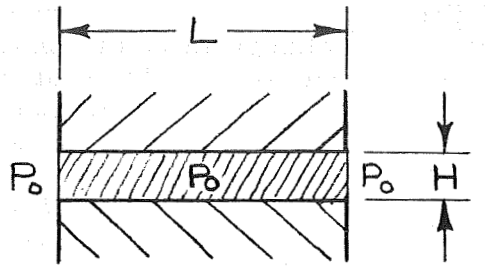

a) No acceleration

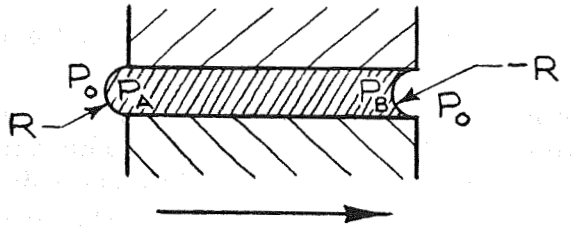

b) Acceleration A applied

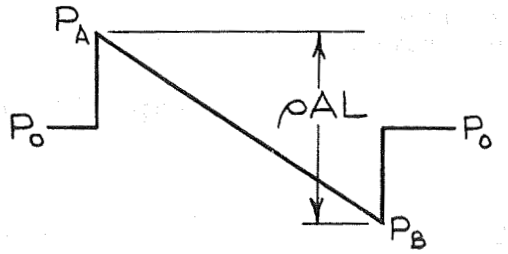

c) Pressure Diagram

FIGURE 39. Capillary Containment of Liquid in a Gap

Due to hydrostatic pressure $\Delta P = P_A - P_B = \rho AL$ where ρ is the density of the liquid. Therefore

$$\rho AL = \sigma\left(\frac{1}{R} + \frac{1}{R_{2A}}\right) - \sigma\left(\frac{1}{-R} + \frac{1}{R_{2B}}\right)$$

Since $R_{2A} = R_{2B} \gg R$ in most cases

$$\rho AL = 2\sigma/R$$

The minimum radius $R = H/2$ so the maximum acceleration is

$$A = 4\sigma/HL\rho$$

The radial gap ring of Figure 37 features a very "stiff" suspension of the gallium because the change in radius R is maximized versus mass shift in the liquid metal. The total volume of the retained gallium does not change with either radial or axial displacements of the rotor with respect to the stator. It is very resistant to slosh and can be filled to adequate accuracy using visual reference. It is easy to wet the rings with gallium using abrasive techniques. A barrier film of perfluorinated polymer can be applied to the "lands" before or after filling is complete.

The steady-state acceleration capability of this design is:

Axial acceleration: $A_a = 15.2$ g ($149\ ms^{-2}$)

Radial acceleration: $A_r = 1.3$ g ($13\ ms^{-2}$)

This assumes a conservative surface tension of 600 dynes/cm for gallium and a nominal gap of 0.020 inch (0.5 mm). The acceleration capability is proportional to 1/gap so that a gap of 0.002 inch (0.05 mm) would permit a radial acceleration of 13 g ($127\ ms^{-2}$) on a ring 2.4 inches in diameter.

The cup gap configuration shown in Figure 38 needs reservoir capacity to account for axial displacement of the rotor with respect to the stator. It is filled by adding a specific weight of gallium. It is a very safe configuration for handling in a one gravity environment.

The steady-state acceleration capability of this design is:

Axial acceleration:

Up: $+A_a$ = unlimited

Down: $-A_a = 17.9$ g ($176\ ms^{-2}$)

Radial acceleration: $A_r = 1.5$ g ($15\ ms^{-2}$)

again assuming 600 dynes/cm for gallium. This is an ultimate capability which is achieved only when a circumferential expansion chamber (reservoir) has been filled and the liquid is attempting to escape through the outer gap.

Slip Ring Assembly

The inner rings each attach to the shaft by a single screw which positions the ring axially and provides the pressure for the high current electrical connection (see Figure 36). Radial runout and wobble are controlled by a close fit of the ring on the shaft. Total indicator readings less than 0.002 inch (0.05 mm) were permitted.

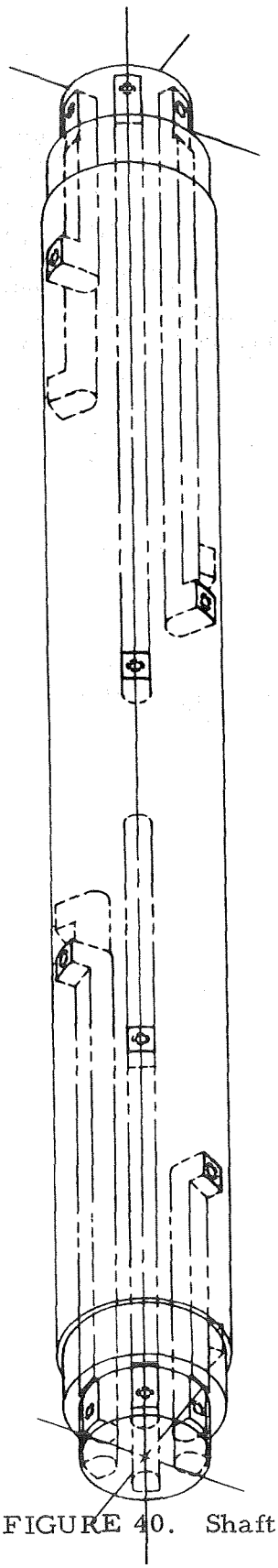

FIGURE 40. Shaft.

The outer rings attach to the insulating posts by means of nylon-typped set screws in the outer rings which press against each post. The axial position of each radial gap outer ring is set simply by visual reference to the inner ring. The cup gap outer rings were set using a 0.020 inch (0.5 mm) feeler gage in the outer gap. This assembly method proved fast and adequate.

The shaft was cast of filled epoxy with copper inserts as shown in Figure 40. The shaft is 13.75 inches (34.9 cm) long and 1.400 inches (3.55 cm) in diameter. The shaft provides current conductors for 12 rings. Ten rings were used, eight of which carried current. The copper bus bars for these eight rings have a total length of 104 cm and a cross-section of 0.56 cm^2 for a resistance of 316 $\mu\Omega$ at room temperature. The four jumpers used to connect the bus bars at the ends of the shaft add another 24 $\mu\Omega$ for a total of 340 $\mu\Omega$ at room temperature and 425 $\mu\Omega$ at 85°C (358K).

If contact resistances are neglected, a voltage drop of 42.5 millivolts can be expected in the shaft bus bars and jumpers at 100 A and 85°C (358K). This results in a heating rate of 4.25 watts in the shaft. At 200 A the power loss becomes 17 watts. This power is conducted into the copper slip rings and dissipated by radiation.

The shaft design provides a close approach to a flight prototype design but has the simplicity and versatility required of an engineering test model.

The three 0.75 inch (1.905 cm) diameter posts were cast from the same filled epoxy as the shaft so as to minimize the difference in thermal expansion between shaft and frame.

The outer rings are jumpered by heavy copper straps which can be seen in Figures 34 and 35. Three are used between rings where current is to be carried and the resulting resistance through the copper is only 2.0 $\mu\Omega$, neglecting contact resistance.

Two sets of heavy copper bus bars are used to conduct the current from the rings to the base plate. This permits operation of rings 1 through 5 at different voltage levels than rings 6 through 10. These bus bars have a cross-section of 0.91 cm^2

and a total length of 160 cm. The resistance at 85°C (358K) is 375 μΩ and the power loss at 200 A is 15 watts.

The total dissipation for the ETM was expected to be 40 to 50 watts at 200 A and there was some question as to whether this power could be dissipated by radiation in the vacuum chamber without exceeding 85°C (358K). The difficulty of designing for high current is obvious.

The metal-to-metal spacing between rings was made 3/16 inch (0.475 cm) and the insulating baffles were placed so as to require a free or surface arc to travel nearly twice that distance. This was considered to provide ample insulation for operation with 3000 volts between rings. This spacing could not be used in the shaft, where the clearance between the conductors is a minimum of 0.060 inch (0.152 cm) through the cast epoxy. However, the insulation between the upper and lower ring sets is ample as can be seen in Figure 40.

The insulating baffles attached to each inner and outer ring as seen in Figure 36 are made of the epoxy-glass fabric laminate per the selection of the screening test.

Voltage taps separate from the current connections are provided on each ring and are brought out in separate bundles for rings 1 through 5 and rings 6 through 10, using teflon insulated wire, unshielded.

Voltage taps are also provided on the inner rings but connections could not be made to them during vacuum testing because of the shaft rotation.

A copper-constantan thermocouple is provided on each outer ring.

The shaft is supported by thin-ring ball bearings mounted in the stainless steel top and bottom plates of the slip ring assembly. The bearings are 440C stainless steel and are dry-lubricated with molybdenum-disulfide for vacuum operation. Wavy washers provide preload to the bearings.

A shaft angle indicator with divisions every 30 degrees is provided at the top of the assembly.

A 12-inch (30 cm) square by 3/8 inch (0.95 cm) thick stainless steel base plate is provided for convenience in supporting the slip ring assembly, drive assembly, thermal shroud, terminal board and bus clamps. A cutaway base ring supports the slip ring assembly on the base plate and provides access to the stainless steel bellows-type coupling between the slip ring shaft and the drive assembly.

Drive Assembly

The drive assembly turns the slip ring assembly shaft at 1 rpd and 20 rpd as required by the statement of work and also at 0.45 rpm for convenient positioning.

The drive assembly consists of a permanent magnet, bifilar-wound DC stepping motor turning a harmonic drive gear assembly. The stepper motor provides 200 steps per revolution. The harmonic drive has a gear reduction of 100 to 1 so that the slip ring shaft turns 0.018 degree per pulse to the stepper motor.

The stepper motor and harmonic drive are reconditioned for high vacuum use by removing all materials, such as paint, which might outgas, providing scavenging holes and dry lubricating all bearing surfaces.

A copper-constantan thermocouple is provided on the case of the motor.

The control panel for the drive system has switches for on-off, CW-CCW, manual stepping, and speed selection. Speed is controlled by selecting the R-C network to use with a multivibrator. A translator module controls the stepper motor. The control panel has its own d-c power supply and requires only 117 volts, 60 Hz line power for operation.

Thermal Shroud

The temperature of the slip rings is controlled by adding heat by means of a thermal shroud. The thermal shroud has three electrically heated radiators and three reflectors as seen in Figure 41. They are arranged around the slip ring assembly so as to provide minimum interference with the viewing of the slip rings through the view port in the vacuum chamber.

Each radiator is a copper rod 0.5 inch (1.27 cm) in diameter by 12 inches (30.5 cm) long, wound with electrical resistance wire to provide 33.3 watts at 30 volts rms. They are operated in parallel from a 30 Vdc power supply. Calculations indicated that the total heat required would be 34 watts (approximately 11 watts per radiator) if the slip ring assembly had no dissipation of its own. The radiator temperature is expected to be 91°C (364K) at that point. A radiator temperature in excess of 100°C (373K) is undesirable because of possible outgassing from the epoxy adhesive used to hold the heater wire in place and from the black epoxy paint applied to the radiator to increase its emissivity.

Each radiator is fitted with a copper-constantan thermocouple.

The reflectors are of polished stainless steel with circular arc cross-

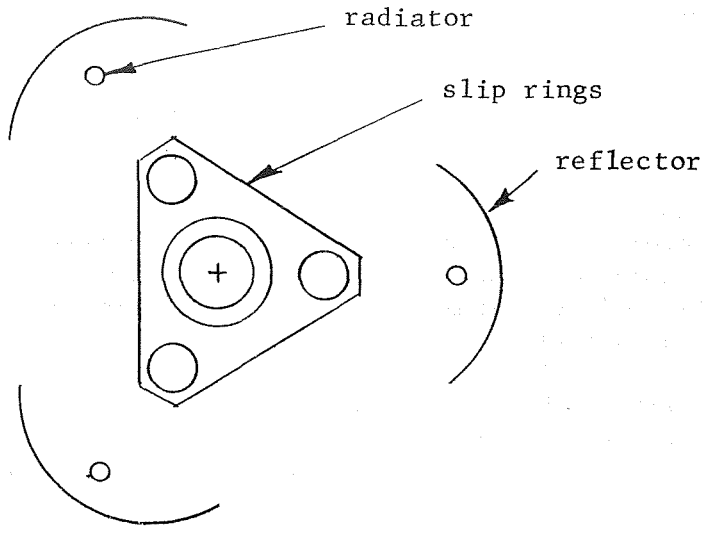

FIGURE 41. Cross-Section of Slip Ring Assembly with Thermal Shroud

sections which approximate parabolas so as to spread the radiation evenly across the slip ring assembly.

Fabrication and Trial Assembly

Shaft

The shaft and the three support posts were cast of filled epoxy and machined to final dimensions. The epoxy-filler combination used was:

Shell Epon 815:	100 parts (by weight)
Lithium aluminum silicate: (Carborundum Lithoflex 2123)	174 parts
HV amine hardener	20 parts

The casting was done using a setup as in Figure 42. The mold was covered by more than 1/2 inch of asbestos insulation and preheated for several hours at 190°F (361K). It was then placed in the bell jar and pumped to a vacuum of 10^{-4} torr in less than 20 minutes. The epoxy was mixed and preoutgassed, then transferred into the degassing reservoir without breaking the vacuum. This permitted thorough outgassing. The mold with its reservoir was then removed from the vacuum chamber and a vacuum established by a tube to the top of the overflow reservoir. The valve below the

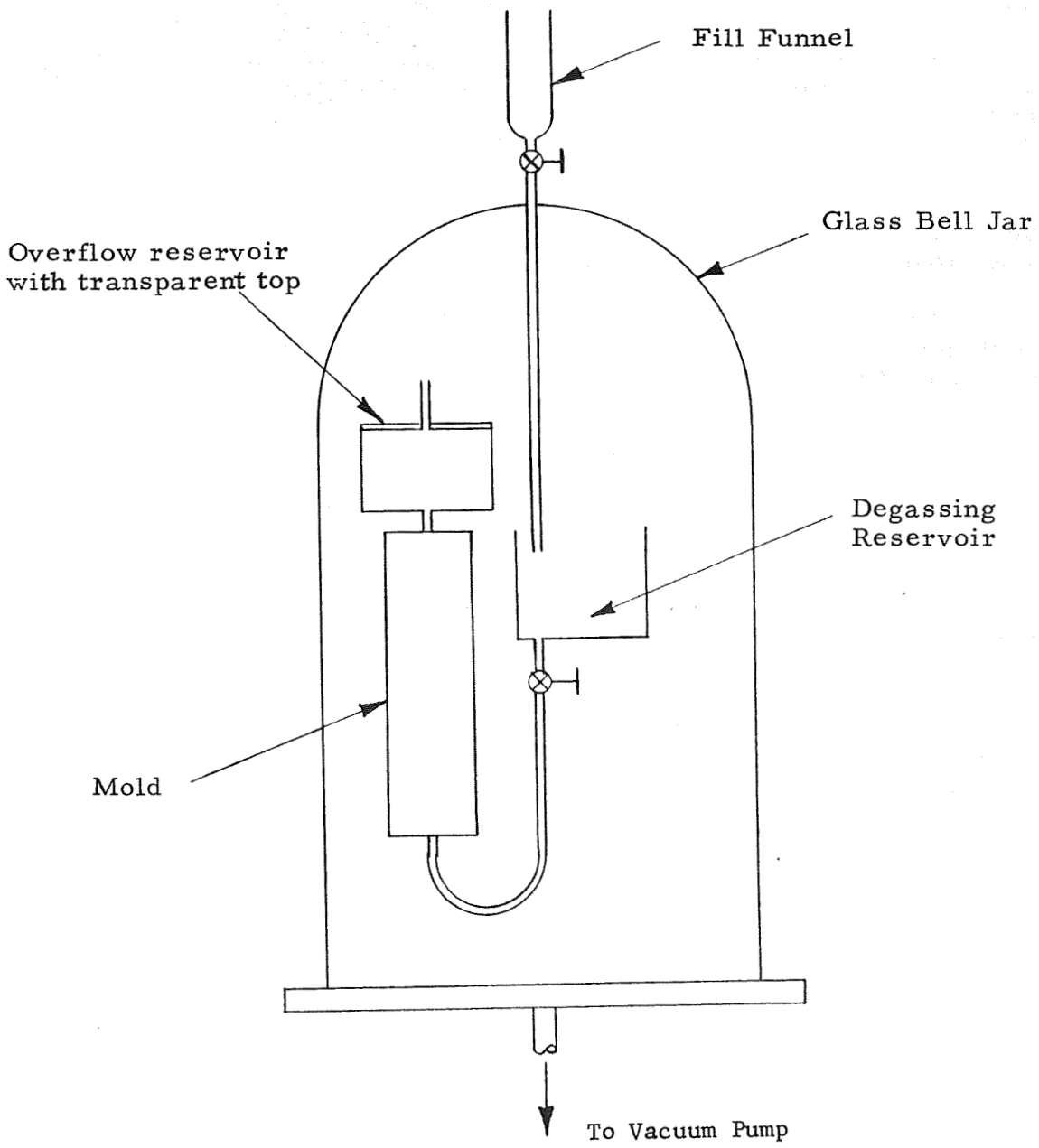

FIGURE 42. Setup for Casting the Shaft

degassing reservoir was then opened, allowing atmospheric pressure to force the epoxy mix up through the mold and into the overflow reservoir. The valve was then closed and the mold and reservoirs transferred to a heated pressure vessel where a pressure of 100 psi (6.89×10^5 N m^{-2}) and a temperature of 190°F (361K) were established.

The above operations involved waiting for the viscous epoxy mix to flow. The mold was in the pressure vessel within one hour of adding the hardener to the epoxy/fill mix. The epoxy mix was still pourable when the 100 psi pressure was applied.

The mold was removed from the pressure vessel after four hours at 190°F and post-cured for 64 hours at 190°F. The temperature was chosen to be close to the 85°C (358K) operating temperature of the ETM.

The mold was removed from the shaft by machining. The screws which held the insert conductors were found to be adhered despite the mold release coating used. Some screws had to be machined out and three holes (out of 24) required threaded inserts to restore the threads in the conductor ends.

Only one bubble was found in the shaft during grinding to size, and it is well away from any conductors. The three support posts, cast of the same material, had a few bubbles, none of which interfere with the function of the posts.

Slip Rings

The soft copper slip rings were machined with a smooth finish in the areas to be contacted by the gallium. This was quite difficult in the cavity type outer rings due to the softness of the copper. Copper would quickly build up on the cutting edge of the carbide tool, causing gouging, unless the rake and undercut angles were carefully controlled, the width of cut was very small and the depth of cut was adequate to avoid skating.

The slip rings were nickel plated by a vendor who specializes in obtaining uniform plating thickness. One inner ring, No. 8, was apparently dropped on an uneven surface before plating and had a badly dented area in the active surface. The plating appears sound on all rings but has some built-up nodules which were removed with a whetstone. A thorough mechanical scrubbing was necessary to remove a discolored film. Steel wool proved effective for this task.

Trial Assembly

The ETM was first assembled with superficial cleaning and without liquid metal in the rings. The rework required was minor and all critical fits were found to work well. Of particular concern were the sliding of the inner rings over the cast epoxy shaft and the sliding of the outer rings over the three cast epoxy support posts. The bearings were free and were set up

with very little axial compliance using wavy washers as shims. Runout of inner rings was slight except for the intentional eccentricity of five rings.

Wiring and attachment of thermocouples was accomplished at this time. The drive assembly and control panel were checked out and the pulse period of 4.32 seconds for 1 rpd adjusted to within 0.1 percent.

The ETM was then disassembled to permit thorough cleaning of all parts and subassemblies prior to final assembly which was accomplished as part of Task 3.

ENGINEERING TEST MODEL TESTING AND EVALUATION

Introduction

The objective of the testing was to obtain experimental technical information on the performance of the ETM which would enhance our understanding of the characteristics of liquid metal slip rings and thus provide increased capability to design liquid metal slip rings for use in space vehicles.

The testing was primarily a two-month test of the slip ring assembly at elevated temperature in a high vacuum, followed by evaluation of the effects of the testing on the slip ring materials.

The final assembly and testing comprised contract Task 3. The final assembly was included because various test data were collected at that time.

The slip rings were arranged as listed in Table 20. Ring 1 was at the top.

TABLE 20. Slip Ring Arrangement for Testing

Ring No.	Current	Gap Configuration	Eccentricity		Gallium Fill percent	Barrier Film
			inch ± .002 inch	mm ± 0.05 mm		
1	no	cup	0	0	100	A
2	yes	cup	0	0	100	A
3	yes	cup	0	0	100	B
4	yes	cup	.010	0.5	100	A
5	yes	cup	.010	0.5	50	B
6	yes	radial	0	0	100	A
7	yes	radial	0	0	100	B
8	yes	radial	.010	0.5	100	A
9	yes	radial	.010	0.5	50	B
10	no	radial	.010	0.5	50	B

Barrier films A and B are the top-rated choices from the screening test. A is the natural oxide film on the slip ring material and B is the perfluorinated polymer coating.

Note that rings 2 and 3 are the same except for barrier film and so are 6 and 7. This is to permit the most accurate determination of the nominal voltage drop per ring under vacuum conditions.

Eccentricity of 0.010 inch means a runout of 0.020 T.I.R. Eccentricities of rings 4, 5, 8, 9 and 10 are at approximately the same angular location.

Assembly and Preliminary Measurements

All parts of the ETM were cleaned in the vapor degreaser followed by ultrasonic cleaning in freon. Parts were thereafter handled only with nylon gloves. Assembly took place in a laminar flow bench in the clean room.

Each inner and outer ring was carefully examined under a stereoscopic microscope and photographed. No significant defects in the nickel plating were found. Figure 43 shows some of the rings before wetting with gallium. No defect was found in the plating of the dented area of inner ring 9 seen in Figure 43d). Several of the rings had slight dents in the copper which had been received before plating.

It was found that the nickel plating was readily wetted with gallium by rubbing the gallium into the surface with the stretch nylon cloth used in the materials experiment. Steel wool and two varieties of industrial treated-paper wipers could also be used for wetting, but they left behind a great deal of debris which had to be wiped off with the lint-free stretch nylon. Too much pressure on the paper wipers inhibited wetting. Wetting was much improved after the scrubbing with steel wool to remove the discolored film which was on the nickel after plating.

The gallium only wets the nickel when sufficient pressure is applied, so that the chance of inadvertently wetting a surface is small. However, in order to attain a well-defined edge to the wetted area, masking tape was used as shown in Figure 44. The masking tape was readily removed with no visual residue. Unwet bands of from 0.010 inch (0.25 mm) to 0.030 inch (0.75 mm) remained in the corners of the inner and outer rings of the cup gap configuration. The coverage of the center lands of the radial gap rings was generally complete. Several dents in the damaged area of inner ring 9 were not wet at the bottom. No attempt was made to protect the bottoms of the small grooves, but only a few slight spots of gallium adhered there.

The excess gallium was removed from the rings. The gallium faithfully reproduced the nickel surface except that scratches were mostly filled in. The "orange peel" texture was accentuated by the wet, shiny surface. Some

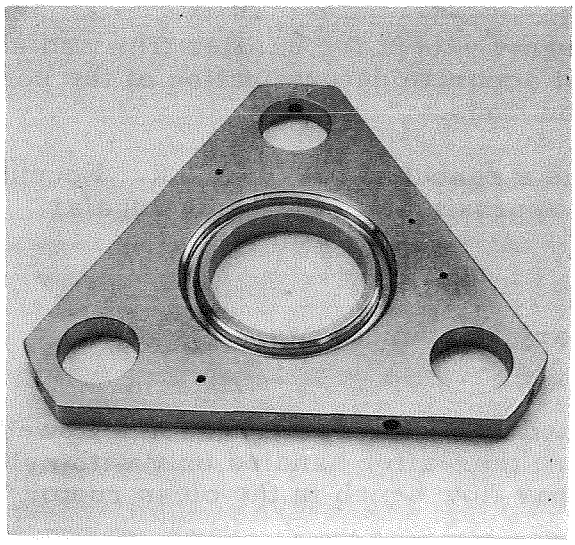

a) Cup Gap Outer Ring

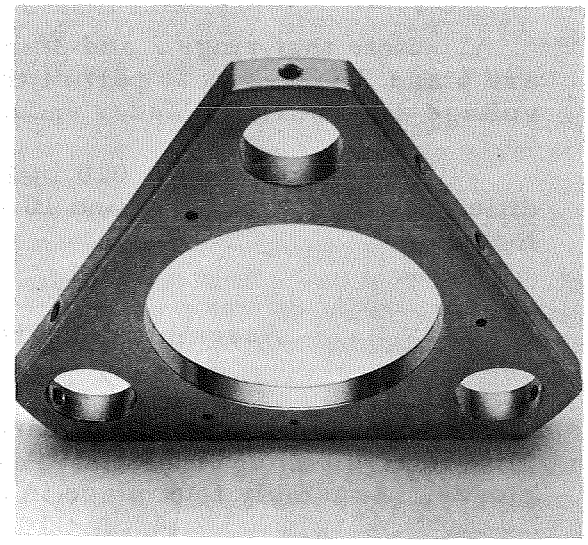

b) Radial Gap Outer Ring

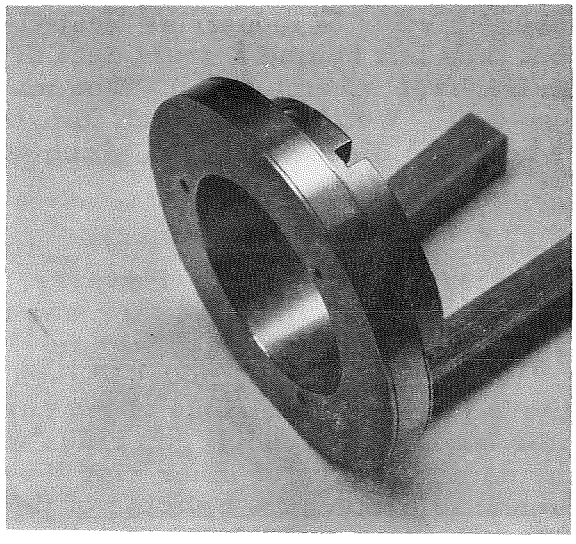

c) Radial Gap Inner Ring

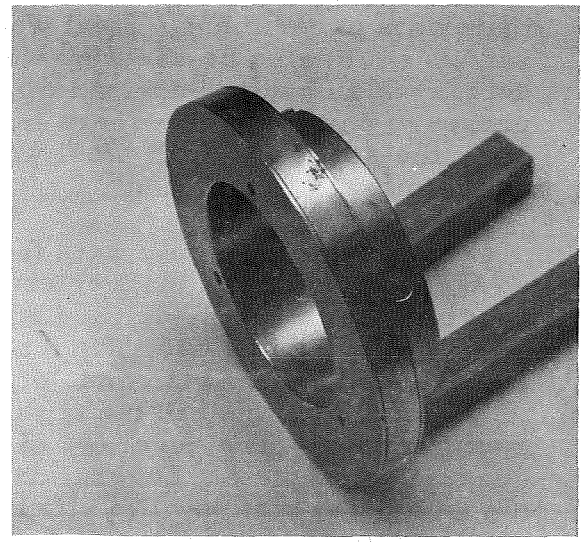

d) Damaged Inner Ring 9

FIGURE 43. Slip Rings Before Wetting with Gallium

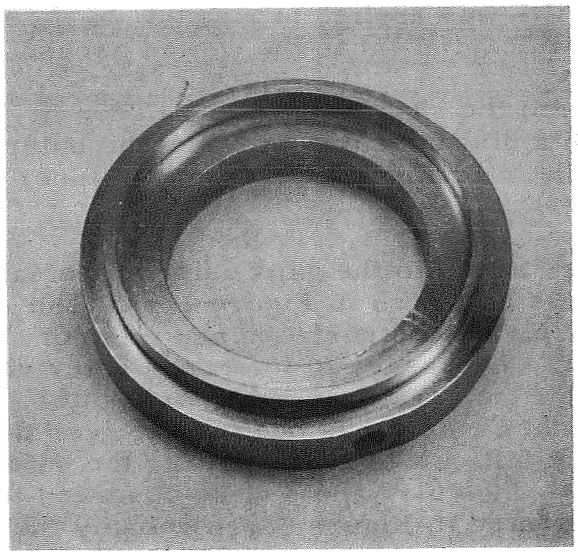

a) Ring 5 After Cleaning

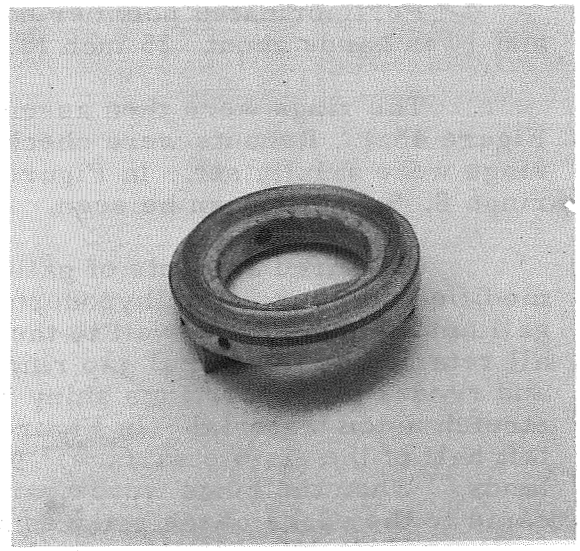

c) Ring 4 Wetted with Gallium

b) Ring 4 with Masking Tape Applied

d) Ring 4, Masking Tap Removed

FIGURE 44. Initial Wetting of Cup Gap Inner Ring

rings seemed slightly dry and frosty in appearance. Under the microscope the wetting looked 100 percent and there was no evidence of bridging.

Perfluorinated polymer barrier film was applied to rings 3, 5, 7, 9 and 10 in bands about .25 inch (0.6 cm) wide adjacent to the wetted areas.

The rings were then assembled onto the shaft and posts as seen in Figure 45a). Runouts were checked with a dial indicator and then the outer rings were axially set. In Figure 45b) the intentional eccentricity of inner rings 8, 9, and 10 can be seen.

Measured amounts of gallium were added to the gaps using a specially modified stainless steel hypodermic needle as shown in Figure 45c). The gallium did not adhere well to the previously wetted surfaces and was not all retained by the radial gap rings. It was necessary to lower the outer rings and render the inner rings shiny wet with excess gallium using swabs of stretch nylon material. In Figure 45d) inner ring 7 has been rewet over the left half of the visible surface. It was not difficult to avoid wetting the outer lands. When the rings were again filled, rings 6, 7 and 8 were observed to come to the edges of the grooves as illustrated in Figure 37. Probably the gallium surfaces were actually convex because of the excess gallium but this was not easily observed in the narrow gaps.

In half-full radial gap rings 9 and 10 the surface tension forces predominated over gravitational forces and the gallium dispersed unevenly over the wetted ring surfaces rather than settling evenly to the bottom half of the ring.

The gallium did not readily flow into the 0.5 mm gaps of rings 1 through 5, which are configured per Figure 38, despite the prewetting. The rings had to be heated above 30°C to avoid the gallium freezing in the hypodermic needle. Three grams were to be added to "full" rings 1, 2 and 3. The last gram in each ring simply filled the outer diameter reservoir and did not flow through to the inner diameter.

Inner and outer rings 1, 2 and 3 were then removed from the ETM and made shiny wet with the cotton cloth swabs and more gallium. The three gram of gallium was added to the cavity of each outer ring before reassembly. At reassembly the gallium disposed itself as had been expected. Figure 46 shows ring 2 before and after rewetting.

It was clear that having the rings quite wet is necessary before filling the gaps. Also, the rings should be wetted just prior to fill. A weekend had elapsed between wetting and the first attempted fill with liquid gallium.

Resistance

The resistance from the inner to the outer rings of each set was essentially unmeasurable with available instrumentation. From calculations, the resistance through the gallium was expected to be 0.16 microhms for the

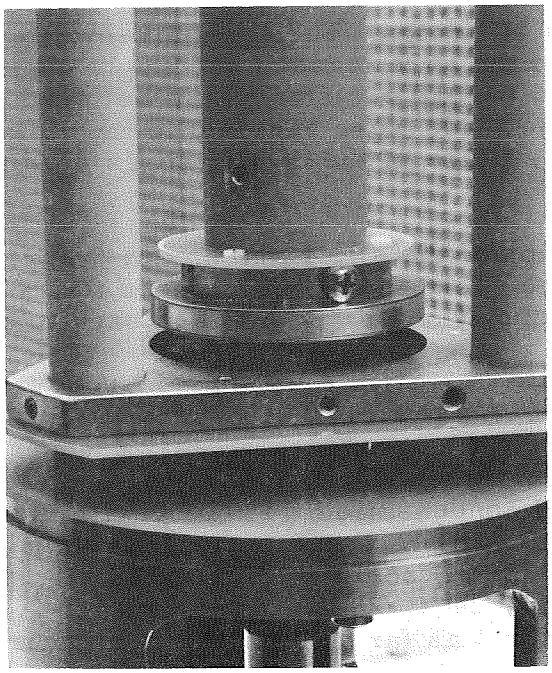

a) Wetted inner ring 10 in place, outer ring lower

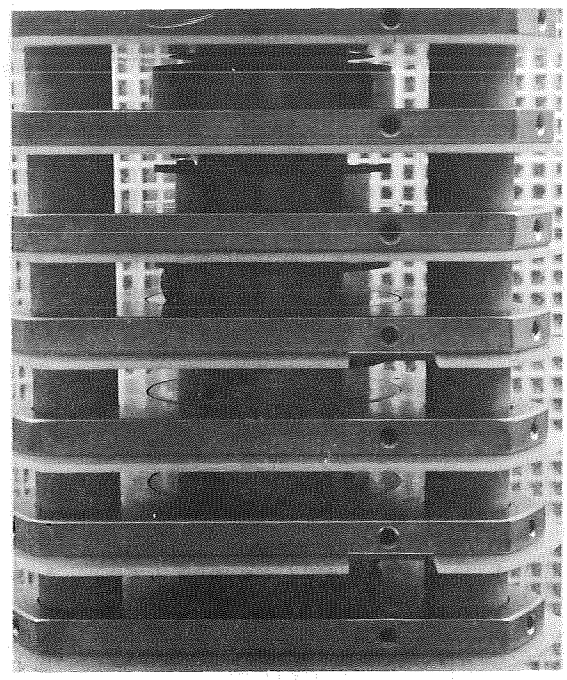

b) Rings 5 through 10 in place, ready for fill

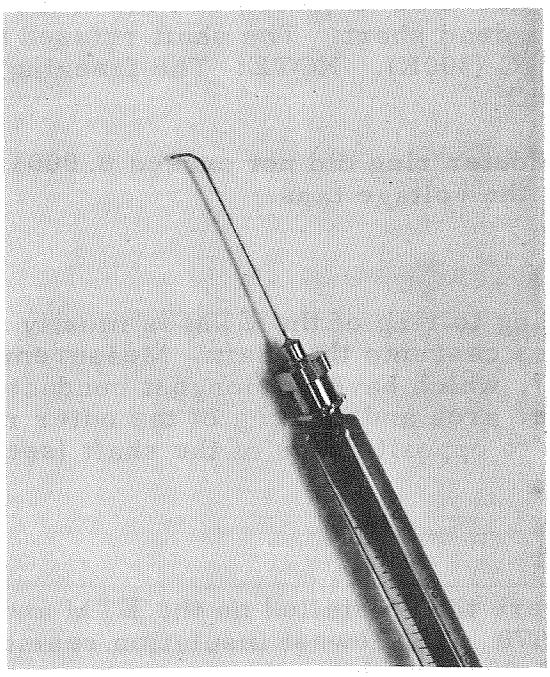

c) Specially modified hypodermic needle for filling slip rings

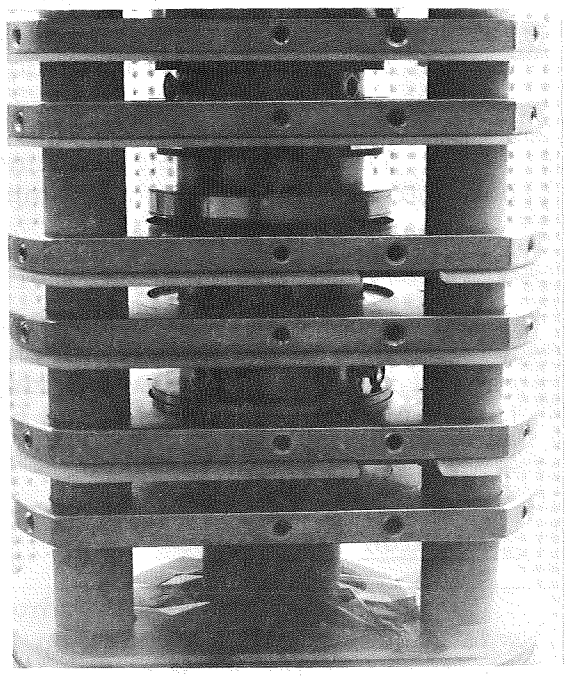

d) Inner ring 7 being rewetted

FIGURE 45. Assembling and Filling the Slip Rings

full rings and 0.32 microhms for the half full rings. Such measurement was swamped by the 19 milliohm resistance of the wire leads. The slight changes of resistance on the data sheets compared to lead resistance are believed due to contact resistance where the lugs on the leads were screwed to the voltage taps on the rings, and to changes in temperature of the copper leads resulting from handling and current flow.

This condition prevailed for rotation of the slip rings and even for measurements from ring to ring where the resistance path included the current bus through the shaft to the jumpers at shaft end and then back to the other ring.

Freezing the Rings

The gallium in the rings was frozen by chilling the ETM to -3.3°C (270K) in the glove box using LN2 to avoid condensation. Probing with the hooked hypodermic needle verified that the gallium was frozen. During chilling, with a ring temperature of 15°C (288K) some gallium was still molten. After return to room temperature, 24°C (297K), the gallium remained frozen and remained a "dead short" as far as resistance measurements could determine.

The chilling required less than 1 hour in the glove box. There seems no reason to believe there will be trouble freezing an operational liquid metal slip ring.

It was necessary to heat the rings above 30°C (303K) to remelt the gallium. Again the rings appeared to be a dead short. The shaft refused to turn as the ring temperature cooled to 27°C (300K). NOTE: The freezing/melting point of gallium is 29.7°C (302.9K).

The resistance from inner ring to outer ring did not exceed 0.0001 ohm for any of the 10 rings, measured at the voltage taps.

Capacitance

The capacitance measured from ring to ring of the ETM is mostly attributable to the heavy copper conductors cast into the shaft. Measurements ranged from 55 μμF between rings 6 and 7, which have the longest conductors, to 20 μμF between rings 5 and 6, where the area and spacing of the outer rings predominates because the conductors run to opposite ends of the shaft (see Table 21.

Insulation Resistance

Final wiring and thermocouples were then installed on the ETM and it was checked with a Megger on 10 April 1970. The lowest insulation resistance measured on the ETM at 500 Vdc was 300,000 megohms.

a) Inner ring after attempted fill. Circumferential track is from dial indicator used to check runout.

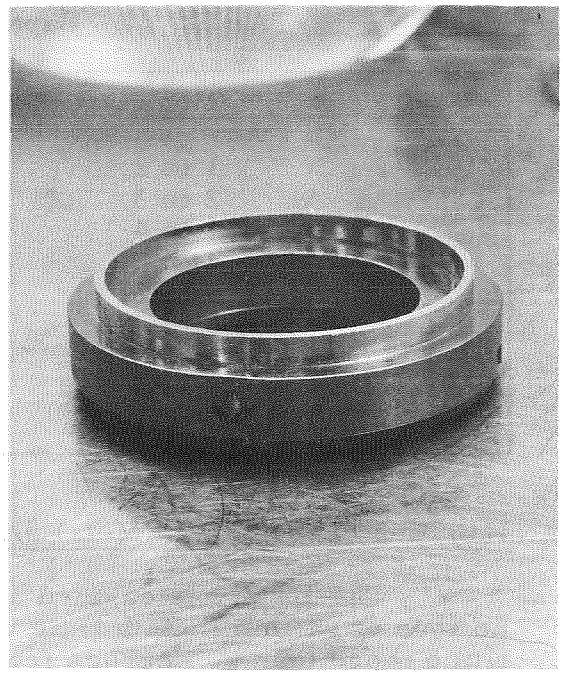

b) Inner ring made shiny wet before reassembly.

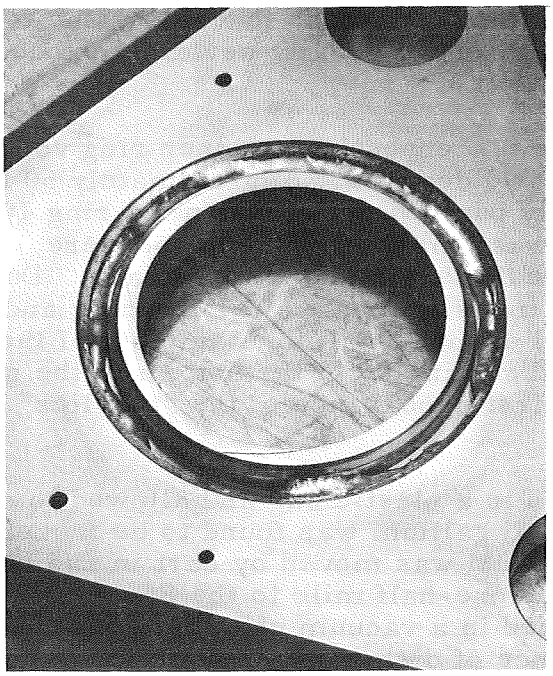

c) Outer ring after attempted fill. Note that some areas are wet and some are not.

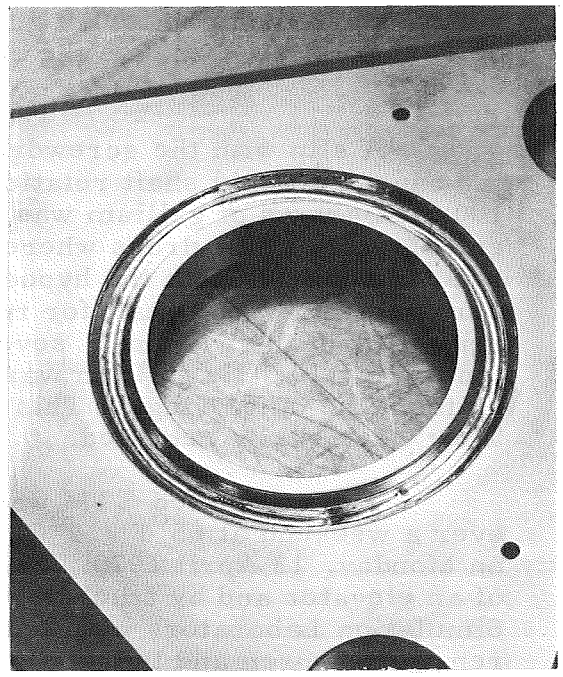

d) Outer ring rewetted and filled.

FIGURE 46. Rewetting of Ring 2.

TABLE 21. Capacitance Between Slip Rings

Rings	Capacitance, μμF
1 to 2	42
2 to 3	46
3 to 4	50
4 to 5	54
5 to 6	20
6 to 7	55
7 to 8	50
8 to 9	45
9 to 10	39

Handling of the Liquid Metal Slip Ring Assembly

The ETM was carried about and taken in and out of the glove box with no loss of gallium. At a time when the gallium was all molten the ETM was tilted more than 30 degrees from the vertical. The gallium was readily observed through the 0.030 inch gap on the open side of the eccentric radial gap rings. No motion of the gallium was observed during the tilting and no evidence of sloshing was seen when the ETM was shaken manually while tilted.

The calculated radial acceleration capability of the radial gap ring with a 0.030 inch gap is 0.9 g. The "tilt test" indicates that this value may be conservative, because the radial component of gravity certainly exceeded 0.5 g.

A slip with the screwdriver while disconnecting an inner ring voltage tap caused a rapid shaft rotation of about 90 degrees. Approximately 50 to 100 milligrams of gallium was apparently pumped out of eccentric ring 10, emerging in small drops where the gap was smallest. The drops were readily removed with the hypodermic needle leaving no visible trace. During slow rotation of the shaft for resistance measurements after freezing and remelting of the gallium, several small drops of gallium came out of the top of ring 10. No gallium was observed coming from the bottom of the gap or from the other rings. This was the first appearance of the "twirlies". They were easily removed.

The completed ETM was enclosed in a plastic bag and allowed to chill over a weekend at 65°F (18°C, 291K). All gallium was found to be frozen on Monday, 13 April 1970. The bagged ETM was moved by cart in and out of an elevator and by truck approximately one-half mile to the Space Simulation Laboratory where it was placed in a vacuum chamber. The gallium remained frozen and there was no evidence of disturbance due to the transportation.

Thermal-Vacuum Performance Test

Test Setup and Instrumentation

The vacuum chamber used is the C-6 chamber located in the Space Simulation Laboratory in the Hughes Aircraft Company El Segundo facility. It has a 22-inch inner diameter steel bell jar 32 inches high with a 5-inch diameter view port about half way up. It is pumped by a peripherial ion pump consisting of fifteen 60 liter per second modules. Roughing is accomplished by a gas aspirator pump and a set of three sorption pumps.

Installation of the ETM in the vacuum chamber and connection of power supplies and instrumentation were accomplished per the Test Plan with the following differences: A 100 amp regulated power supply was substituted for the battery which had been planned for use during measurements of electrical noise, and current was not supplied to rings 2 through 5 during the high voltage test. Figures 47 and 48 show the test setup and instrumentation.

It was found that the voltage drop at the high voltage, high current vacuum feedthroughs from ring 2 to ring 5 was 0.41 volts at 200 amps and that from ring 6 to ring 9 was 0.44 volts instead of the desired 0.2 volts maximum. The power loss in the vacuum chamber was 170 watts. This was after doubling up on the cables used as current busses within the vacuum chamber. We were thus forced to operate with a higher heat input to the vacuum chamber than had been anticipated.

Four small "twirlies" were seen to form on ring 10 when correct operation of the drive assembly was verified. These were observed through the viewport in the vacuum chamber.

Insulation resistance was well over 100 megohms on the completed installation when all connections to rings 1 through 5 were disconnected external to the vacuum chamber.

Pumpdown and Formation of Gallium Residue

Pumpdown began 16 April 1970. A pressure of 11 microns ($1.5\ Nm^{-2}$) was obtained in the first hour and was 5×10^{-6} Torr ($6.7 \times 10^{-4}\ Nm^{-2}$) after 2 hours. During the second hour, 0.03 inch (0.8 mm) diameter balls of gallium formed on the four "twirlies" on ring 10. Looking through the 0.020 inch (0.5 mm) axial gaps, there appeared to be lumps in the gallium in the outer reservoirs of rings 3, 4 and 5 which were probably air bubbles.

Four hours after the start of pumpdown the pressure remained near 5×10^{-6} Torr. The shaft was rotated 180 degrees in an attempt to break the bubbles. This appeared to be successful in the cup gap rings (1 through 5) but it caused twirlies to form on radial gap rings 6 through 10. Three small drops fell from the bottom of ring 10. Some gallium had also fallen

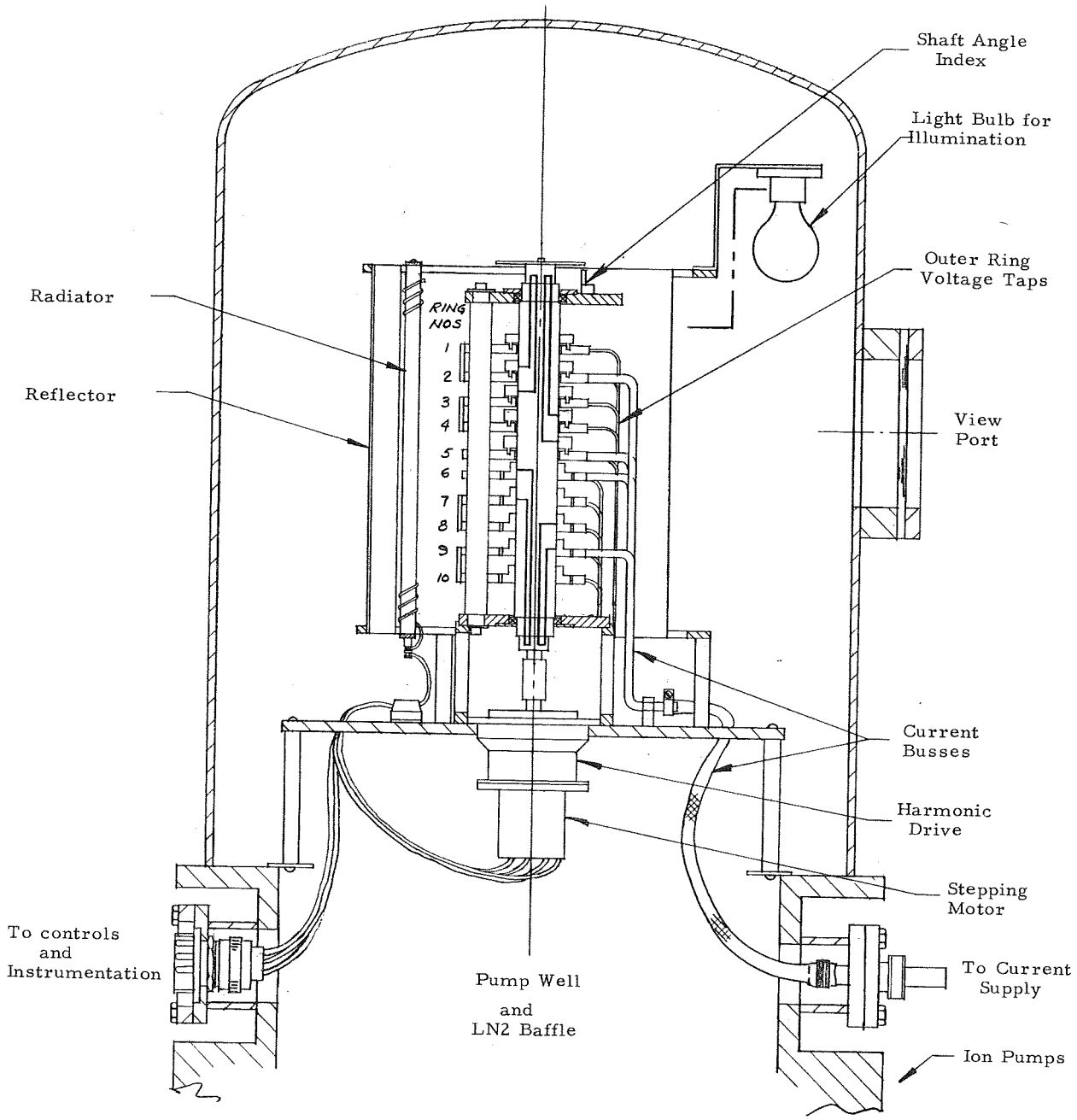

FIGURE 47. Vacuum Test Setup

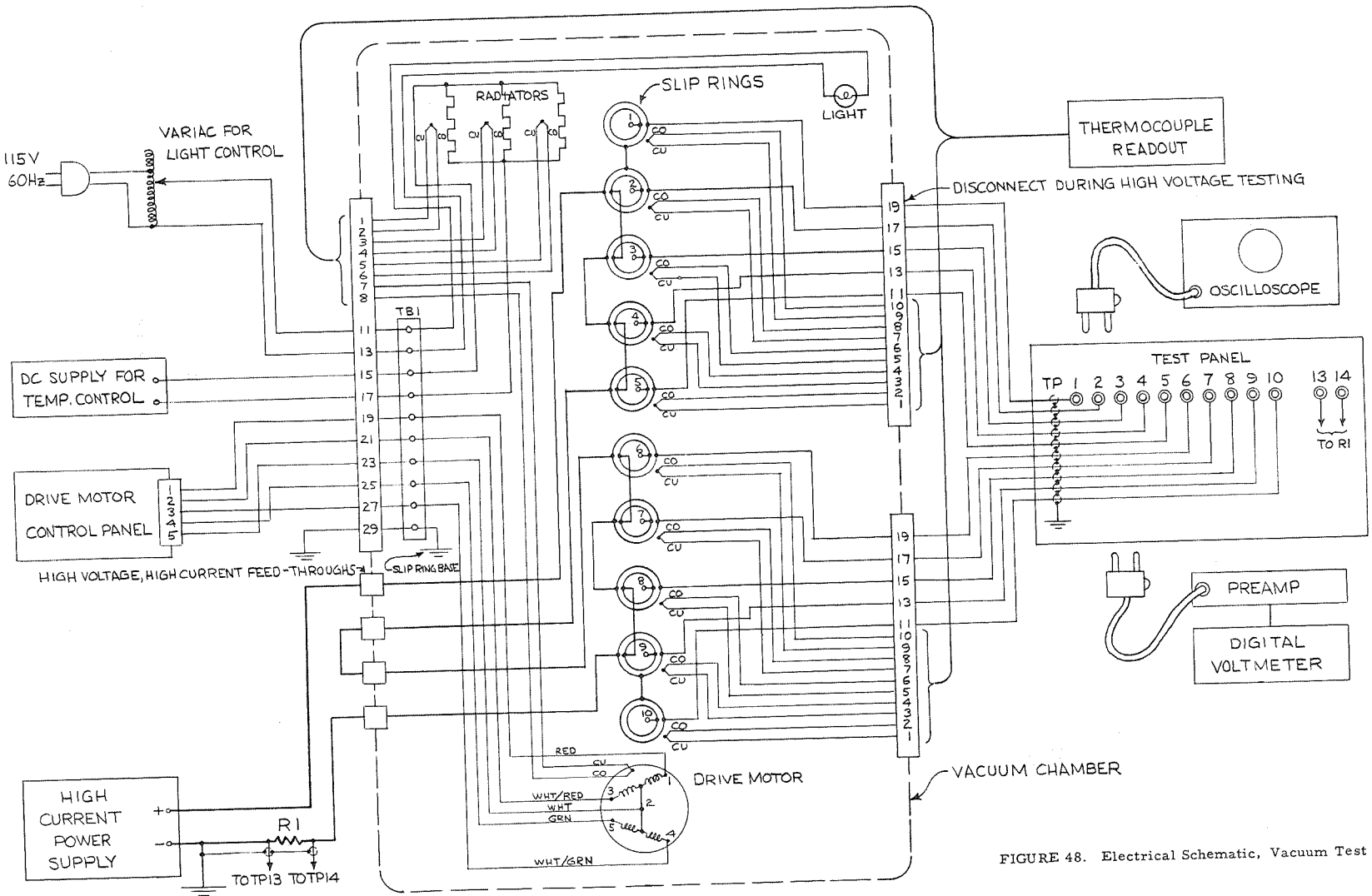

FIGURE 48. Electrical Schematic, Vacuum Test

from rings 6 through 9, but it was caught by the inter-ring insulation and was not visible.

"Twirlies" is the name we have given to helical formations of gallium residue which may roll up between the inner and outer rings of the radial gap configuration. They are the same diameter as the gap between the opposing unwetted portions of the ring. They appear to be caused by gallium oxide film which shears due to the shaft rotation, snags on the side wall of the radial gap and rolls up between the parallel unwetted outer lands of the inner and outer ring like a machining chip. They are cylindrical in form with their axes parallel to the shaft axes. The outside surface is wrinkled and silvery and probably is the oxide film. They were seen to grow as long as 0.06 inch beyond the ring and are typically 0.02 inches in diameter.

The gallium balls noted during pumpdown on the four twirlies on ring 10 were probably gas bubbles.

Twirlies also formed on the bottom of the rings but they could not be seen until the ETM was removed from the vacuum chamber.

Rotation was allowed to continue at 1 revolution per day in the hope that the twirlies might find their way back into the gaps. This did not happen. After 20 hours the vacuum was at 1×10^{-6} Torr (1.3×10^{-4} Nm^{-2}) and twirlies had formed all around concentric rings 6 and 7 and were bunched where the gap is narrow on eccentric rings 8, 9 and 10. Several more small drops were noted to have fallen from the bottom of ring 10.

The 100 A current was turned on 23 hours after the start of pumpdown.

After four days the vacuum was 5×10^{-7} Torr (6.7×10^{-5} Nm^{-2}) and the temperature was stabilized at 85°C (358K) in the rings (2 through 9). which carry current. The twirlies on rings 6 through 10 were generally swept into one or two irregular wrinkled piles about 0.06 inch wide, 0.04 inch high and 0.2 inch long which straddled the gap but primarily turned with the inner rings.

The largest pile was on ring 8. Ring 8 had been 100 percent filled with gallium. It has 0.020 inch (0.5 mm) T.I.R. radial runout and uses only nickel oxide as a barrier film. The gallium residue on this ring was a pile about 3/4 of an inch (2 cm) long and contained an estimated 0.2 gram of gallium. A full ring has 3 grams of gallium. The residue on the top of the remaining rings was less than 0.1 gram each.

The residue did not show significant change after the fourth day in vacuum. After two weeks the vacuum was 1.8×10^{-7} Torr (2.4×10^{-5} Nm^{-2}) and it was clear that twirlies were no longer forming. The top surface of the gallium in ring 8 could be observed where the gap was widest and it appeared to be level, smooth and flush with the edge of the groove.

It is important to note that rings 1 through 5, which have a significantly different configuration for retaining the gallium, displayed no tendency to

form twirlies or otherwise discharge gallium after the slight bubbling during initial pumpdown.

Barrier Films

The debris piles on the slip rings formed tracks on the end surfaces of the outer and inner rings adjacent to the gaps as they were carried around. The tracks consisted of many tiny balls of gallium, each less than 0.008 inch (0.2 mm) diameter). The tracks were quite distinct on rings 7 and 10 which had the perfluorinated polymer coating. There was very little track on rings 6 and 8 which used only the nickel oxide as a non-wetting barrier. Ring 9 had only a slight track despite the perfluorinated polymer coating probably because it had very little debris.

Slip Ring Drive

The step motor drive turned the slip rings at 1 revolution per day with an error on the order of 0.1 percent. At the slew speed of 20 RPD the time for 1 revolution was 72 minutes, 40 seconds, an error of 0.9 percent.

The slip rings were observed to not rotate during parts of 19 May and 20 May 1970 despite normal currents to windings of the stepper motor. This condition corrected itself and the slip rings turned reliably for the remaining four weeks of the test.

Electrical and Thermal Data

Temperature stabilization at 100 A in the vacuum occurred with an average ring temperature near 85°C (185°F, 358K) so data was not attempted at 30°C (303K). With a current of 200 A the temperature increased rapidly.

Table 22 presents the basic data collected near the beginning and end of the test. The voltage drops in the large copper conductors are so high as to swamp the 16 and 32 microvolt drops expected for full and half-full rings respectively at 100 A. The voltage data is between voltage taps on the outer rings. The combination indicated by "jumper on shaft" in the "Remarks" column of Table 22 include two slip ring gaps in series. The calculated 0.032 millivolts for the liquid metal gaps of rings 2 and 3 is very small compared to the 17 millivolts measured. Therefore, slight changes in temperature and current masked any changes in the slip ring gaps.

The voltages measured between rings 1 and 2 and between rings 9 and 10 where there was no intentional current are due to the location of the voltage taps slightly removed from the current taps. The large voltage between rings 5 and 6 includes the current busses on the ETM, the cables inside the vacuum chamber, the vacuum feedthroughs, a cable connecting the feedthroughs outside the vacuum chamber, and the contact resistance of eight connections. The power loss in this series is 22.5 watts at 100 amps.

The data at 200 A on 20 April was taken during a 20-minute period

following a 45-minute cooling period. Note the steadily rising temperatures at 1 rpd and then at 20 rpd, culminating in a temperature of 205°F (96.1°C, 369.3K) on ring 9. This relatively high temperature at ring 9 might partly be due to the resistance through the liquid metal gap, which may be higher for ring 9 than any other current-carrying ring because of its 50 percent fill and poorly wetted outer ring. The high temperature is more likely to be due to heating in the bus bar. Note the steadily rising temperatures in rings 2, 5, 6 and 9, which have outer ring bus bars attached, as time progresses.

It was necessary to use the thermal shroud heaters to maintain the ring temperatures above 80°C (176°F, 353K) after 23 April, increasing to 14 watts on 6 May. The radiator temperature then reached 200°F (367K), the limit for the black epoxy paint. The reason the heaters were needed was the slow decrease in temperature of the vacuum chamber due to the LN2 cold trap. Note the temperature of the drive motor, which is not covered by the thermal shroud.

The significant reduction in voltage drops at 100A between 20 April and 15 June are attributed to improvements in electrical contact resistance between the nickel-plated copper rings and the bare copper bus bars and jumpers due to the vacuum. The power loss in the rings and shaft reduced from 9.6 watts on 20 April to 8.3 watts on 15 June due to the lower contact resistances.

Resistance versus Shaft Angle

The voltage drops and currents through the current-carrying rings were measured every 30 degrees (0.524 rad) at a rotation rate of 20 revolutions per day on 30 April. The resistances were calculated and the averages subtracted for each ring pair. The deviations from average are plotted in Figure 49. There is a clear indication of sinusoidal variation. Fourier analysis was used to extract the best fit sinusoid. The data point at zero shaft position was discarded to reduce the effect of settling transients. Table 23 shows the resulting reduction in the deviations of the data.

The significant reduction in deviations after removal of the sinusoids indicates that factors such as ring eccentricity, wetting as a function of angular location on the ring, and the position of the current taps on the inner and outer ring may cause measurable variations in resistance as a function of shaft angular position. Note that rings 2 and 3 and rings 6 and 7, which are not eccentric, have larger sinusoidal variation than rings 4 and 5 which are purposefully eccentric.

TABLE 22. VOLTAGE AND TEMPERATURE DATA, VACUUM TEST OF ETM

Date	20 April	20 April	20 April	20 April	15 June	15 June	Remarks
Pressure, 10^{-8} Torr	47	47	210	270	3.6	3.7	Note increase with high current.
10^{-6} N m^{-2}	63	63	280	360	4.8	4.9	
Current, Amperes	101.7	101.7	203.7	207.4	100.4	100.4	Using R1, 100 μΩ
Rotation, rpd	1	20	1	20	1	20	
Millivolts							
Ring 1 to 2	+ 0.05	+ 0.04	+ 0.05	+ 0.06	+ 0.15	+ 0.15	No current
Ring 2 to 3	- 17.87	- 17.85	- 36.22	- 37.16	- 16.35	- 16.38	Jumper on shaft
Ring 3 to 4	- 2.26	- 2.27	- 4.24	- 4.29	- 1.26	- 1.28	Jumpers on outer rings
Ring 4 to 5	- 26.25	- 26.29	- 52.57	- 54.38	- 22.98	- 22.95	Jumper on shaft
Ring 5 to 6	-225.4	-225.4	--	--	-225.73	-225.80	Jumper outside vacuum
Ring 6 to 7	- 22.64	- 22.68	- 45.57	- 47.70	- 20.43	- 20.54	Jumper on shaft
Ring 7 to 8	- 1.41	- 1.49	- 3.07	- 3.19	- 1.24	- 1.22	Jumpers on outer rings
Ring 8 to 9	- 23.97	- 23.95	- 47.71	- 50.00	- 20.32	- 20.33	Jumper on shaft
Ring 9 to 10	- 0.04	- 0.03	+ 0.02	- 0.02	+ 0.15	- 0.18	No current
Ring 1, °F	155.4 (341.7K)	155.4 (341.7K)	146.4 (336.7K)	156 (342.1K)	161.3 (345.0K)	161.3 (345.0K)	No current
Ring 2, °F	180.0 (355.4K)	180.0 (355.4K)	166 (347.6K)	187 (359.3K)	176.7 (353.6K)	176.8 (353.6K)	
Ring 3, °F	179.0 (354.8K)	179.0 (354.8K)	167 (348.2K)	181 (355.9K)	175.8 (353.1K)	175.8 (353.1K)	
Ring 4, °F	157.7 (343.0K)	157.7 (343.0K)	148 (337.6K)	160 (344.3K)	161.4 (345.1K)	161.3 (345.0K)	Poor thermal connection
Ring 5, °F	186.4 (358.9K)	186.4 (358.9K)	169 (349.3K)	196 (364.3K)	182.5 (356.8K)	182.4 (356.7K)	
Ring 6, °F	187.6 (359.6K)	187.5 (359.6K)	169 (349.3K)	201 (367.1K)	186.30 (358.9K)	186.0 (358.7K)	
Ring 7, °F	179.7 (355.2K)	179.7 (355.2K)	167 (348.2K)	184 (357.6K)	178.8 (354.7K)	179.2 (354.9K)	
Ring 8, °F	186.0 (358.7K)	186.0 (358.7K)	173 (351.5K)	191 (361.5K)	184.0 (357.6K)	183.8 (357.5K)	
Ring 9, °F	185.7 (358.6K)	185.7 (358.6K)	171 (350.4K)	205 (369.3K)	183.2 (357.2K)	183.2 (357.2K)	Note at 200 A
Ring 10, °F	181.2 (356.1K)	181.2 (356.1K)	167 (348.2K)	184 (357.6K)	179.3 (355.0K)	179.5 (355.1K)	No current
Radiators, °F	139.3 (332.8K)	139.3 (332.8K)	134 (329.8K)	137 (331.5K)	198.5 (365.7K)	198.7 (365.8K)	Heater not on, 20 April
Drive Motor, °F	124.3 (324.4K)	124.4 (324.5K)	124 (324.3K)	129 (327.1K)	119.0 (321.5K)	119.2 (321.6K)	

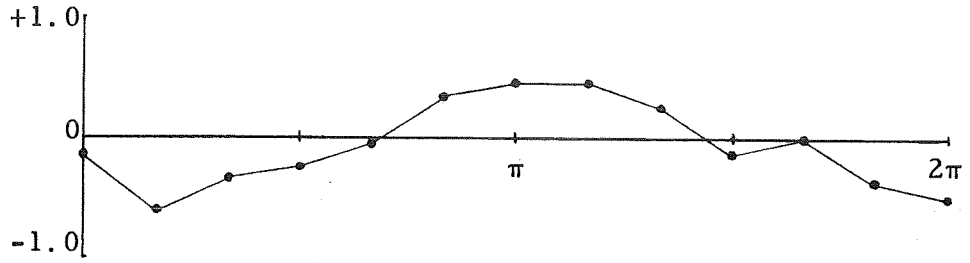

a) Rings 2 and 3

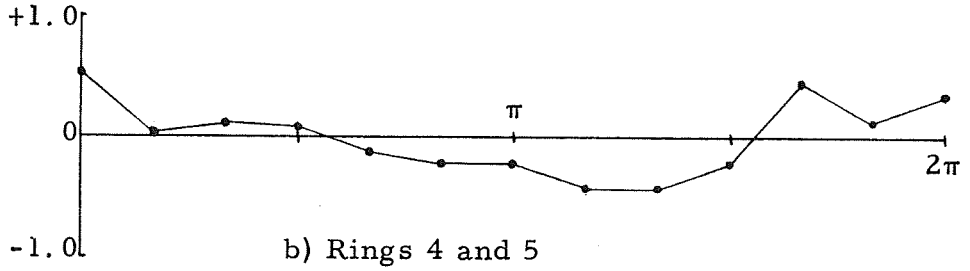

b) Rings 4 and 5

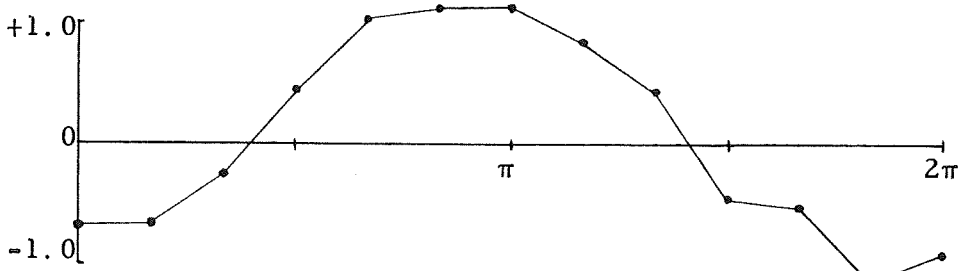

c) Rings 6 and 7

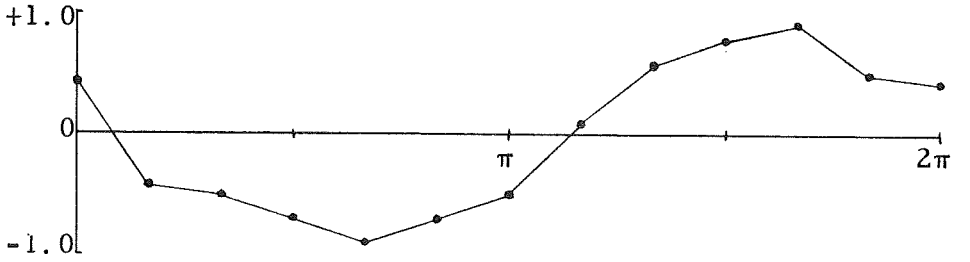

d) Rings 8 and 9

FIGURE 49. Variation of Slip Ring Resistance with Shaft Angular Position

TABLE 23. Sinusoidal Component of Resistance vs Shaft Angle Data

(All Figures are Microhms)

Rings	2 and 3	4 and 5	6 and 7	8 and 9
Standard deviation before extraction of sinusoid	0.33	0.31	0.67	0.64
Amplitude of best fit sinusoid	0.48	0.31	1.11	0.87
Standard deviation, sinusoid extracted	0.10	0.16	0.13	0.12

Electrical Noise

The electrical noise was examined with an oscilloscope connected across the voltage taps of the rings in pairs 2 and 3, 4 and 5, 6 and 7 and 8 and 9. With the vertical scale factor at one millivolt per centimeter there was no noise visible that was not synchronous with the 60 Hz line and thus attributable to sources other than the slip rings. Notice was particularly taken of possible noise occurring when the drive motor was stepping but nothing could be seen at 1 rpd or 20 rpd. Electrical noise across any of the ring pairs was thus much less than 100 microvolts peak to peak.

High Voltage Testing

High voltage was applied to rings 1 through 5 while 100 amps continued to flow through rings 6 through 9 at low voltage. All connections to rings 1 through 5 were removed on the outside of the vacuum chamber except for the current bus to ring 5 which was used to introduce the high voltage. Current busses, voltage taps and thermocouples remained connected inside the vacuum chamber. Note that rings 1 through 5 are connected together with very low resistance.

On 1 May 1970 the application of 1000 volts to ring 5 caused a breakdown somewhere in the vacuum chamber. Leakage current went to 700 microamps and the ionization gage was overloaded. The ionization gage was then turned off. The illuminating light had burned out earlier in the day so the inside of the chamber was quite dark. High voltage was again applied until breakdown occurred at 1100 volts but no corona discharge could be seen.

Continuous application of high voltage over a period of 30 minutes caused the leakage current meter to jump to a peak current, which caused the voltage to drop. As the voltage increased the breakdown would again occur. After 30 minutes the voltage was varying between 1700 and 1900 volts with peak leakage current of 400 microamps. No corona discharge was observed on the rings.

It is believed that the discharge took place where a 39-pin connector attaches the voltage taps and thermocouples from rings 1 through 5 to the vacuum feedthrough inside the vacuum chamber. This location is inside a projecting tubing (see Figure 47) and the pressure was probably in the corona region between the faces of the connector and the vacuum feedthrough.

The full 3000 V was successfully applied for 30 minutes on 2 June 1970. The pressure as indicated by the ion gage went from 4.5×10^{-8} Torr (6.0×10^{-6} N m^{-2}) to 2×10^{-7} Torr (1.7×10^{-5} Nm^{-2}) in the first 15 minutes and was then turned off. The leakage current remained steady at 25 microamps, indicating an insulation resistance of 120 megohms for rings 1 through 5 and their bus bars, power cables, instrumentation cables and connectors in the vacuum chamber.

On 16 June 1970 3000 V was again applied for 10 minutes, the last electrical test. Leakage current was down to 20 microamps. The voltage control was turned to the upper stop. The voltage resulting was off the meter scale but the current went to 30 microamps, indicating a potential in excess of 4000 V.

Post-Test Examination

The thermal vacuum testing of the ETM was completed on 16 June 1970 after 60 days at pressures less than 10^{-6} Torr (1.33×10^{-4} N m^{-2}), temperature of 85°C (358K) and 100 amperes of current through 8 of the 10 rings.

Gallium Debris and Contamination

A concerted effort was made to exclude air from the ETM while samples of the surface debris were collected. The vacuum chamber was back-filled with argon, and a plastic sheet was taped in place around the bell jar to dam in the heavy gas while the bell jar was lifted and a plastic bag placed over the ETM. This bag was sealed with tape and continuously flushed with argon. Samples were obtained through slits cut in the tape.

These precautions did not forestall the appearance of a dark powder on the insulator below ring 10 and under the gallium gap. This dark powder may have been on the insulator since the formation of the debris during pump-down, but was invisible until the atmosphere changed its color.

All lumps of gallium residue, including a shiny drop below ring 10, appeared to shrink 50 percent during back fill of the vacuum chamber with argon gas.

Samples of the grey residue from the twirlies and of the dark powder were collected for analysis by X-ray diffraction. These samples were sealed

in an argon atmosphere. Samples were also collected of the gallium from each ring and of the residue and subjected to analysis by emission spectrograph. Table 24 tabulates the emission spectrograph results. Note that for rings 6 through 10 the copper is low but the nickel is high.

The report of X-ray analysis states that ". . . no oxides, hydroxides, nitrides, or other atmospheric reaction products of gallium, nickel, or copper exist to a measurable extent." The dark powder showed a few very faint reflections of d = 2.14A, d = 2.0A and d = 3.1A. These could not be matched with any data in the ASTM X-ray diffraction file. This pattern is considered to be more characteristic of intermetallic compounds than oxide or hydro forms. The report of X-ray analysis is given in Appendix C.

The contamination of the gallium came in three forms:

- Grey debris rolled up from the gallium (twirlies)
- Lumps in the liquid gallium, herein called sludge
- Dark powder which seemed to spray from the gallium surface

The twirlies and sludge are spongy and gelatinous and they freeze when the gallium in them freezes. It seems likely that both are formed of the surface film when gallium is exposed to air. The twirlies contain many voids. Heat to over 100°C does not significantly change the resiliency of a twirly or dissolve sludge. The substance which provides the semi-solid consistency remains unidentified.

The gallium readily froze at room temperature and the ETM was transported to the clean room for examination and disassembly in the flow bench.

Examination of Slip Ring Drive

On disassembly, it was found that many flecks of MoS_2 lubricant had fallen to the top of the stepper motor from the harmonic drive. No other evidence of malfunction was found. It has been concluded that the faltering rotation was due to heavy loading of the drive compounded by a fleck of solid lubricant lodging in the gearing. The heavy loading could be expected due to the shaft heating of more than 8 watts at 100 amperes. This caused it to expand relative to the three posts which space the ball bearings and produced a high thrust loading on the bearings. The fleck of solid lubricant was displaced by the constant torque pulsing from the stepper motor.

Electrical Breakdown of Lamp Circuit

Examination of the ETM disclosed that extensive arcing had occurred from one line of the illuminating lamp circuit to the stainless steel base of the ETM across the surface of a Bakelite terminal strip. Strangely, this breakdown did not occur between the much more closely spaced terminal

TABLE 24. CONTAMINATING ELEMENTS FOUND IN GALLIUM FROM ENGINEERING TEST MODEL AFTER THERMAL-VACUUM TESTS

(All Values in Parts per Million)

Ring No.	Sample No.	Cu	Ni	Be	Mg	Cu	Remarks
1	1	20					
	11	19					
2	2	21					
	12	21					
3	3	260					
	13	21					
4	4	11	6				
	14	19		3			No known source of beryllium
5	5	33					
	15	20					
6	6	4	17				
	16	2	27				
	21	6	600				Grey debris
7	7	9	40				
	17	6	86				
	22	< 2	34				Grey debris, small sample
8	8	0.5	19				Ring 8 had least sludge, most debris
	18	0.6	8				
9	9	0.4	170				Ring 9 had least debris of rings 6-10
	19	2	160				
	24	0.7	22		5	0.4	Grey debris, large sample
10	10	< 0.4	58				Ring 10 had most sludge
	20	< 2	1100				Small sample, less sensitive
	25	< 2	68				Grey debris, small sample

screw and the base. The arcing probably took place during pumpdown and was due to corona discharge (see Figure 50).

The illuminating lamp burned out after two weeks when it was adjusted to full 115 volts to try to balance the temperature distribution across the rings. The 40-watt appliance bulb was clearly not able to dissipate this power adequately in the vacuum.

Resistance

The electrical resistance from each outer ring to its corresponding inner ring remained below the 0.2 milliohm threshold of the impedance bridge used, including the effect of rotating the slip rings. The insulation resistance was found to be decreased from 300,000 megohms to 190,000 megohms.

Post-Test Examination of Slip Rings

Each slip ring was found to contain soft lumps or sludge in the gallium (see Figure 51) ranging from an estimated relative volume of less than 10 percent in ring 8 to 50 percent in ring 10. Ring 8 had the most external debris, was 100 percent filled, and was eccentric. The gallium wetted the previously unwetted lands at the narrow gap, forming a ramp which probably carried the surface debris out (see Figure 52). Ring 10 was only 50 percent full and eccentric and therefore had a large area of gallium exposed to the atmosphere before testing.

Rings 1 through 5 had moderate sludge but only one small twirly, which lodged in the reservoir of ring 2.

In Figure 52 near the right-hand post will be seen one of the few pieces of surface debris which remained after collection of samples for analysis. This fragment was formed as a twirly. In Figure 52 on top of the inner ring insulator are some very small fragments from the bottom of ring 7.

The gallium in the gap at the right is seen to have wetted the outer land of the radial gap and now comes nearly flush to the edge of the ring.

The shaft and posts of the ETM were not damaged by the assembly, testing or disassembly. They are shown in Figure 53. The slight surface stain is nickel transferred from the rings while sliding them on and off with no lubricant in the close fits. The nylon-tipped set screws which hold the outer rings were found to be snug but were not tight after the testing.

Figure 54 shows the outer rings of the cup gap configuration before the gallium was removed. The shiny gallium exaggerates the slight unevenness of the gallium on the wetted lands in the reservoirs. Compare to Figures 38 and 46. Rings 4 and 5 were not rewetted at final assembly and it appeared that the gallium did not penetrate to the inner reservoir in these rings. Ring 5 was only 50 percent filled with gallium. Figure 54(f)

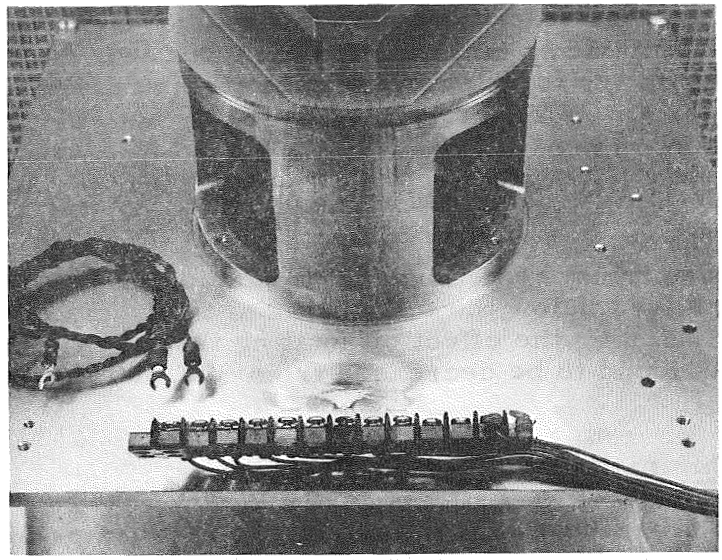

FIGURE 50. Discoloration and Tracking due to Electrical Breakdown of Lamp Circuit

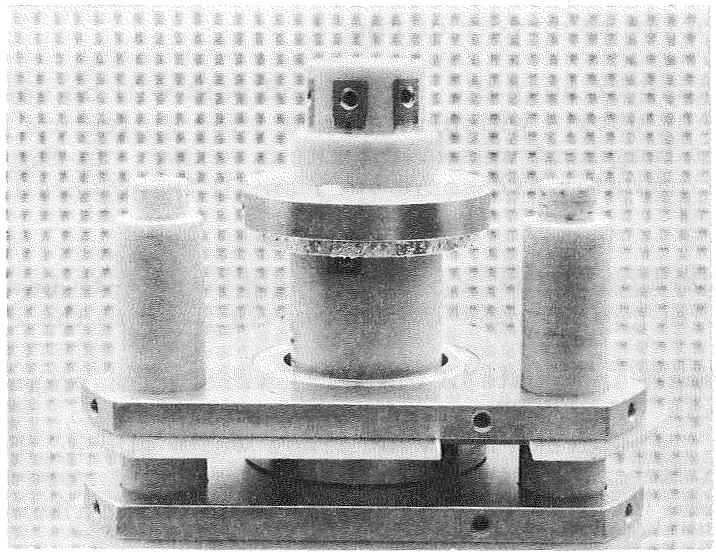

FIGURE 51. Gallium Sludge on Ring 1 at Disassembly

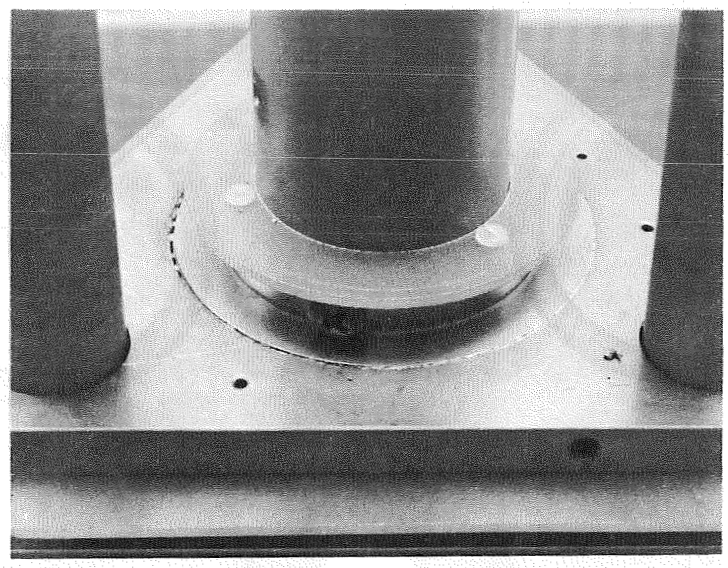

FIGURE 52. Ring 8 Prior to Disassembly

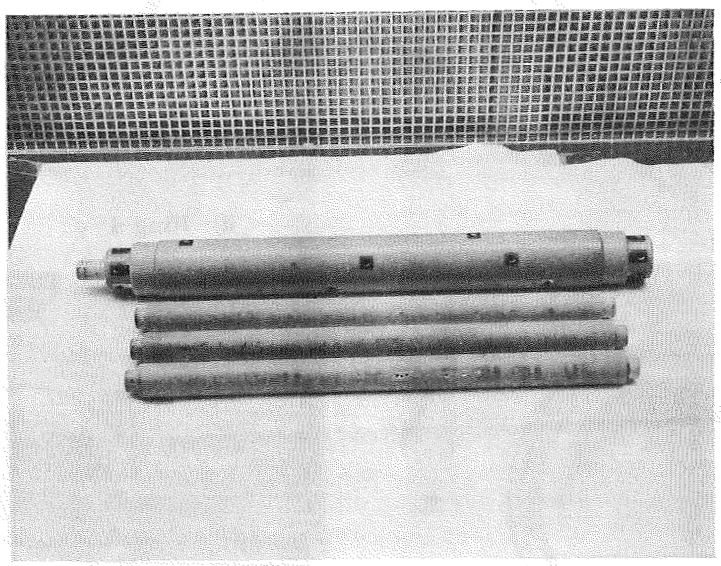

FIGURE 53. Shaft and Posts After Disassembly of ETM

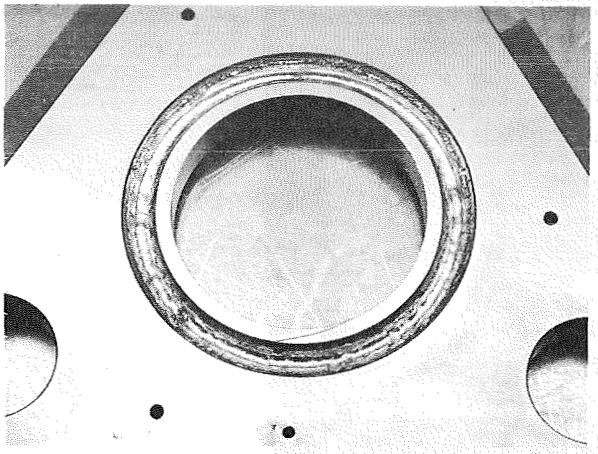

a) Ring 1

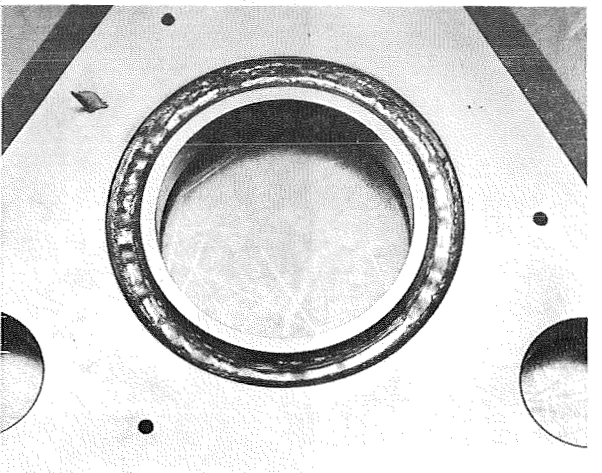

b) Ring 2

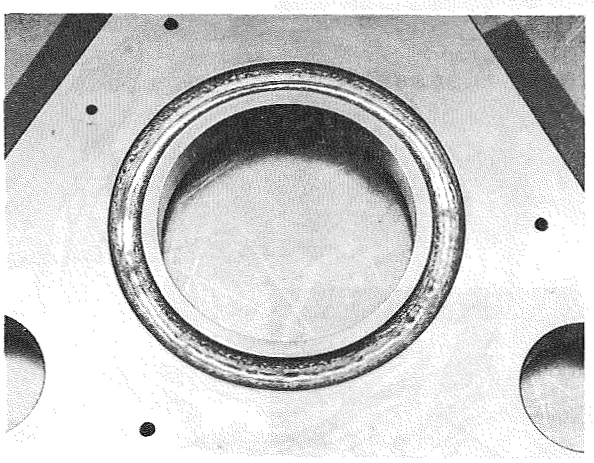

c) Ring 3

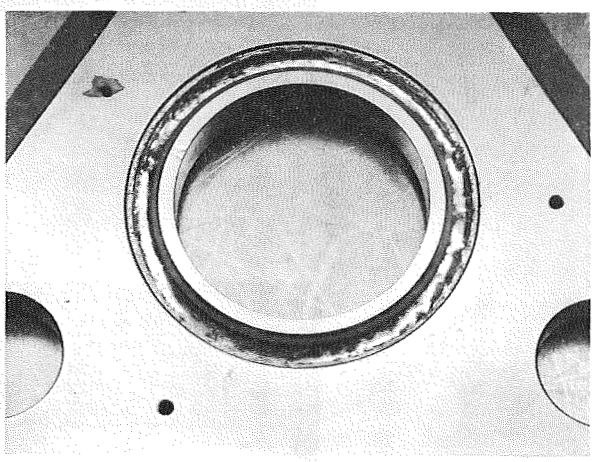

d) Ring 4

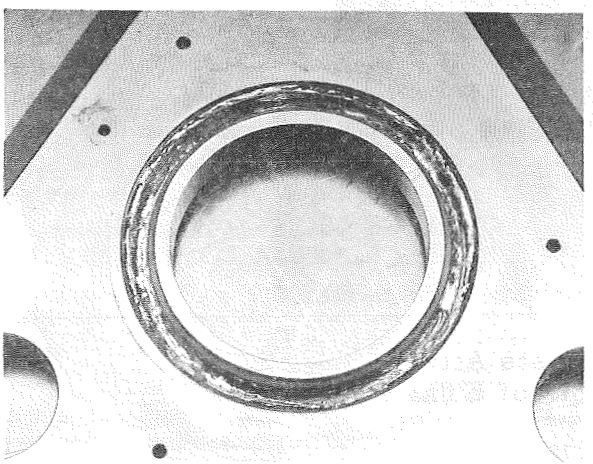

e) Ring 5

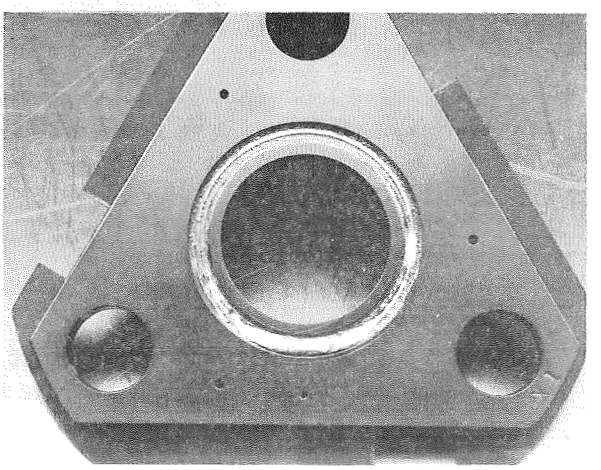

f) Ring 1 tilted

FIGURE 54. Cup Gap Outer Rings After Thermal Vacuum Testing

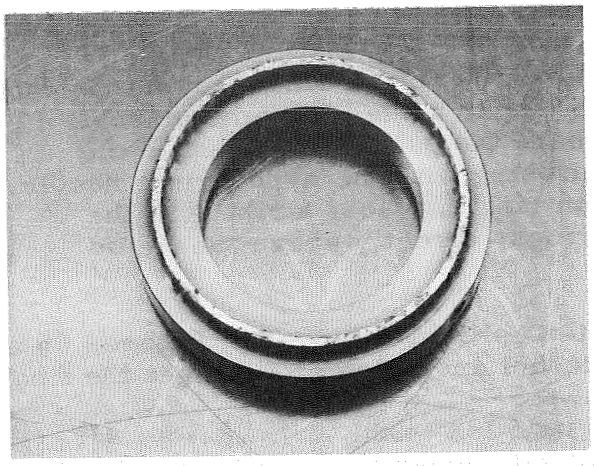

a) Ring 1

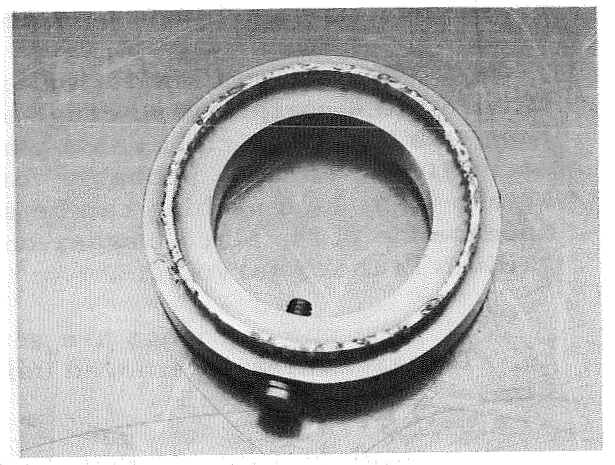

b) Ring 2

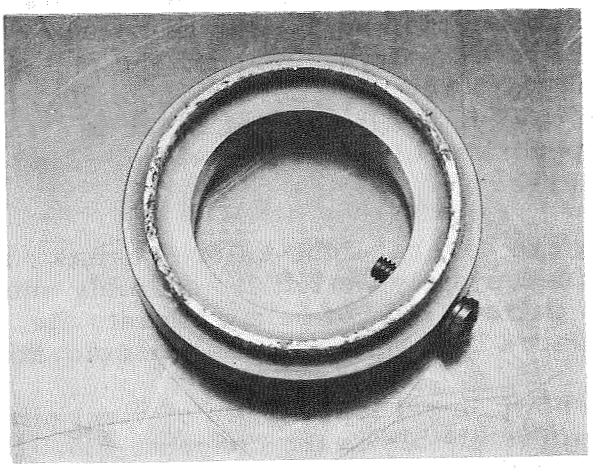

c) Ring 3

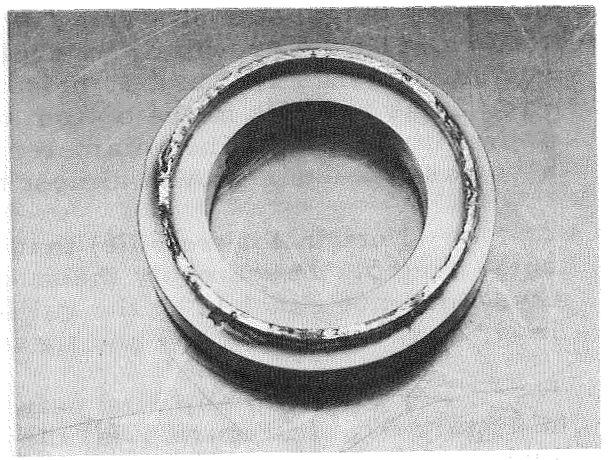

d) Ring 4. Note black powder.

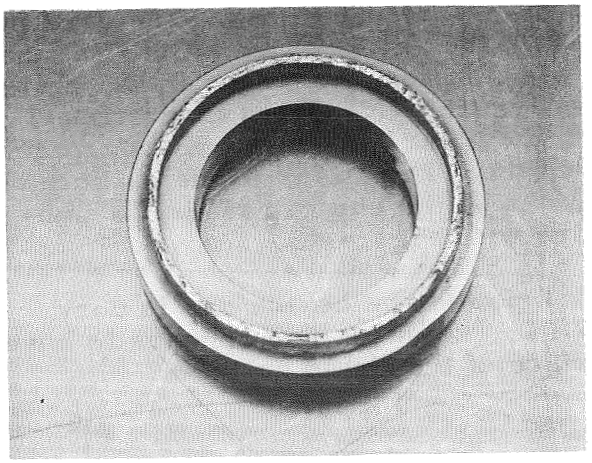

e) Ring 5

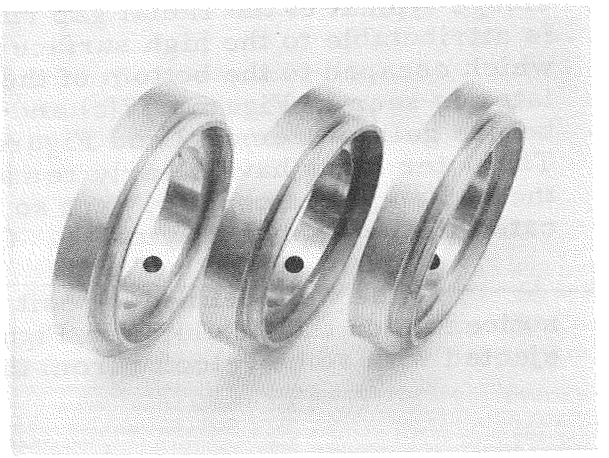

f) Rings 1, 2, 3 after gallium removal

FIGURE 55. Cup Gap Inner Rings After Thermal-Vacuum Testing

shows ring 1 tilted to display its load of gallium and the way the wet-nonwet boundary is still observed. The surface of the gallium has many wrinkles due to the surface film. Rings 3 and 5 have the slight stain from the brushed-on perfluorinated polymer barrier film.

The cup gap inner rings are shown in Figure 55. The sharp edges of the wetted portion were rough and no longer wetted in some places. Ring 4 in the lower right has a place where the gallium has wetted the normally unwet land, probably during probing with the hypodermic needle. Marks from such probing can be seen on ring 2. Most striking is the appearance of the black powder on all rings, directly above the liquid gallium in the reservoirs.

The cup gap rings are seen after gallium removal in Figures 55 and 56. The gallium was removed using alcohol and nylon cloth to get the final film.

Note in Table 25 that the dissolved copper is much higher in rings 1 through 5, which are the cup gap configuration. This is probably due to a thinner deposit of nickel over the copper in the outer ring cavities. This is borne out by greater blistering of the nickel-plated surface in these outer rings and by the growth of several small gallium crystals under the nickel surface of rings 1, 2 and 3; those which were rewetted during assembly. Ring 2 has two pits in the bottom of the cavity, the largest of which is approximately 0.01 inch diameter by approximately 0.01 inch deep. Ring 2 also has a bulbous growth almost this large.

Note in Figure 56(e) that there are several light-colored areas on outer ring 5. Presumably these were inadequately wetted at assembly and thus were not attacked by the gallium. Gallium did not penetrate into the inner reservoir of ring 4 and these surfaces have only minimal discoloration.

Radial gap slip ring pair 6 is shown in several stages of disassembly in Figure 57. In Figure 57(a) the gallium is visible in the concentric 0.020 inch (0.5 mm) gap. There is no debris on the inner ring insulator from cup gap ring 5 which was above it. Figure 57(b) shows the film curtain and the sludge typical of the radial gap rings as they were separated. The curtain is attributable to the high surface tension of the gallium. Some of the gallium which escaped to the bottom of the ring via twirlies and lodged in the insulator is seen in Figures 57(c) and 57(f). Figure 57(d) shows inner ring before gallium removal and Figure 57(e) the outer ring with gallium removed. The outer lands have clearly remained unwet. The attack of the gallium on the nickel-plated copper is not so severe as on the cup gap rings, as indicated by the lighter grey color. Compare with Figure 43.

The well-defined deposit of black powder below the gap is very noticeable on the insulator in Figure 57(f). The substance appears to have ejected with some velocity from the surface of the liquid gallium.

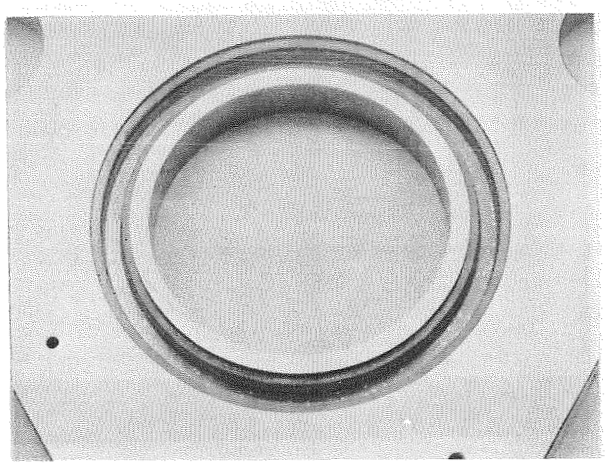

a) Ring 1

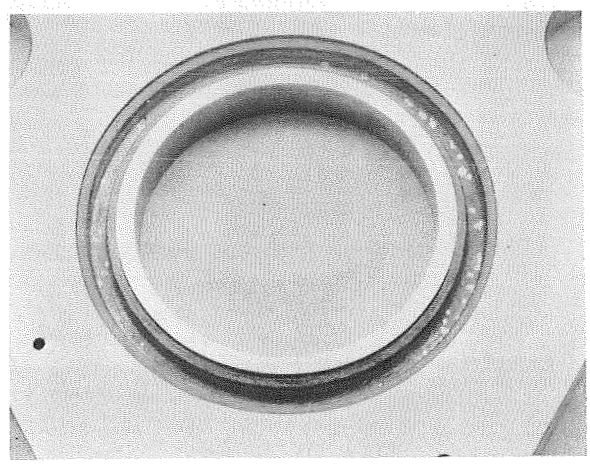

b) Ring 2. Note gallium crystals under nickel plating.

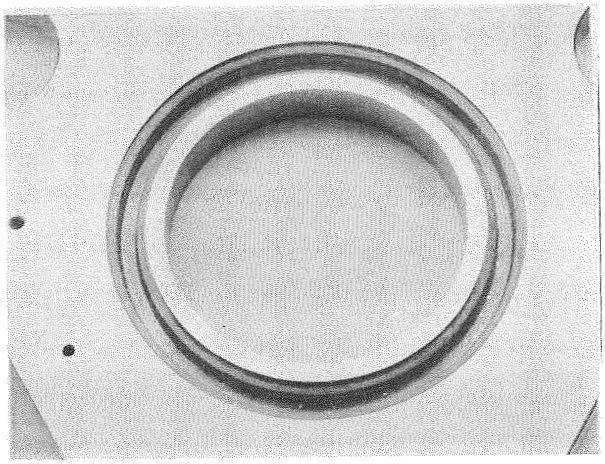

c) Ring 3

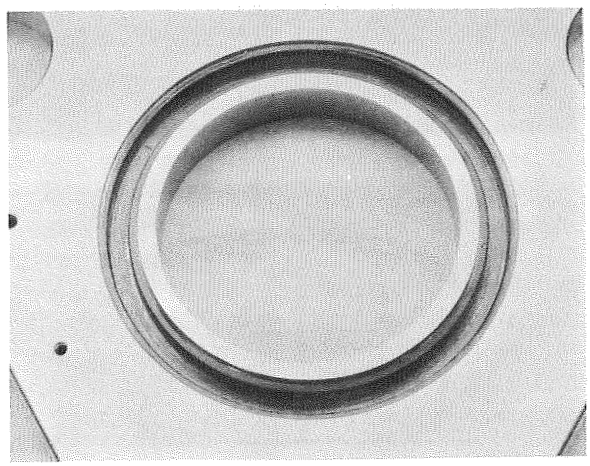

d) Ring 4

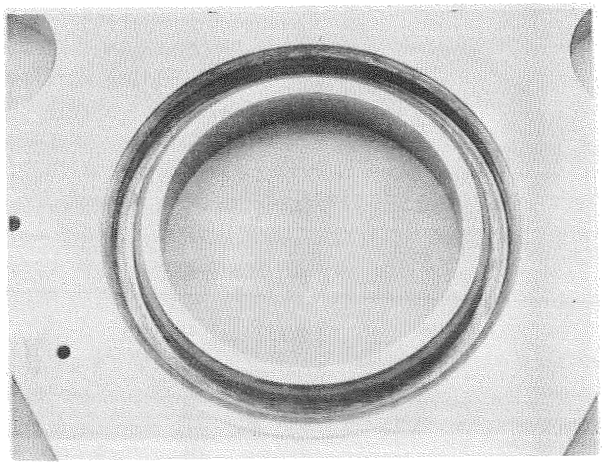

e) Ring 5. Note light-colored areas.

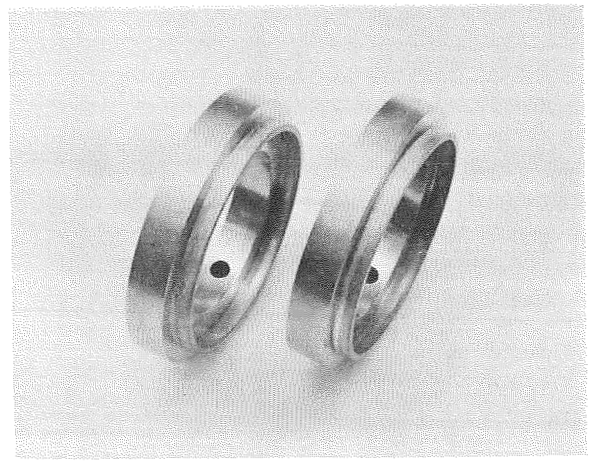

f) Inner rings 4 and 5

FIGURE 56. Cup Gap Rings with Gallium Removed

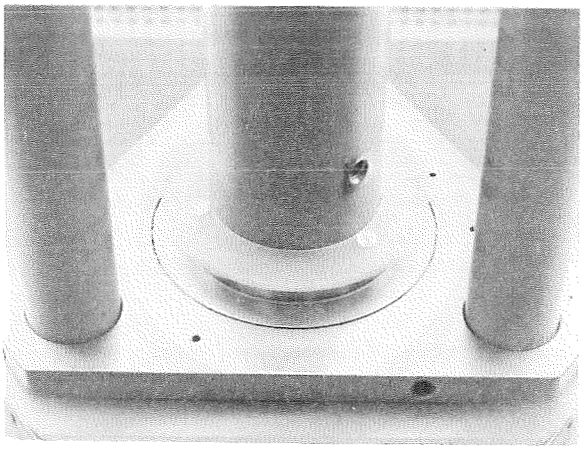

a) Rings in place on test model

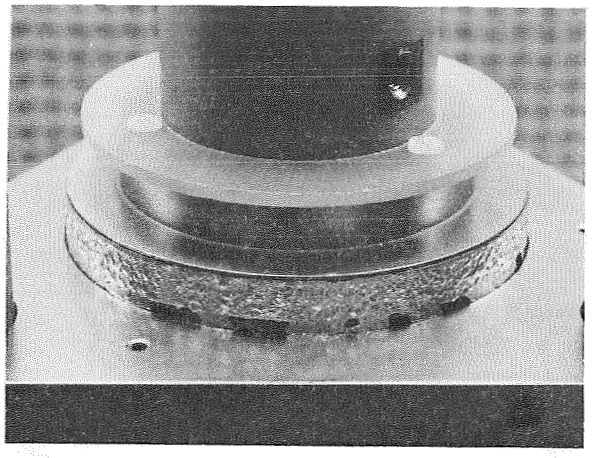

b) Gallium film during removal of inner ring

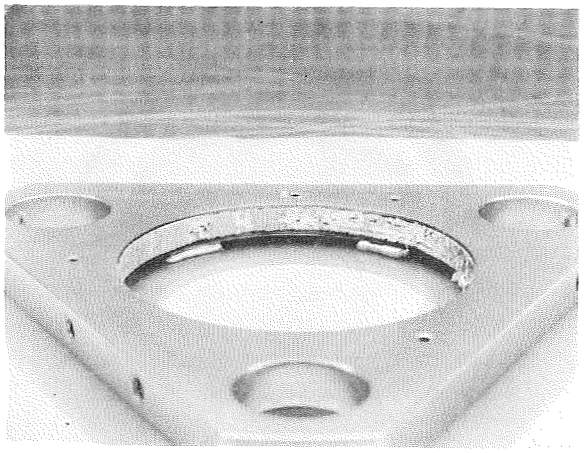

c) Outer ring with gallium

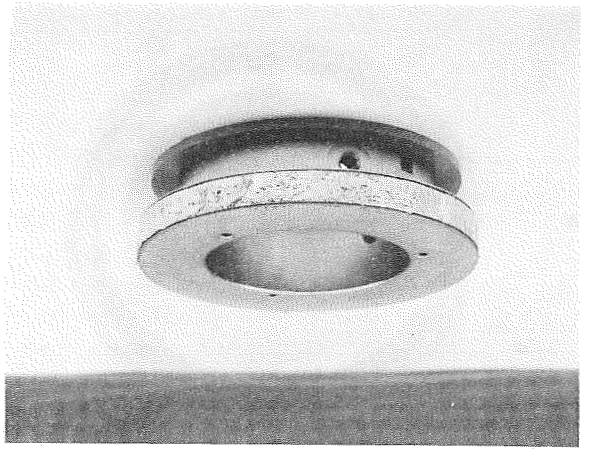

d) Inner ring with gallium

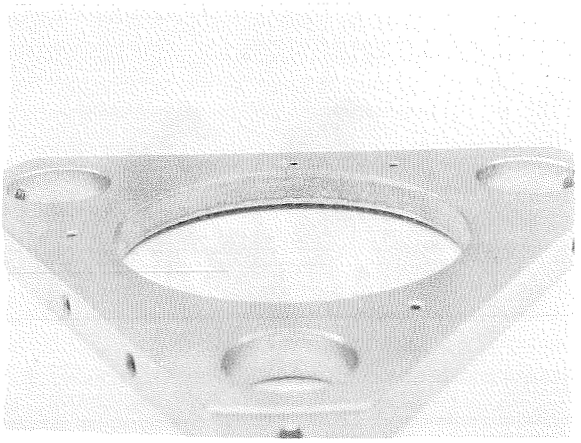

e) Outer ring with gallium removed

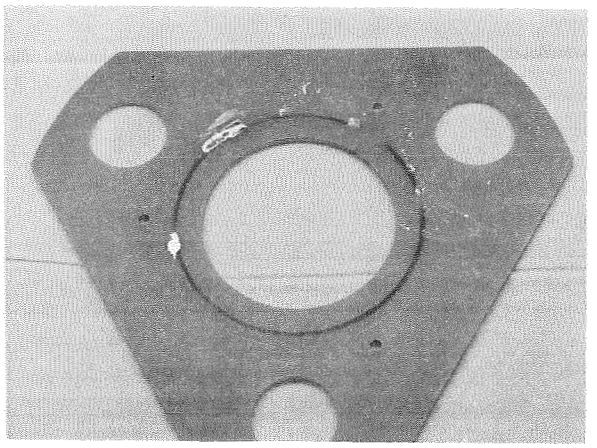

f) Insulator showing track of debris

FIGURE 57. Disassembly of Slip Ring 6

Figure 58 shows inner rings 6 through 10 after gallium removal. Attack by the gallium was mild, even in the damaged area of ring 9.

The gallium in the rings remained frozen during disassembly and it was necessary to use a heat gun to remove the inner rings. It was possible to remove ring 10 with the inner and outer rings bonded together by the frozen gallium as seen in Figure 59. Note the pendant drops formed during the radial motions when the other rings were removed. Note also the voids in the wide (0.03 inch, 0.75 mm) portion of the gap. Ring 10 had been only 50 percent filled and had lost several drops of gallium due to twirlies.

Figure 60 shows the outer ring insulators from the remaining radial gap rings. The black residue from ring 7 is comparable to that from ring 6. Surprisingly, ring 8, which had the most twirly residue, shows little black powder. Neither does ring 9, which had the least twirly residue. The ring 10 insulator is smudged by the gathering of residue samples. This insulator had been allowed to rest on the lower bearing plate during vacuum testing and some of the residue on it was thus visible through the view port. The black powder had not been visible until the argon (and some air) contacted the ETM.

Figure 61 shows the remaining radial gap rings. The low sludge content in ring 8 is apparent. Markings on inner ring 9 indicate that the gallium collected at the bottom of the ring and in the narrow (0.010 inch, 0.25 mm) gap portion but drained from the upper portion of the wide gap. See Figure 61(c). This drained area was lightly coated with the black powder. The markings in this coating are from probing for samples with the stainless steel hypodermic needle.

Ring 9 was identical to ring 10 except that ring 10 did not carry current and was thus at a lower temperature. Ring 9 had much less sludge than ring 10 and also much less black powder residue. Ring 9 had the least debris from twirlies and no drops came out of the bottom (see Figure 60(c)). Ring 9 thus had the best performance of the radial gap rings with respect to debris formation overall. Table 25 compares the 10 slip rings from several aspects.

The nickel surface of all rings was found to be grey when the gallium was removed from the wetted areas. Generally, the nickel areas which had been purposfully left unwet remained unwet. The exception was in the narrow (0.010 inch, 0.25 mm) gaps of eccentric rings 8, 9 and 10, where the outer lands became wetted. Surfaces which originally were not adequately wetted (to allow the gallium to immediately spread upon touching) were found to be mostly wetted after the long contact with gallium, but some such areas on ring 10 remained largely dry and showed little attack by the gallium. The grooves in the radial gap rings were almost entirely free of wetting and corrosion.

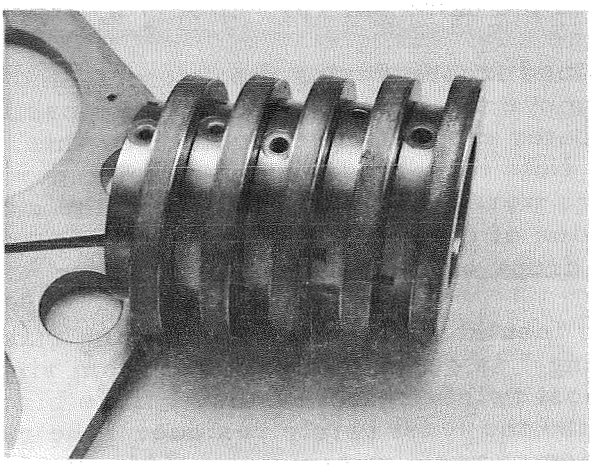

FIGURE 58. Radial Gap Inner Rings, Gallium Removed

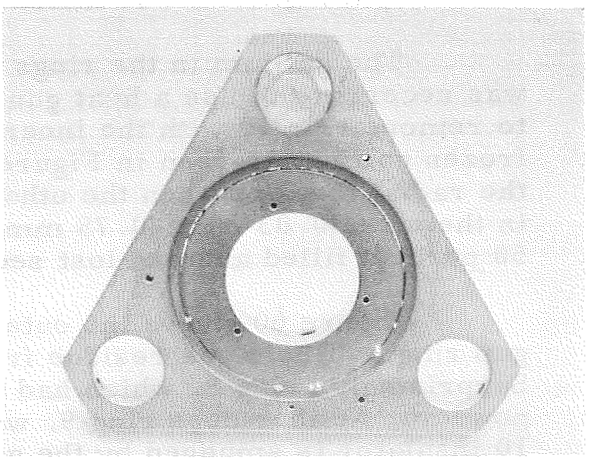

FIGURE 59. Ring 10, Gallium Frozen

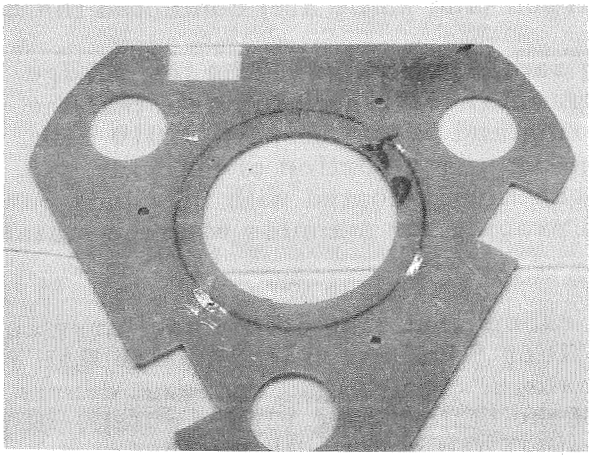

a) Ring 7

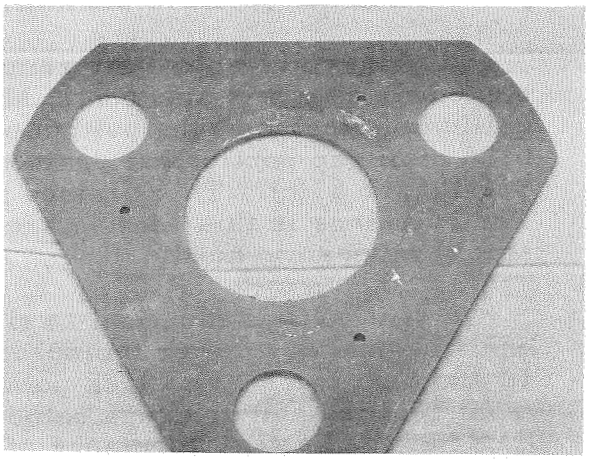

b) Ring 8

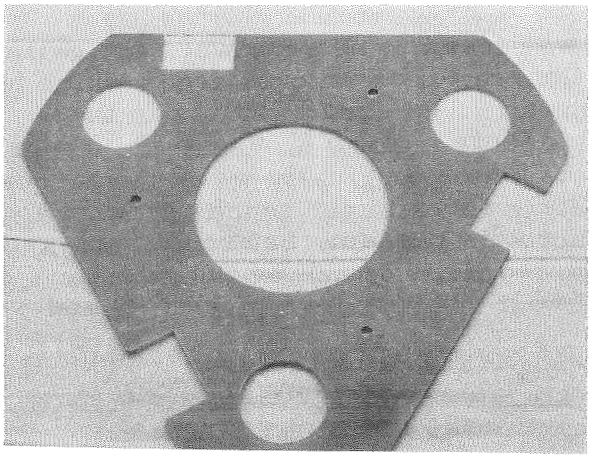

c) Ring 9

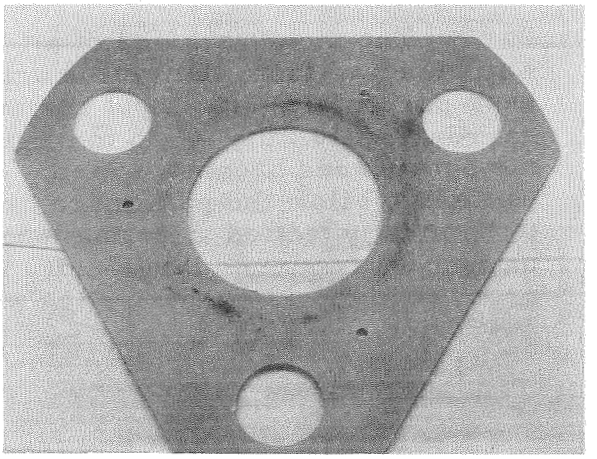

d) Ring 10

FIGURE 60. Insulators of Radial Gap Rings, Showing Black Powder Residue

Barrier Films and Insulators

The gallium debris did not wet the ring surfaces except where there was mechanical abrasion during sample collecting. It did adhere in small droplets to the perfluorinated polymer coating as previously described. This was probably due to the mechanical softness of the coating.

Figure 61(a) is mounted inverted to show its relationship to the outer ring below. The inner ring pictured was removed from the assembly in the attitude shown and positioned for photography without disturbing the debris pile which is seen to adhere to the bottom of the ring in preference to the epoxy-glass laminate insulator. It did not, however, wet the oxided nickel surface. The metallic gallium debris was readily removed from the coated and uncoated nickel surfaces and from the epoxy glass laminate using a soft nylon brush. The black powder tended to smear as seen in Figure 60(d) and required some wiping with solvent for removal.

Ball Bearings

The bearings were free with the gallium melted. The top bearing was clean. It turned freely and the balls were unmarked as observed under the microscope. Gallium was seen on several of the balls of the lower bearing. It is probably debris from ring 10. The bearing remained relatively free and the gallium was not frozen at 25 ^{o}C (298K).

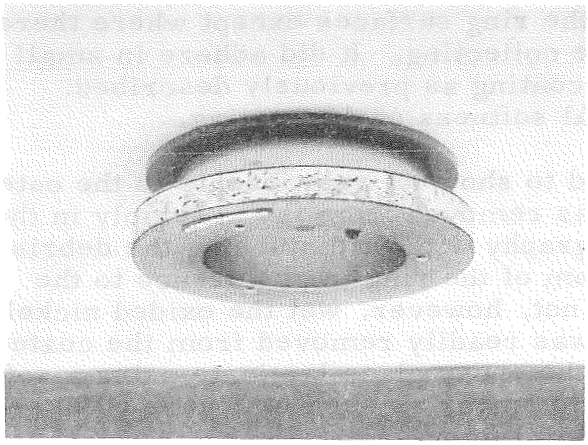

a) Inner ring 7 with gallium

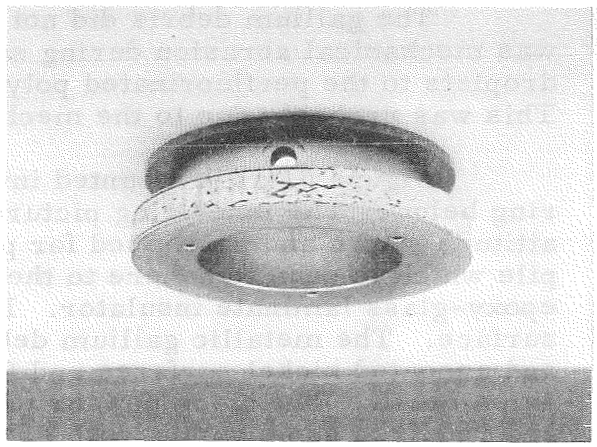

b) Inner ring 8 with gallium

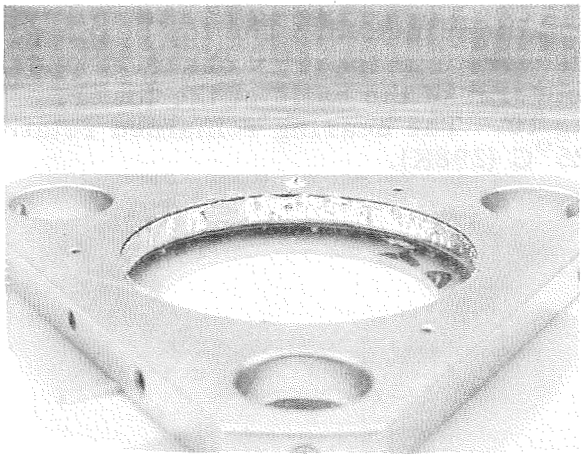

e) Outer ring 7 with gallium

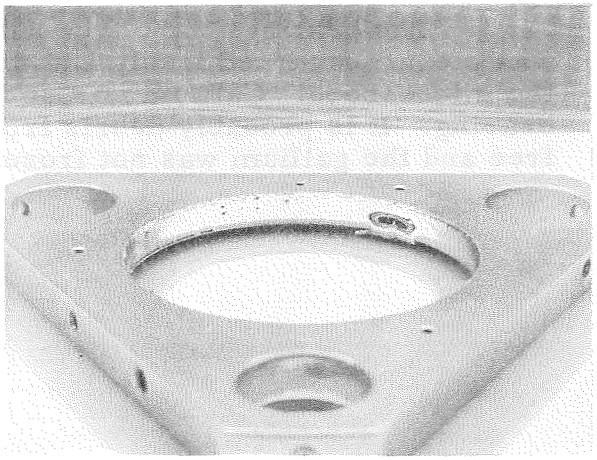

f) Outer ring 8 with gallium

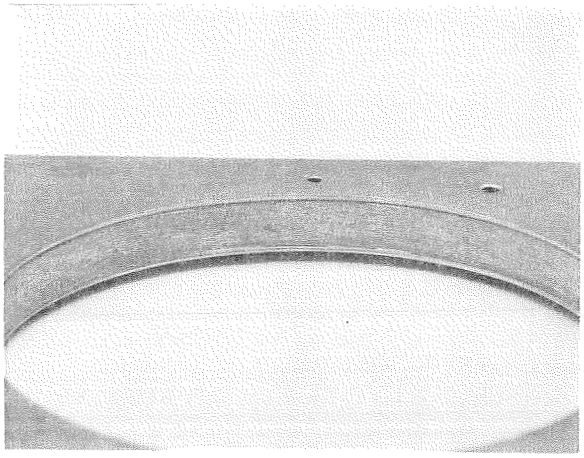

i) Outer ring 7, gallium removed

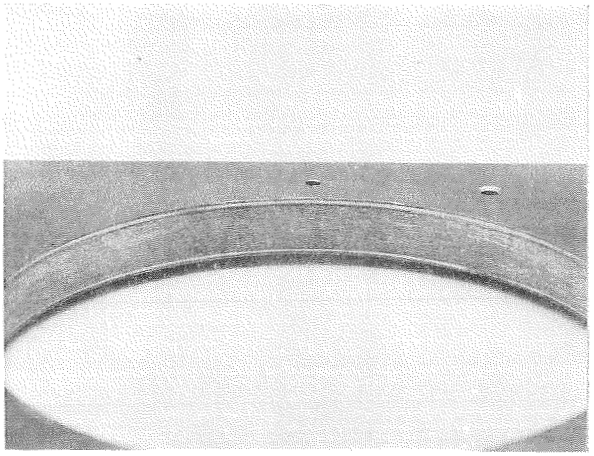

j) Outer ring 8, gallium removed.

FIGURE 61. Radial Gap Slip Rings at Disassembly

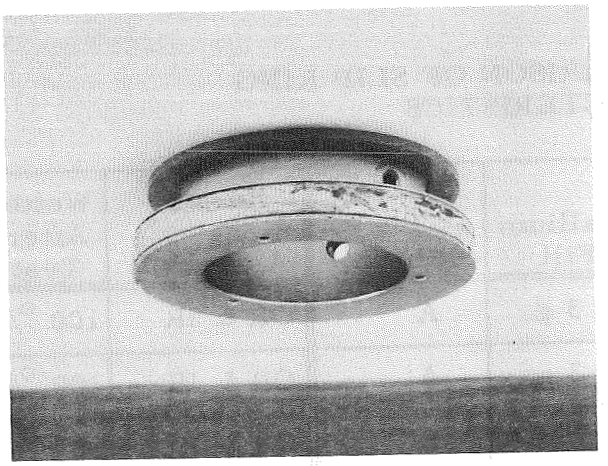

c) Inner ring 9 with gallium

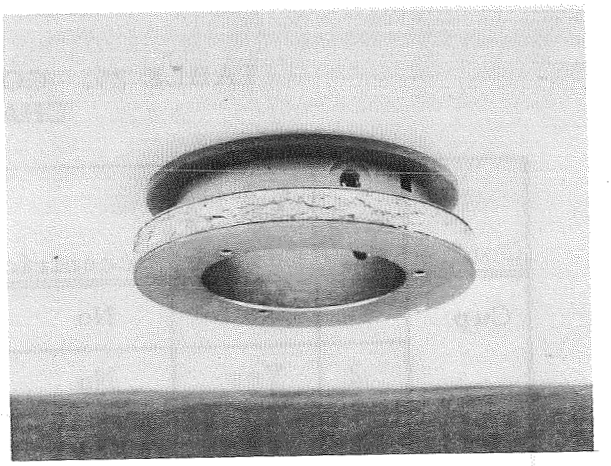

d) Inner ring 10 with gallium

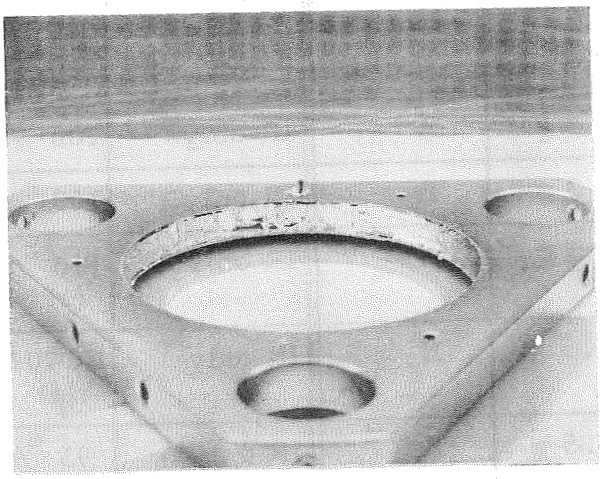

g) Outer ring 9 with gallium

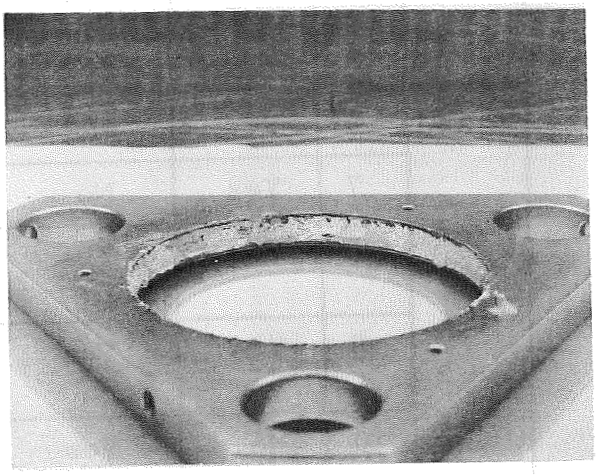

h) Outer ring 10 with gallium

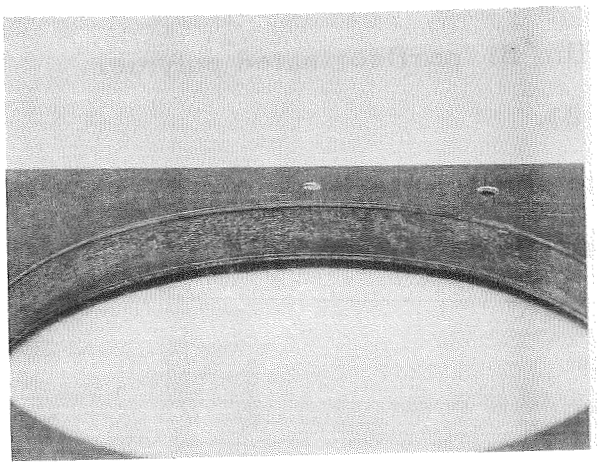

k) Outer ring 9, gallium removed

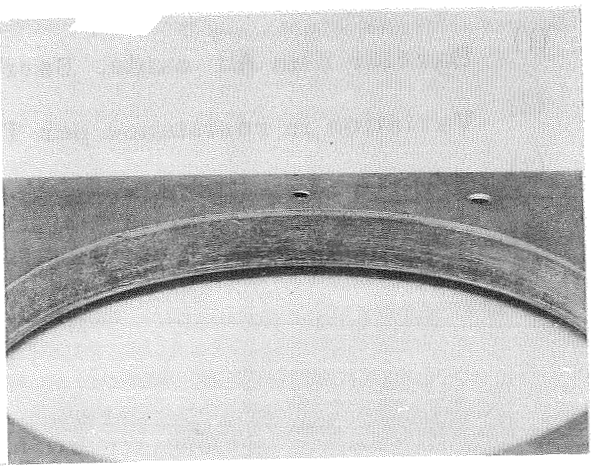

l) Outer ring 10, gallium removed

FIGURE 61. (concluded)

TABLE 25. COMPARISON OF SLIP RING CHARACTERISTICS

Conf.	Ring No.	Current	Eccentric	Gallium Fill	Film[1]	Rewet at Assembly	Wetted After Test
Cup	1	No	No	3 g	A	OR & IR	100 %
	2	Yes	No	3 g	A	OR & IR	100 %
	3	Yes	No	3 g	B	OR & IR	100 %
	4	Yes	Yes	3 g	A	No	80 %
	5	Yes	Yes	1.5 g	B	No	60 %
Radial	6	Yes	No	3 g	A	IR only	100 %
	7	Yes	No	3 g	B	IR only	100 %
	8	Yes	Yes	3 g	A	IR only	110 % (4)
	9	Yes	Yes	1.5 g	B	IR only	IR 70 % (4)
	10	No	Yes	1.5 g	B	IR only	95 % (4)

(1) Barrier film A: oxide, Barrier film B: perfluorinated polymer.

(2) Variation in resistance per Table 23.

(3) Gallium crystals under nickel plate of outer rings

(4) Barrier lands wetted, outer ring and inner ring.

TABLE 25. (concluded)

Debris			Sludge	Surface Corrosion	Variance in Resistance[2]	
Twirlies	Track	Black Powder			Sine	Random
None	--	little	25 %	much[3]	--	--
None	--	little	25 %	much[3]	.48	.10
One inside	--	little	25 %	much[3]		
None	--	some	25 %	varied	.31	.16
None	--	some	25 %	varied		
< .1 g	slight	much	25 %	little	1.11	.13
< .1 g	heavy	much	25 %	little		
.2 g	slight	some	< 10 %	some	.87	.12
< .05g	slight	some	25 %	some		
< .1 g	heavy	much	50 %	some	--	--

DISCUSSION OF RESULTS

Materials Selection

Electrode Materials

The criterion for good electrical performance was found to be good wetting of the electrode material by the liquid metal. The most readily wetted materials of those tested, beryllium-copper and nickel, were attacked and to some extent dissolved by gallium. Stainless steel wetted more easily after long exposure to gallium and the wetted surface turned slightly darker in color. Thus it appears that good wetting is associated with some chemical attack. This corresponds to the findings of Reference 5.

The reason that beryllium is noted in the literature as resistant to attack by gallium at high temperatures must be that beryllium quickly develops a surface compound in the presence of gallium and other contaminants which is electrically insulating and which inhibits further attack. Beryllium might be a successfull slip ring material if all contamination could be excluded. This would be quite difficult because beryllium is typically a sintered material and is thus filled with voids which trap contamination. The beryllium electrodes had very low voltage drops despite their poor contact resistance and there was only the one instance of deterioration in the static screening test.

The tungsten used in the material selection experiment was also a sintered material. This may be a factor in the poor wetting properties. The tungsten and the beryllium electrodes typically lost weight in the dry argon atmosphere and elevated temperature, presumably due to the evaporation of water and other volatiles. The poor wetting properties of tungsten probably stem primarily from its resistance to chemical attack by gallium.

The inertness of the tungsten to attack by gallium indicates that successful non-wetting slip rings might be made of tungsten if the high contact resistance were not objectionable. MEF 55 had a non-wetted electrode and high contact resistance, but the resistance did not show significant change during the 30-day screening test.

Beryllium-copper is considered a failure as an electrode material due to the growth of significant deposits on the electrode surfaces under the gallium. It may be expected that any copper-rich alloy would also be attacked by the gallium based on the similar deposits which later became evident on the nickel-plated copper electrodes.

The correlation of wetting properties with relative surface energies was not as expected. The surface energy of copper is much lower than that of tungsten (both are greater than gallium) but beryllium-copper wets readily with gallium and tungsten does not. The wetting method used in the materials

evaluation test, machining in a bath of liquid gallium, should provide the cleanest possible tungsten surface to the gallium, particularly since no trace of the carbide cutting bit was ever seen in the emission spectrograph results. On the other hand, low surface energy materials such as teflon were wetted by the gallium. Apparently the surface energy mechanism with respect to wetting is considerably different from the surface energy measured by ring removal or sessile drop methods. The surface tension of a liquid metal as measured by mechanical means may not be significantly lowered by a surface film composed of low surface energy contaminants. The surface contamination was visible during the ring pull tests on the gallium but did not appear to affect the results.

The choice of electrode materials based on the results of this project is divided between stainless steel and nickel. The nickel must apparently be a much thicker plating than used in this experiment if it is to protect copper. Gallium obviously can diffuse through nickel plating to attack vulnerable substrates. Preferably the nickel would be used in bulk.

There is some question as to the eventual extent of corrosion of nickel by gallium. The nickel-plated copper electrodes used in the screening and long-term evaluation tests showed an average weight gain in six months equivalent to an increase in nickel of 0.00076 inch (19.2 μm) over the surface wetted by gallium. The spread was from 0.00010 inch (2.6 μm) to 0.0016 inch (40.5 μm). This poor showing is undoubtedly due to the corrosion of the copper and to the rough machine finish more than to the corrosion of the nickel. The lowest figure was obtained with the most careful procedure and good surface finish and may be representative of solid nickel. This indicates a growth of 0.002 inch (50 μm) in 10 years, which should be acceptable using gaps of 0.020 inch (0.5 mm). It seems unlikely that the growth would continue at a constant rate. The contribution of nickel to the surface films and debris is not known, but the wetting and electrical properties of liquid metal slip rings with solid nickel electrodes and gallium fill would be excellent.

The stainless steel remained quite clean and excelled as a non-contaminating container for gallium. Several gallium samples from stainless steel material evaluation fixtures were found to contain no impurities measurable by the emission spectrograph. The surface film on the stainless steel was the best non-wetting coating found for metals. Stainless steel AISI 304 can therefore be recommended for use as a container for gallium.

The weight gain during six months for the stainless steel electrodes used in the screening and long-term evaluation tests was equivalent to an average increase in stainless steel thickness over the wetted area of 0.00009 inch (2.3 μm), with a spread from -0.00006 inch (-1.4 μm) to +0.00025 inch (6.3 μm). The apparent maximum rate of corrosion would result in a growth of 0.005 inch (125 μm) in 10 years. The visual evidence belies such a growth rate and it is believed to be mostly experimental error in weighing.

The high electrical resistivity is a drawback to the use of stainless steel for high current slip rings. One other questionable area was the change in resistance manifested by MEF 44 used with the gallium-indium-tin alloy in the screening test and again in the long-term evaluation test using pure gallium. The AISI 304 stainless steel is otherwise well suited for use as an electrode material for liquid metal slip rings.

It is expected that other metals will be found to have a moderate chemical attack by gallium which will result in good wetting properties and low contact resistance without excess deterioration.

Barrier Films

Barrier films were sought primarily to enhance the non-wetting characteristics of the bare electrode surface where the liquid metal was not wanted. None of the applied coatings (see Table 5) were as successful at resisting wetting by gallium as the natural oxide film on the metals, particularly stainless steel.

The other function desired for a barrier coating was electrical insulation. This requirement is still valid, particularly for slip rings to operate at very high voltages. These functions would best be separated in the slip ring configuration so that an insulating film could be chosen on the basis of its insulating properties. Most films so chosen will probably have adequate resistance to chemical attack by gallium. Gallium did not appear to attack the organic coatings tested and it was readily removed from them.

Insulators

Two very satisfactory structural insulators were found which have excellent resistance to wetting by gallium: epoxy-glass fabric laminate per L-P-509, Type IV, Grade G-10 and alumina ceramic, 96 percent pure. The remaining 4 percent consists of oxides of silicon, calcium and magnesium. There was no adhesion of the gallium to either of these materials. In this respect they were superior even to the oxide coating on the stainless steel. The gallium in contact with them was free of contamination except that attributable to dust. These materials can also be recommended for use in containers for gallium if precautions are taken to permit expansion of the gallium on freezing.

The epoxy-glass fabric laminate used is the product of a particular manufacturer and is green in color. Other manufacturers may use different epoxy resins and therefore may not have the same resistance to wetting by gallium. Note that in the barrier film testing the epoxy conformal coating was wetted by gallium. Testing of each product intended for use with gallium will be necessary.

Liquid Metals

The experience with the gallium-indium-tin alloy was limited but discouraging. The three cases of changes in contact resistance were in

material evaluation fixtures which were using or had used the alloy. The surface tension measured was 20 percent lower than pure gallium. No advantage is seen for the alloy except its low melting point. It was of interest to note that the alloy with its high percentages of alloy constituents other than gallium (21.5 percent indium, 16.0 percent tin) retained the tendency to supercool that is characteristic of pure gallium.

The gallium presented only a few problems in handling:

- The tendency to supercool
- The tendency to squirt (momentum-dominated behavior due to the high density)
- The formation of the semi-plastic surface film.

Another possible problem was anticipated and therefore gave no trouble: the expansion on freezing. A 4 milliliter glass beaker full of scrap gallium was collected to see if it would break when the gallium froze. It did.

The high chemical activity of gallium was expected to cause a problem, particularly on aluminum surfaces. In a peripheral experiment, gallium was placed in an aluminum foil cup. It rolled readily on the oxidized surface leaving no mark. When the cup was floated on water in an ultrasonic cleaning bath however, the gallium penetrated the .004 inch (0.1 mm) foil in seconds, leaving a hole which continues to increase in size at this writing, one year later. Epoxy coatings provided adequate protection from attack for the aluminum thermal chambers and glove box. The gallium was readily cleaned from work benches, tools and floors leaving no visible trace using alcohol as a "solvent".

The cost of the 0.999999 pure gallium required in the 10 large slip rings would be less than $30.00 if they were all full. Waste due to wetting was very small, less than 50 percent. The lower cost of lower purity gallium is probably not justified in view of possible increase in surface films.

The 108-day high vacuum exposure of 0.1 cm^3 drops of gallium on insulation and barrier film samples resulted in a measured weight loss of 0.28 percent. Assuming that all this weight loss is evaporation, the rate of evaporation is 1.0 percent per year for these samples with a large ratio of exposed area to volume. The gallium in a slip ring with only narrow edges exposed would evaporate at a much slower rate.

The utilization of the attractive properties of liquid gallium, such as low resistivity, low rate of evaporation and high surface tension has been adequately demonstrated to justify the selection of gallium as the most advantageous liquid metal for slip rings for the proposed spacecraft function of transferring high power from solar arrays. The surface film on gallium is the only problem for which suitable control measures have not been demonstrated.

Electrical Characteristics

The bulk resistivity of gallium, 28 $\mu\Omega$cm, is low enough that slip rings of a size and configuration that is mechanically feasible will almost always have a current-carrying capacity in excess of the attached conductors, provided that the interface resistance to the slip ring material is in the region of 10 $\mu\Omega$ cm^2 and below. This level of interface resistance was achieved on the 65 material evaluation fixtures tested with only three exceptions: one each for beryllium, stainless steel and tungsten. See Tables 9 through 13. Assume a current of 100 A, a surface area of 1.0 cm^2 between the gallium and each electrode, a gap (electrical path through the gallium) of 0.1 cm, and an interface resistance of 10 $\mu\Omega$ cm^2. The resistancethrough the gap is

$$R = \left[10(1.0) + 28(0.1) + 10(1.0)\right] \times 10^{-6} \text{ ohms}$$

$$R = 22.8\ \mu\Omega,$$

the voltage drop is $V = 100\ (22.8 \times 10^{-6}) = 2.28$ millivolts, and the power is

$$P = .00228(100) = 0.228 \text{ watts.}$$

This low power would readily be conducted away by electrical conductors which could handle 100 amperes. The assumed gap is the same as used in the material evaluation fixtures.

The power loss of 9.6 to 8.3 watts in the 8 rings of the ETM at 100 A is an average of 1.12 watts per ring at 85°C (358K). At room temperature this would be less than 1 watt per ring. The loss is from the outer ring current connection to a current connection on the end of the shaft, plus a small contribution from the jumpers. Two such "average" rings operated at 100 A with a potential of only 25 V direct current between rings would transfer 2.5 kW with an efficiency exceeding 99.9 percent.

The 10-ring assembly operated with 100 amps per ring and 3000 volts direct current between rings could transfer 1.5 megawatts with an efficiency of 99.9993 percent including the losses due to leakage current.

The conclusion is that liquid gallium slip rings can be smaller and lighter than any high power brush-ring combination known and still have excess current capacity. There is little likelihood of open circuit or overheating due to loss of gallium. The loss would have to be almost 100 percent.

High currents in large gaps may result in a sensitivity to magnetic fields. The forces involved are readily calculable. Motion of the gallium due to the sudden application of electric current was not observed during this project, even on MEF 41 which had a very poor fill of gallium and had a pendant drop of gallium to exaggerate any motion. The surface tension forces required to support the gallium for testing in earth's gravity will certainly retain the gallium in all but very strong magnetic fields.

The interface resistance was found to be below 1.0 $\mu\Omega$ cm^2 when good wetting was obtained between gallium and any of the five electrode materials tested. For the nickel-plated copper electrodes the interface resistance for 12 out of 13 MEFs was less than 1.0 $\mu\Omega$ cm^2 and for the four 20-ampere nickel-plated copper electrodes it averaged 0.07 $\mu\Omega$ cm^2. There seems a possibility that the variations measured were largely experimental error and that the interface resistance approaches zero as the wetting becomes 100 percent.

As a consequence of the very low resistance through a liquid metal slip ring with wetted electrodes the electrical noise is negligible. Electrical noise attributable to the slip rings was not identified during the project with the following exceptions:

- MEF 41, beryllium electrodes with gallium-indium-tin alloy as the liquid metal, showed a gradual increase in voltage drop at 20A from less than 0.5 millivolt to 40 millivolts in two days due to an increasingly unwet condition of one electrode.

- MEF 44, stainless steel electrodes with gallium-indium-tin alloy, showed a gradual increase in voltage drop at 20A from 292 μV to 350 μV in 30 days, probably due to an increasingly unwet condition.

Such gradual increases could readily be detected by suitable sentry circuits so that the likelihood of unanticipated failure of wetting and interface resistance is extremely remote. Tungsten MEF 55 operated reliably for the screening test period despite a poorly wetted electrode such as would have been detected at or before acceptance test of a prototype slip ring assembly.

The only variation in resistance attributable to the slip rings in the engineering test model was the cyclic variation with shaft angle. The maximum was 0.23 millivolt peak to peak at 100 A (see Figure 49c). This variation was several times the calculated resistance through the gap. The most likely cause of the measured variation was the placement of the high current connections at discrete locations on the inner and outer rings. When these connections on the inner and outer rings are 180 degrees (π rad) from each other, the resistance becomes a maximum. The effect is unlikely to be noticeable except at high shaft speeds.

Slip Ring Configurations

The design of a cross-section for a liquid metal slip ring gap is dominated by the following considerations:

a) Retention against acceleration (and possibly magnetic) forces.

b) Provision for relative radial and axial displacements of the slip ring rotor and stator, particularly during a shock to the spacecraft.

c) Avoidance of escaping residue and sludge.

Consideration of the electrical characteristics of the gap is likely to be unimportant unless the electrode material has high resistivity, such as stainless steel.

Other considerations in the design of prototype gallium slip rings are:

- Adequate electrode cross-section area for control of voltage drop and power loss.
- Adequate electrode cross-section area for mechanical strength and dimensional stability.
- Adequate electrical connections.
- Suitable mechanical support and alignment provisions.
- Electrical insulation between rings and to structure.
- Provision for chilling the rings to freeze the liquid metal for transportation and launch.

Retention of gallium against acceleration forces in a vacuum was demonstrated in both the long-term evaluation test and the vacuum testing of the ETM. The key parameters are high surface tension vs density for the liquid metal, wetted contact to the electrodes, and maximum change in radius of the liquid metal surface vs displacement of the mass of the liquid metal.

The surface tension of the gallium was found to be insensitive to contamination. Wetted contact was found to be very important. Gallium was poorly retained in MEFs and slip rings with poorly wetted surfaces. No gallium was lost from well-wetted electrodes with the same gap. It is necessary to establish wetted contact to develop the full surface tension of the gallium. Control of wetting is thus likely to require more attention than control of surface tension with respect to retention of gallium.

The radial gap configuration of Figure 37 was chosen to maximize the change in radius of curvature of the liquid metal surface vs mass displacement for a given gap diameter, length and thickness. The non-wetted outer lands were intended to protect the bulge in the gallium on the high pressure side, see Figure 39. This configuration proved unacceptable for a slip ring assembled in air due to the escape of residue.

The cup gap configuration of Figure 38 was not difficult to wet and it proved preferable for ease of filling. It retained all residue as well as could be observed and it did not form twirlies to a significant extent, although it did form sludge.

The cup gap configuration is expected to be more tolerant of radial shock than the radial gap configuration due to the shorter path the liquid must travel to accommodate radial displacement. The expected sensitivity to sudden axial displacement might be overcome by undercuts in the rotor which would return squirted gallium to the gap.

Both configurations demonstrated adequate retention capability for assembly and handling purposes. Freezing of the assembly presented no problems except that of verifying that the gallium was frozen. This was done with a mechanical probe (a hooked-end hypodermic needle). The only handling problem was that rotation of the shaft resulted in loss of small amounts of gallium from the radial gap rings due to twirlies.

It is thus considered that the cup gap configuration is usable in its present form, but the radial gap configuration is unsafe unless design changes can eliminate the tendency to form twirlies.

The distribution of current in the liquid metal does not appear to be a significant concern. More important, and having almost the same effect on design, is that the lowest possible volume of liquid metal should be used to reduce sloshing and aid in retention. Both considerations result in an even thickness of gap throughout the ring.

Note that the cup gap ring will tend to compensate for changes in resistance with shaft angle due to radial runout of the interface surfaces if this should be determined to be a significant design factor. The location of the current taps, the cross-sectional area of the rings, and the resistivity of the slip ring material are likely to be as important in this respect as eccentricity in the gap.

The avoidance or minimization of eccentricity is axiomatic. Where it is unavoidable it would appear that reduction in the fill is desirable. Ring 8 and ring 9 were both eccentric but ring 8 was full and produced the most twirlies (but the least sludge) while ring 9 was only half-full and produced the fewest twirlies of any radial gap ring (despite its dents). Ring 10 was also eccentric and half-full and produced its share of twirlies and the most sludge, probably because it was poorly wetted and at a lower temperature.

Note that contact angle did not turn out to be an important parameter in that the electrode materials which displayed good wetting characteristics also had contact angles near zero. The use of tungsten as an electrode material would require much more careful design of the retention features because the significant contact angle of gallium on tungsten would permit the gallium to have more mobility unless the rings were quite full. More important than contact angles is that the wetted/non-wetted line on the

surface of the electrode be definite and even so that stress concentrations on the surface film are reduced.

Sharp internal and external corners are generally to be avoided. Sharp corners in the present ring designs were utilized to help define the wetted/non-wetted line. A sharp internal corner in the wetted area would be hard to clean and to wet, and very hard to plate. A sharp external corner in the wetted area is attacked by the gallium. This should be corrected in the present design of the cup gap rings.

The gap between electrodes should be limited in height (H in Figure 39) and length (L in Figure 39) to avoid problems with the gallium expansion on freezing. Normally the gallium was noted to freeze starting from crystals near the center of a melt, but too great a ratio of L to H could trap molten gallium while it is being frozen and cause very large forces to be developed. A maximum ratio of 20 to 1 was used in the ETM and no damage was noted. Ratios of L to H smaller than 4 encourage "holes" in the gallium such as are seen in Figure 59.

Gallium Residue

The freedom from residue expected for liquid metal slip rings was not achieved with gallium in the present project. Two types of external residue and an internal contamination of the gallium were encountered during the project.

- "Twirlies" caused soft grey wrinkled lumps of the surface film from gallium mixed with liquid gallium to be removed from the radial gap rings.
- Black powder, finely divided, was found on all slip rings on surfaces opposite to gallium surfaces.
- Sludge is soft lumps in the liquid gallium found in all ten slip rings.

None of these forms of contamination was noted in the static testing of the materials selection experiments. A surface film which exhibits plastic flow behavior is almost always found on the gallium. It might be characterized as scum except that it is extremely thin. It formed on the gallium in seconds, even in the argon atmosphere in the glove box. See Figures 22(b) and (c). It is believed that the twirlies and the sludge are largely composed of this film.

Analysis by X-ray diffraction failed to identify the substances, other than pure gallium, of the twirlies or the black powder. Reference 5 cites examples, page 43, of the hydroxide of gallium, $Ga_2(OH)_3$, being amorphous to X-ray under certain conditions. Gallium suboxide, GaO, is described as a dark-brown to black substance and amorphouse, page 29.

Higher temperatures than experienced in this project are cited as necessary for the formation of most gallium oxides, hydroxides and gallates. The literature in general often refers to the oxide film on gallium, probably without true knowledge of the composition of the film.

It was noted that the twirlies ceased to form after a few days in vacuum. The black powder was observed only after the vacuum was broken. These clues strongly indicate that the contamination may include amorphous forms of gallium oxides, hydroxides, nitrides and/or gallates, despite the statement in Appendix B that ". . . no oxides, hydroxides, nitrides, nor other atmospheric reaction products of gallium, nickel or copper exist to a measurable extent."

The film, which we will assume to be amorphous, that is, having no crystalline structure, is something other than liquid and commonly displays wrinkles. It tears without causing substantial change to the surface tension of pure gallium even though it contains measurable contamination by nickel, copper and other contaminants. The contaminants concentrate in the surface film. The extent to which the contaminants influence its formation and properties merits further study.

Some insights into the behavior of the film, and the probable formation of the sludge and twirlies, can be obtained by noting that the film does tear and that the twirlies formed on the radial gap rings where the principal radius of the gallium surface was convex. Sludge formed in the cup gap rings where the principal radius was concave.

When the rings were rotated the film would wrinkle and then shear. In the radial gap rings with the convex surface, a bundle of wrinkled film, wet on one side, might break loose and be rolled up between the non-wetted walls of the gap, forming a twirly. Sometimes the twirly would roll out of the gap, forming the observed debris. Sometimes the twirly would roll into the liquid gallium, forming the sludge.

In the cup gap rings with the concave surface, the wrinkled fragment of surface film would be folded under the surface to form only sludge.

The prospects for a non-wetted configuration to be free of twirlies seem dim because of the convex surface of the gallium in a non-wetted gap.

If the above explanation is correct: twirlies can be avoided by design, sludge will persist until the surface film on gallium can be avoided or destroyed. A limited amount of sludge can probably be tolerated by a slow speed slip ring operating in a vacuum as in the projected application. High speed gallium slip rings operating in air do not appear feasible. The effect of sludge on the friction characteristics of a slip ring would be an interesting investigation.

The black powder may simply be microscopic droplets of gallium which have evaporated from the gap and have condensed on opposing surfaces. They would be rapidly oxidized on contact with air. The powder may be a

secondary product of the surface film. This possibility is suggested by the uneven deposition of powder as in Figure 55(d) and by the fact that the black powder was not noted after the 100-day vacuum test of material evaluation fixtures (see Figure 30). A black powder was at times noted in the corroded region between gallium and beryllium.

The powder adhered to the surfaces on which it was deposited. It should therefore be readily retained by a simple labyrinth as in the cup gap ring configuration.

Metals are much more active chemically when liquid than solid. Corrosion and the formation of surface films would be reduced by retaining the gallium in a frozen state as much as possible. Assuming that the surface film is due to oxygen and/or water vapor, operations with the gallium molten should be accomplished only in an inert gas environment or in a vacuum. Fewer problems with surface film were encountered on this project when working in the glove box.

Specifications, Procedures and Controls

Liquid metal slip rings for spacecraft will require careful attention to design, material selection, fabrication techniques, assembly facilities and procedures, handling and testing procedures, transportation methods, launch procedures and environment, and operating modes and environment. The following list of measures is recommended based on the project findings as discussed above.

Material Selection

- Electrodes: AISI 304 stainless steel for signal rings. Consider solid nickel, 99.97 percent pure, for rings where the current is in excess of 1 ampere.
- Insulation: Epoxy-glass fabric laminate per L-P-509, Type IV, Grade G-10 or alumina ceramic, 96 percent pure, unglazed.
- Liquid Metal: Gallium 99.9999 percent pure. Obtain in polyethylene containers, gas free or with argon gas.
- Test all materials for wetting/non-wetting as required.

Design of Slip Rings

- All contacting surfaces between gallium and electrodes to be 100 percent wetted.
- Current not to exceed 100 A/cm^2 of wetted area per electrode.

- Interface resistance between gallium and electrode not to exceed 10 $\mu\Omega$ cm^2 for stainless steel or 1.0 $\mu\Omega$ cm^2 for nickel.

- Electrode cross-sectional area must be sufficient to limit the temperature rise due to electrical current to 100°C when the current connection on the rotor is 180 degrees (π rad) from the current connection on the stator.

- Gaps: minimum to accommodate required radial and axial displacements and runouts; not to exceed 0.040 inch (1.0 mm); maximum gap not to exceed three times the minimum gap.

- Wetted areas to be in continuous bands on rotor and stator with edges straight within the minimum gap dimension. Width of band to exceed 4 times the maximum gap and be less than 20 times the minimum gap.

- Wetted bands on rotor and stator to diverge with 60 degree (1.05 radian) to 120 degree (2.1 radian) included angle at edge of wetted area for a width exceeding the minimum gap.

- Surface finish on wetted area to have 32 microinch rms (0.81 μm rms) maximum roughness.

- All outside or inside radii in wetted area to exceed 0.010 inch (0.25 mm).

- Barrier film: Use naturally oxidized surface of electrode.

- Ring fill to be such that both exposed surfaces of gallium are concave in earth's gravity.

- Acceleration capability to be a minimum of 4 g (39.2 ms^{-2}) vertical and 1 g (9.8 ms^{-2}) horizontal with the gallium in the liquid state.

- Retention of debris: Use line-of-sight labyrinth from gallium surface to retain evaporated material. Use a secondary non-wetted gap with rounded entrance to retain liquid metal. This gap should be as small as possible: choose radial or axial for minimum clearance.

- Reservoir volume must be provided between the liquid metal surface and the secondary gap to accommodate liquid metal displaced by relative motion of the rotor and stator rings.

- Recommended gap configuration: The cup gap per Figure 36, modified by rounding the corners of the inner ring wetted electrode surfaces. Avoid the radial gap configuration of Figure 36.

Fabrication

- Machining: The final machine finish on electrodes should be accomplished with chucks and cutting tools cleaned with solvent so as to be free of oil.

- Handling: Use clean gloves to handle clean parts.

- Store all parts by sealing in clean plastic bags.

- If nickel plate is to be used to protect copper electrodes, it must be applied very slowly so as to be dense and free of pores and the thickness of nickel must exceed 0.005 inch (0.13 mm) in all areas wetted by gallium. Electroplated nickel should be used unless electroless nickel plating can be shown by test to give superior protection to the copper from gallium.

Assembly and Test

- Cleaning: All parts and all tools for use in assembly must be thoroughly clean and free of oil. Vapor degreasing with trichlorethylene followed by ultrasonic cleaning in trichlorotrifluoroethane followed by rinsing in distilled water and an oven bakeout, preferably in an inert atmosphere, is recommended for all parts, although cleaning can be omitted for parts machined as outlined above. A preliminary scrubbing with an abrasive such as steel wool is recommended for nickel-plated electrodes.

- Handling: Use clean gloves to handle clean parts. Laundered white stretch-nylon gloves are recommended.

- Assembly environment: All work with liquid gallium should be accomplished in an oxygen-free environment. Wetting and assembly require manipulation and the use of a glove box with an argon atmosphere is recommended. The oxygen content must be maintained well below 0.1 percent for this to be effective. The working area must be free of particulate contamination and soft films such as oil, grease and wax.

- Wetting procedure:

  a) Mask areas to be protected from gallium. Masking tape is acceptable. Precut individual polyethylene masks would be preferable.

  b) Apply liquid gallium to area to be wetted and work into the surface by abrasion. Use laundered stretch nylon cloth for nickel surfaces and emery paper for stainless steel. Part should be at room temperature. Use a slight amount of heat if gallium freezes.

  c) Wipe off contaminated liquid gallium with stretch nylon cloth, note unwet areas, repeat wetting if necessary.

  d) Apply pure liquid gallium to wetted surface immediately after wiping off excess. Spread gallium over wetted surface by shock (such as tapping on a nylon anvil). Note possible bridging and rewet if necessary. Gallium should stop spreading at edge of wetted area. Gallium layer should be thick enough to hide surface finish of electrode.

  e) Freeze gallium immediately after wetting by placing part on cold plate.

  f) Strip off masking tape if used.

- Assembly of rotor and stator:

  a) Use small jig to hold rotor and stator (inner and outer rings) of slip ring in proper relative position.

  b) Heat jig and rings on hot plate just enough to melt gallium.

  c) Add predetermined amount of liquid gallium, using a calibrated glass syringe with a stainless steel hypodermic needle. The use of gallium which has been outgassed in a vacuum is recommended.

  d) Immediately freeze the gallium by placing rings and jig on a cold plate.

- Test each ring assembly for proper contact resistance. A 10-ampere of higher current, separate voltage taps on the electrodes, and a voltmeter capable of reading microvolts will be necessary to obtain suitable accuracy. The measurement can be obtained with the gallium frozen, and should be done quickly before the current heats the rings.

- Complete the slip ring assembly with the gallium frozen and in the glove box if possible.

- Testing of complete assembly: Permit shaft rotation of the slip ring assembly only in a vacuum with a pressure less than 1 micron of mercury equivalent (0.133 Nm^{-2}). Do not allow the gallium to melt until the pressure is below this level. Minimize the number of turns required for testing. Leave the shaft prepositioned for assembly in the spacecraft. Freeze the gallium before readmitting air to the vacuum chamber.

Handling and Transportation

Seal the liquid metal slip ring assembly in an argon atmosphere and maintain the gallium in the frozen state by keeping the temperature of the assembly below 27°C (81°F, 300K) for all handling and transportation operations.

Assembly into Spacecraft

Assembly into the spacecraft should be accomplished without permitting the gallium to melt. All forms of contamination must be excluded from the area of the slip rings, particularly if they are to operate at high voltage. If necessary to turn the shaft for spacecraft testing, the gallium should only be permitted to be liquid in a high vacuum and the number of turns should be kept to an absolute minimum.

Launch

Chill the liquid metal slip ring assembly before launch to a temperature that will assure that the gallium remains frozen through launch and until a low pressure is established in the ring area.

Operation

The gallium should not be melted or the shaft required to turn until the last possible time. Several hours or days in space should be allowed if possible to permit outgassing. This will be particularly important if the rings are to operate with high voltage between the rings. A ring temperature in excess of 80°C (353K) for several hours or days before turning may also prove beneficial.

The above specifications, procedures and controls are but a brief outline of the expected eventual requirements for the slip rings for a prototype solar array orientation mechanism. If such measures are implemented there is a high confidence that the liquid metal slip rings will arrive on station in a condition that will provide:

- electrical performance greatly improved over present state-of-the-art rotary power transfer means

- negligible friction, so that attitude control systems will be simplified
- great reliability due to the simple design, few failure modes, and large power handling capacity.

SUMMARY OF RESULTS

The experimental liquid metal slip ring development project was undertaken to explore the advantages and problems of the use of the liquid metal gallium to conduct electrical power across slowly rotating mechanical joints in spacecraft. The effort is considered successful in that no overwhelming technical problems were uncovered and the electrical characteristics of the liquid metal slip rings were found to be far superior to those of conventional brush-on-ring assemblies.

Exotic or hard-to-work materials such as beryllium and tungsten were not found necessary. Conventional engineering materials such as nickel, stainless steel and epoxy-glass fabric laminate were found to give superior performance. Wetting of the electrode materials by the gallium provides greatly reduced contact resistance and improved retention compared to non-wetted contact.

The wetting was found to be readily accomplished by simple abrasion. Non-wetting of the electrodes where desired is better accomplished by the naturally oxidized metal surface than by any of five materials tried as barrier coatings. Low surface energy materials were found to be wetted by gallium while some high surface energy materials such as alumina ceramic were not wetted. Good wetting of metals appears to be associated with a degree of chemical attack on the electrode material by the gallium.

The gallium was retained in the gaps between the electrodes by capillary forces so that rubbing seals were not required. The friction torque of the slip rings therefore consists of the viscous shearing force in the liquid gallium, which is negligible at the operational speed, one revolution per day, of the application.

Very careful attention must be given to the design and to assembly procedures and controls to minimize the effects of an unidentified surface film which forms on the gallium. The surface film can cause debris to escape from the gap between the rings, and causes soft lumps in the gallium which might interfere with free rotation. High speed applications, especially in air, are considered unlikely for gallium slip rings due to the debris from the surface film. The surface film does not form in a vacuum and probably contains amorphous oxides and hydroxides of gallium.

Evaporation of the gallium is slight. A simple baffle intercepts the vapor and minimizes possible contamination of other surfaces by condensing the gallium. Operation of the slip rings at 100 amperes in a high vacuum at temperatures from 30 ^{o}C (303K) to 85 ^{o}C (358K) presented no problems other than dissipation of the electrical heating losses in the electrodes and cabling.

The gallium is readily retained in the rings for transportation and spacecraft launch by maintaining the gallium frozen at temperatures below 29.7 ^{o}C (301.9K).

The electrical performance of the liquid gallium slip rings is outstanding. The interface resistance for gallium on nickel was consistently less than 1.0 $\mu\Omega cm^2$ and is believed to approach zero with perfect wetting. The 10-slip ring assembly tested is capable of transmitting 1.5 megawatts (100 amperes at 3000 volts in each of five circuits) with an efficiency of 99.9993 percent. The power loss in the liquid metal of one ring at 100 amperes is 1.6 milliwatts.

The electrical "noise" in the slip rings tested was a maximum of less than one-quarter of a millivolt peak to peak at 100 amperes and consisted mostly of a sinusoidal variation as a function of shaft position.

The number of failure modes in a liquid metal slip ring are few and incipient failures can be detected by voltage drop measurements. High reliability is thus expected. The longevity of gallium slip rings in space applications may be determined by the rate of chemical attack of liquid gallium on the electrode material and by evaporation of the gallium. Measured rates indicate that slip ring life should readily exceed 10 years.

APPENDIX A

BIBLIOGRAPHY

Documents reviewed as part of the literature search which presented information of value to the liquid metal slip ring project.

Key: (H) High applicability to liquid metal slip ring project
(L) Low applicability to liquid metal slip ring project

Adam, Neil Kensington
"The Physics and Chemistry of Surfaces"
Dover Press, 1968 (H)

American Chemical Society
"Contact Angle, Wettability and Adhesion" Advances in Checmistry Series No. 43
The American Chemical Society, Washington, DC, 1964 (H)

American Society for Metals (ASM)
"Metals Handbook" 8th Edition, Vol. 1, "Properties and Selection of Materials"
ASM, Metals Park, Ohio, 1961

Anonymous
"Properties of Indium-Gallium Alloys"
Semiconductor Materials Data Sheet No. 5
Alpha Metals, Inc. (H)

Anonymous
"Gallium at Your Disposal"
Aluminum-Industrie-Aktien-Gesellschaft Research Laboratories,
Neuhausen am Rheinfall, Switzerland, 1956 (H)

Anonymous
"Eutectic Alloys of Gallium, Metals Fluid at Room Temperature"
Technical Bulletin of United Mineral & Chemical Corporation, 1962 (H)

Anonymous
"Pysical, Electrical and Mechanical Properties of Group IIIA Elements"
Williams Precious Metals, Division of Williams Gold Refining Company, Inc. (L)

Brennecki, M. W.
"Gallium" in "Metals Handbook", 8th Edith, Vol. 1
Properties and Selection of Materials
American Society for Metals (ASM), Metals Park, Ohio, 1961 (H)

Breteque, P. de La
"Bibliography on Gallium", 1962 (L)

Buranich, Godfrey F.
"High-Temperature Antenna Investigation" Report No. 9
AD-466971, Div. 8/1, 14/2, 14/1
Cornell Aeronautical Lab., Inc., Buffalo, N. Y., 30 June 1965 (L)

Chaberie et al
"Filling Up" Sliding Electrical Contacts for a
Homopolar Engine" - Electrical Contacts Symposium, 1968 (L)

Colligan, Loomis and Surprenant
"Dendritic Growth in Undercooled Metals", AD-457916,
Div. 17, 25
Thayer School of Engineering, Dartmouth College, Hanover, N. H. (L)

Encyclopedia Britannica
"Gallium", Volume 9
Encyclopedia Britannica, 1963 (L)

Gaggin and Moberly
"Embrittlement by Liquid Metals" - AD639 481, Fld 11/6
Stanford Research Institute, Menlo Park, California
28 February 1966 (L)

Haltner, A. J.
"Adsorption and Surface Energetics", Lecture 13 from
Proceedings Preprint "Interdisciplinary Approach to the
Lubrication of Concentrated Contacts"
Southwest Research Institute, San Antonio, Texas, July 1969 (H)

"Handbook of Chemistry and Physics", 47th Edition
The Chemical Rubber Company (H)

Hultgren, Orr, Anderson, Kelley
"Selected Values of Thermodynamic Properties
of Metals and Alloys"
Wiley (L)

Krieger, G. L.
"The Physical Chemistry of Cleaning", SC-TM-66-428
Sandia Laboratory, Albuquerque, New Mexico, 1966 (H)

Kuczkowski and Buckley
"Friction and Wear of Low Melting Binary and Ternary Gallium Alloy Films in Argon and in Vacuum"
NASA TN D-2721, 1965 (L)

Lemon & Ference
"Analytical Experimental Physics"
The University of Chicago Press, 1943 (L)

Lo, J. M. and Colligan, G. A.
"Electrical Resistivity of Undercooled Gallium and Gallium-Indium Eutectic Alloy"
AIME Metallurgical Soc. Trans. Vol. 236, # 10, October 1966 (L)

Mantell, C. L.
"Engineering Materials Handbook" First Edition
McGraw-Hill Book Company, Inc., 1958 (L)

March, N. H.
"Liquid Metals"
Pergamon Press, 1968 (L)

Masica and Salzman
"An Experimental Investigation of the Dynamic Behavior of the Liquid-Vapor Interface Under Adverse Low-Gravitational Conditions"
Fluid Mechanics and Heat Transfer Under Low Gravity Symposium
USAFOSR & Lockheed MSC, DDC AD 633, 580, 1965 (L)

"McGraw-Hill Encyclopedia of Science and Technology", Vol. 6
McGraw-Hill Book Company, 1966 (H)

Meridian Laboratory, Inc.
"Rotocon Viscous Sliprings"
Technical Data and Specifications, July 1969 (L)

Przybyszewski, J. S.
"Friction and Contact Resistance for Low Speed Gallium Lubricated Sliding Electrical Contacts of Beryllium in Vacuum", NASA TM X-52637
Lewis Research Center, Cleveland, Ohio, 1969. (H)

RCA
"Vapor Pressure Curves of the Elements"
RCA Laboratories, Princeton, N.J., September 1962 (L)

"Reactor Handbook"
McGraw-Hill, 1955 (H)

Reynolds and Satterlee
"Liquid Propellant Behavior at Low and Zero G"
ASTIA N67 15898
Chapter 11, "The Dynamic Behavior of Liquids, 1967 (H)

Sears, F. W.
"Mechanics, Heat and Sound", Second Edition
Addison-Wesley Publishing Company, Inc., 1958 (L)

Sheka, Chaus and Mityureva, "The Chemistry of Gallium",
Elsevier Publishing Company, New York, N. Y., 1966 (H)

Smithells, C. J.
"Metals Reference Book", Vol. II, 2nd Edition
Interscience, N. Y., 1955 (L)

Spalvins, T.
"Energetics in Vacuum Deposition Methods for Depositing
Solid Film Lubricants"
NASA TM X-52549, Lewis Research Center, Cleveland, Ohio, 1969 (L)

Spalvins, Przybyszewski and Buckley
"Deposition of Thin Films by Ion Plating on Surfaces
Having Various Configurations"
NASA TN D-3707, Lewis Research Center,
Cleveland, Ohio, November 1966 (L)

Thompson, A. P.
"Gallium" in "Rare Metals Handbook"
Reinhold, N. Y., 1954 (L)

Vossen, J. L. and O'Neill, Jr., J. J.
"D. C. Sputtering with RF-Induced Substrate Bias"
RCA Review, December 1968 (L)

Weast, Robert C., Editor-in-Chief, Handbook of Chemistry and
Physics, 47th Edition, The Chemical Rubber Co., Cleveland
Ohio, 1966. (H)

Yatsenko, S. P., Loshkin, D. V., and Perel'shteyn, G. N.,
"The Application of Gallium Alloys in Liquid Sliding Contacts,"
Academy of Sciences of the USSR, Ural Branch, Institute of
Chemistry, Transactions, Nov. 12, 1966, Translated by
D. Koolbeck/TDBRO-2, Foreign Technology Division,
WP-AFB, Ohio, AD 684045. (L)

APPENDIX B

X-RAY DIFFRACTION ANALYSIS OF SURFACE CONTAMINATION PRODUCTS FROM LIQUID GALLIUM SLIP RINGS

Introduction

On June 19, 1970, several residues from a liquid metal bearing were received in the laboratory for X-ray diffraction analysis. It was of special interest to determine the identity of the grey residue scum. It was requested that sample preparation be carried out in an argon atmosphere in order to protect the samples from atmospheric contamination. The following report represents the results of the studies and is hereby respectfully submitted.

Samples

Samples were received with the following designations and descriptions:

Samples 6 & 8 . . .	Grey Contamination Residue--Probably Identical
Samples 7, 9 & 10 .	Grey Contamination Residues--May Contain Braycoat (per fluoridated polymer)
Samples 11 & 12 . .	Mostly Gallium Metal Mixed With Contaminant
Sample 13	Contaminant Residue Stuck To Adhesive Tape

Sample Preparation and Study Methods

In order to minimize atmospheric contamination, an argon glove box was used with dry argon flowing through under positive pressure. Prior to flushing with argon, the major por-

tion of air was removed from the box. The original sample containers were opened while in the glove box. Except in the instance of Sample #13 the following technique was used: small amounts of the sample were placed on clean microscope slides and immediately covered with a droplet of 5% cellulose nitrate/amyl acetate solution. The residues were thoroughly mixed with the cellulose nitrate solution, and when the proper consistency was reached the mixtures were formed into .3 mil diameter fibers. After the fibers had dried, they were dipped into 2% cellulose nitrate solution to provide additional protection from the atmosphere. The original containers were then resealed and packed into a plastic bag filled with argon to preserve them for future studies. The fibers were allowed to dry and were mounted into sample holders for study in a Debye/Scherrer powder diffraction camera. Sample #13 was removed from the scotch tape by allowing the adhesive to be softened with a few drops of benzene. The entire adhesive layer and contamination was scrapped off of the tape substrate and placed upon a clean microscope slide. After allowing most of the benzene to evaporate, it was possible to form the sample into a fiber using the softened adhesive as a binding medium This fiber was then studied with the other samples by rotation in the diffraction camera under the following exposure conditions:

Kilovolts Potential	15
Milliamps	30
Target	Copper
Filter	Nickel
Pinholes	.025/.025-TS/SS
Film Type	Ilford Industrial G Type No Screen X-Ray Film
Exposure	8 hours
Development	6 minutes/68^{0}F in Eastman X-Ray Developer

As it was found during sample preparation that the major portion of the gallium was still in liquid phase, additional diffraction studies were performed after freezing the fibers in liquid nitrogen. The studies were repeated as described above except that the exposure time was shortened to 5 hours.

Discussion of the X-Ray Diffraction Data

Sample #6	---	XRD Film Print 3612
		XRD Film Print 3616 (Frozen)
Sample #10	---	XRD Film Print 3613
		XRD Film Print 3614 (Frozen)
Sample #11	---	XRD Film Print 3611
		XRD Film Print 3615 (Frozen)
Sample #13 (on tape)	---	XRD 3622

The enclosed X-ray diffraction film prints are contact prints of the original negatives. Phase identification was made by measuring the observed diffraction line spacing (1 mm = $2^0\theta$) and calculating the interplanar atomic spacing or d values. These were compared with standard data in the ASTM X-ray diffraction file. The X-ray diffraction patterns of the "as received" contaminants show the major phase of each sample to be completely amorphous. The faint broad inner ring represents the scatter from the cellulose nitrate binding medium. On XRD 3622 of Sample #13 there is an additional inner ring which matches that of the adhesive obtained from scotch "Magic Mending" tape. The outer broad ring can be related to the pattern of liquid gallium. Sample #11 visibly contained a large quantity of liquid gallium and shows this broad ring most intensely. All of the samples, except #13, visibly showed liquid gallium in droplets during sample preparation. The presence of elemental gallium in the grey resi-

dues was confirmed by freezing the fibers in liquid nitrogen to crystallize the super cooled metal. X-ray diffraction prints #3614 and 3616 show this transition, and no phases other than the gallium metal appear to a measurable extent. There is some difference between the two patterns which can be attributed to differences in crystallite orientation; in other words, some gallium reflections occur on one pattern that do not occur on the other. Sample #13 was found also to contain a major amount of the amorphous gallium. However, on long exposure a few very faint reflections can be seen on the original negatives. However, these cannot be matched with any data found in the ASTM X-ray diffraction file. Extremely faint indications of the highest intensity reflections found on Sample #13 could also be observed on the one frozen studies of the other samples. These reflections are d=2.14A, d=2.0A, and d-3.1A. No difference could be observed between the samples containing the per fluoridated polymer.

Although no match could be found, it can be definitely stated that no oxides, hydroxides, nitrides, nor other atmospheric reaction products of gallium, nickel, or copper exist to a measurable extent. The following list of compounds were carefully checked against the pattern and in all cases found not to exist:

Nickel, Copper
$NiCO_3$
$NiCO_3 \cdot 6H_2O$
$NiCO_3 \cdot 2Ni(OH)_2 \cdot 4H_2O$
NiO
Ni_2O_3
$Ni_2O_2(OH)_4$
$Ni_3O_2(OH)_4$
β-NiOOH
$4Ni(OH)_2 \cdot NiOOH$
Gamma-NiOOH
$NiGa_2O_4$

CuO
Cu_2O
$Cu(OH)_2$
$CuGaO_2$
δ-Cu_9Ga_4
PHi-CuGa
$Cu_3(OH)_2(CO_3)_2$
$CuCO_3 \cdot Cu(OH)_2$

$Ga(OH)_3$
α-Ga_2O_3
Ga_2O_3
GaO_2H
γ-$GaNi_3$
β-Ga_2Ni_3

It is possible that some as yet unclassified compound is present. The pattern more closely approximates that of inter-metallics in general rather than oxide or hydroxide forms. Spectrographic analysis of the residues may add to this evidence if nickel or copper is found to exist with the gallium.

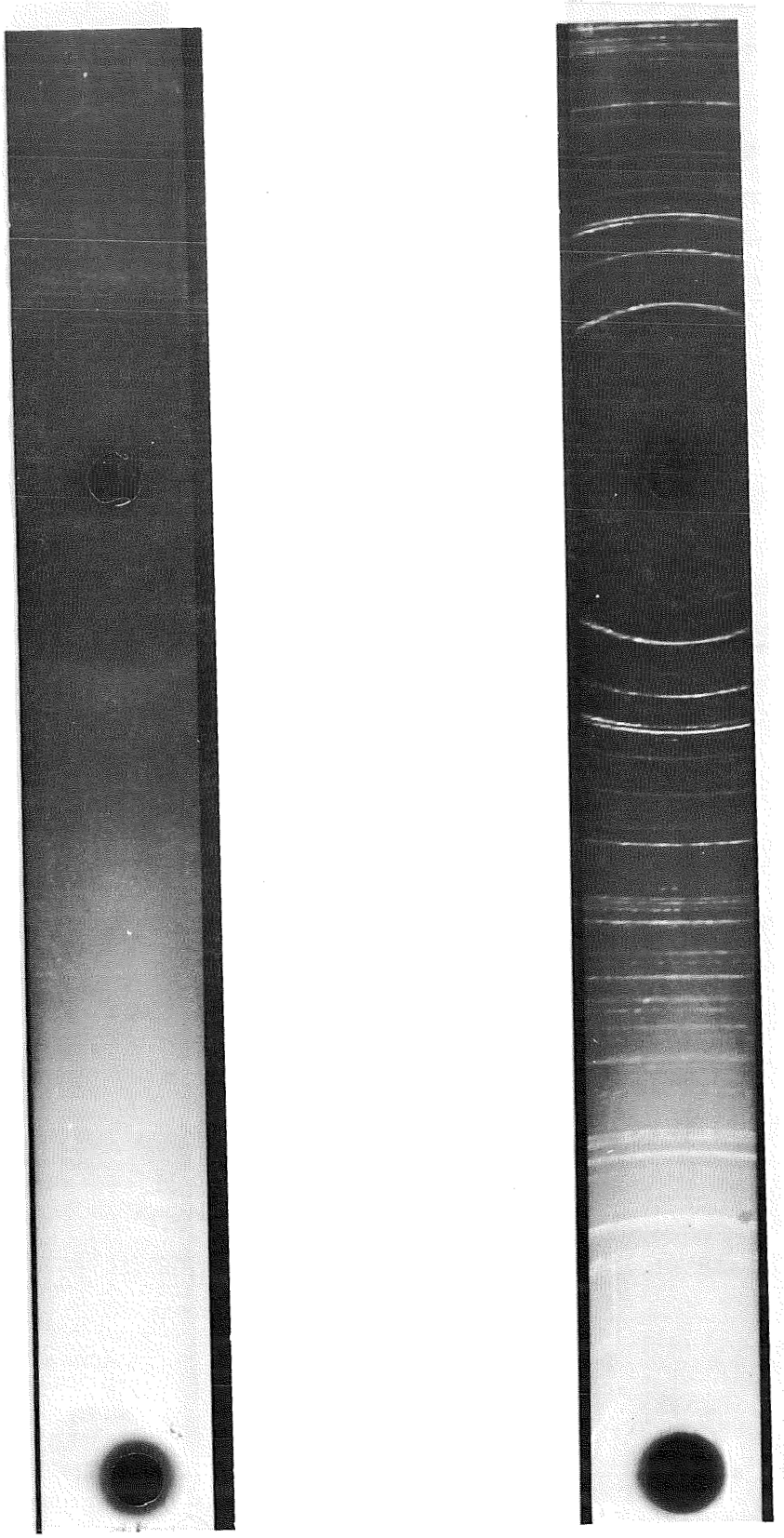

a) Gallium Liquid

b) Gallium Frozen

FIGURE 62. X-Ray Diffraction Film Prints from Sample 6, Grey Residue from Ring 6

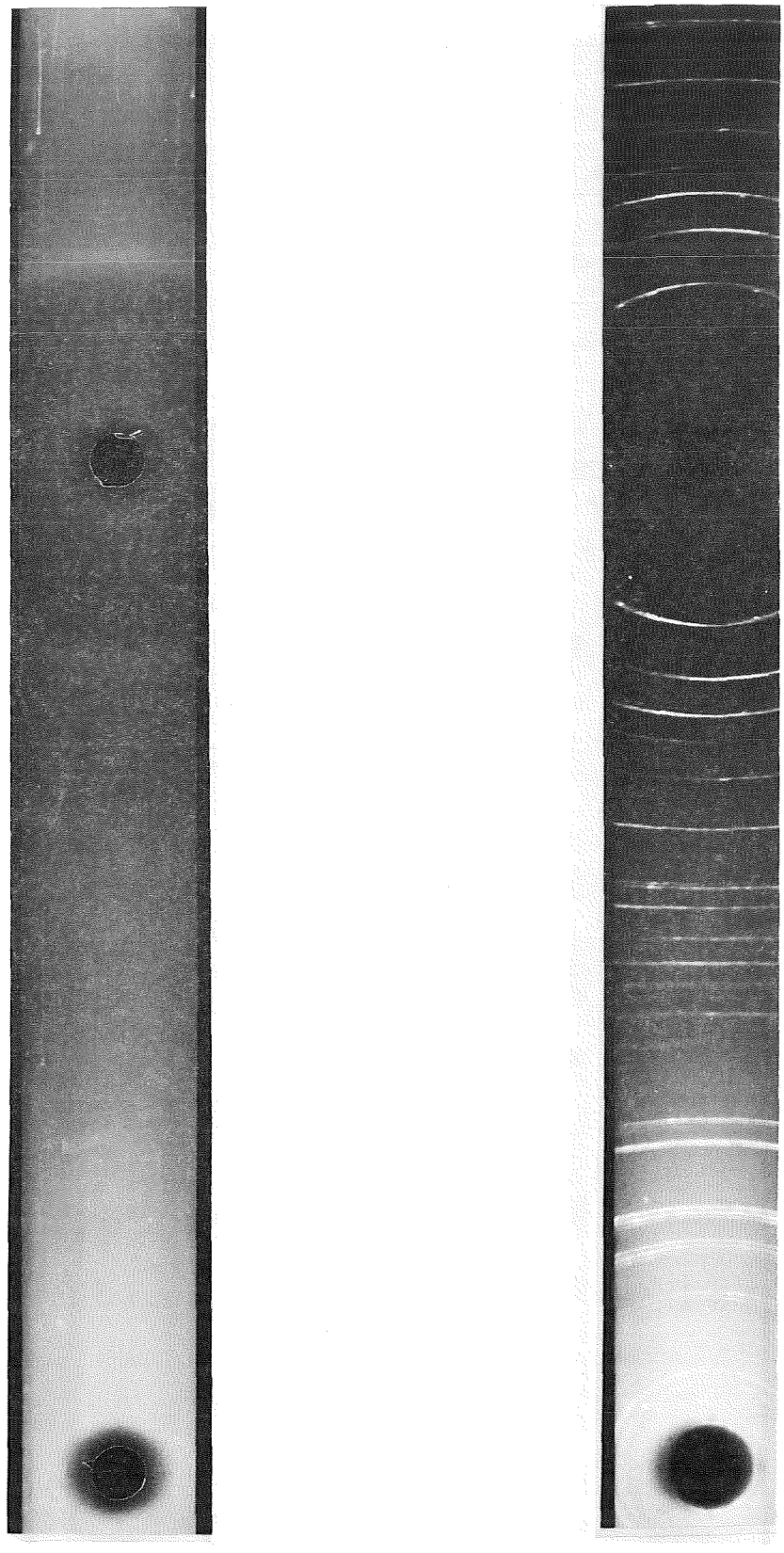

a) Gallium Liquid

b) Gallium Frozen

FIGURE 63. X-Ray Diffraction Film Prints from Sample 10, Grey Residue from Ring 10

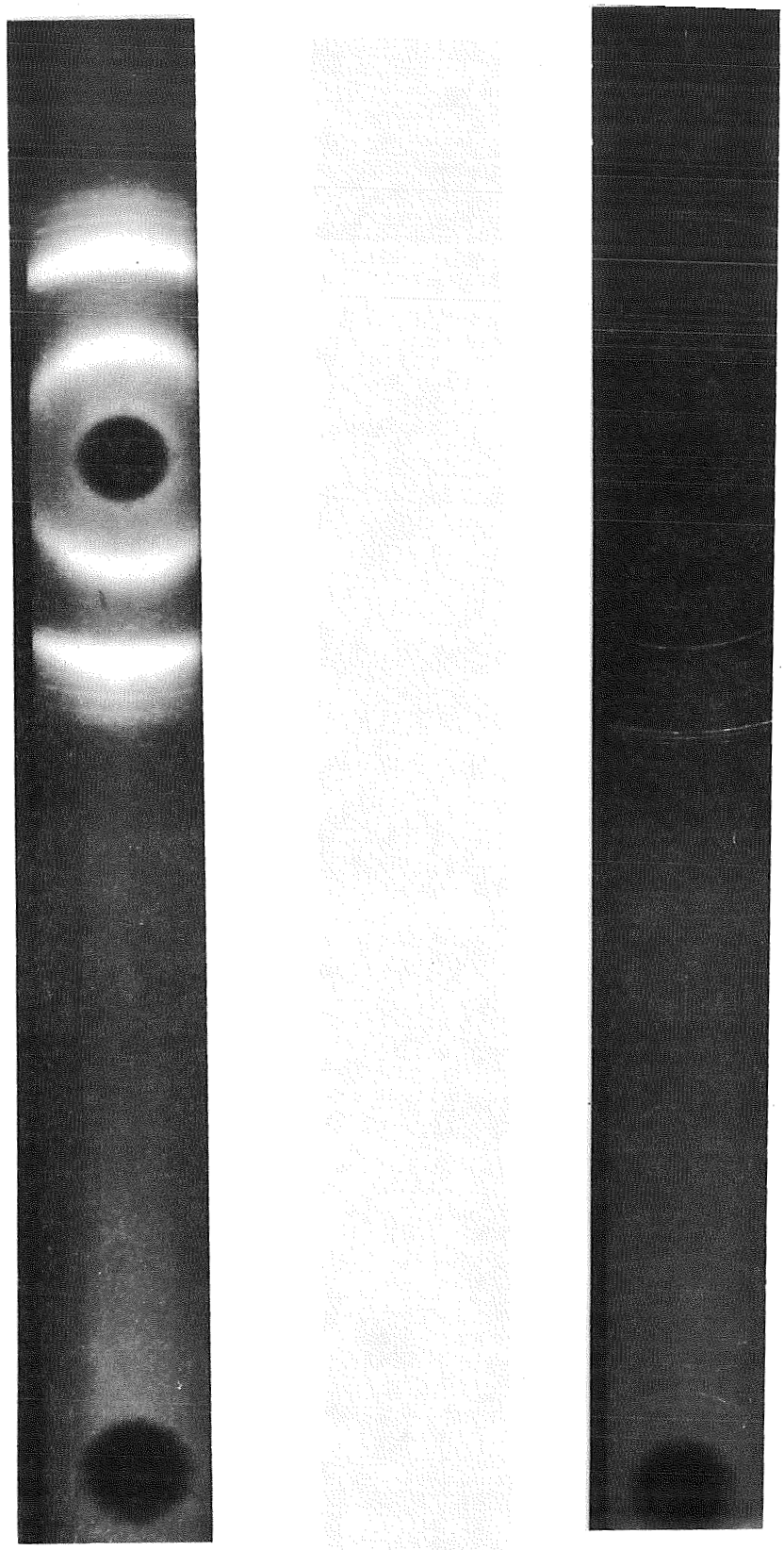

a) Gallium Liquid

b) Gallium Frozen

FIGURE 64. X-Ray Diffraction Film Prints from Sample 11
Gallium Drops from Below Ring 10

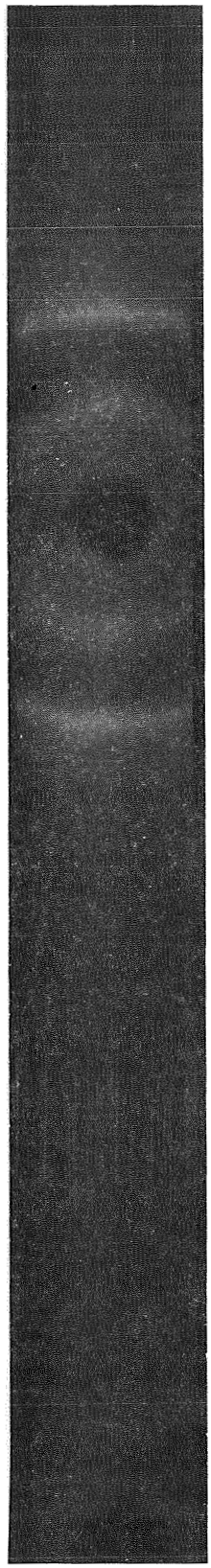

FIGURE 65. X-Ray Diffraction Film Print from Sample 13, Dark Powder Residue from Below Ring 10 (on adhesive tape)

APPENDIX C

NEW TECHNOLOGY

No specific new innovation, discovery, improvement or invention was made as part of the work performed under Contract NAS 3-11537.

REFERENCES

1. Robert C. Weast, Editor-in-Chief, Handbook of Chemistry and Physics, 47th Edition, The Chemical Rubber Company, Cleveland, Ohio, 1966.

2. G. L. Krieger, The Physical Chemistry of Cleaning, SC-TM-66-428, Sandia Laboratory, Albuquerque, New Mexico, 1966.

3. John S. Przybyszewski, Friction and Contact Resistance for Low Speed Gallium Lubricated Sliding Electrical Contacts of Beryllium In Vacuum, NASA TM X-52637, Lewis Research Center, Cleveland, Ohio, 1969.

4. S. P. Yatsenko, D. V. Loshkin and G. N. Perel'shteyn, The Application of Gallium Alloys in Liquid Sliding Contacts, Academy of Sciences of the USSR, Ural Branch, Institute of Chemistry, Transactions, November 12, 1966, Translated by D. Koolbeck/TDBRO-2, Foreign Technology Division, WP-AFB, Ohio, AD 684045.

5. I. A. Sheka, I. S. Chaus and T. T. Mityereva, The Chemistry of Gallium, American Elsevier Publishing Company, Inc., New York, N. Y., 1966.

DISTRIBUTION LIST

National Aeronautics & Space Administration
Headquarters
Washington, D. C. 20546

Attention:	SA/L. Jaffee	1 copy
	SAC/A. M. G. Andrus	10 copies
	SC/R. B. Marsten	1 copy
	RN/W. H. Woodward	1 copy

NASA-Lewis Research Center
21000 Brookpark Road
Cleveland, Ohio 44135

Attention:	S. C. Himmel (M.S. 3-3)	1 copy
	C. C. Conger (M.S. 54-1)	1 copy
	R. E. Alexovich (M.S. 54-5)	1 copy
	Technology Utilization Officer (M.S. 3-19)	1 copy
	Library (M.S. 60-3)	2 copies
	Report Control Office (M.S. 5-5)	1 copy
	N. T. Musial (M.S. 501-3)	1 copy
	R. R. Lovell (M.S. 54-5)	50 copies
	Spacecraft & Support Proc. Section (M.S. 500-110)	1 copy
	J. S. Przybyszewski (M.S. 23-2)	1 copy
	A. F. Forestieri (M.S. 302-1)	1 copy

NASA-George C. Marshall Space Flight Center
Huntsville, Alabama 35812

Attention:	Library	1 copy

NASA-Goddard Space Flight Center
Greenbelt, Maryland 20771

Attention:	Library	1 copy

NASA-Ames Research Center
Moffett Field, California 94035

Attention:	Library	1 copy

NASA-Langley Research Center
Langley Station
Hampton, Virginia 23365

Attention:	Library (M.S. 185)	1 copy

NASA-Manned Spacecraft Center
Houston, Texas 77001

Attention:	Library	1 copy
	F. E. Eastman (EB8)	3 copies
	C. Robinson (EP52)	1 copy

Jet Propulsion Laboratory
4800 Oak Grove Drive
Pasadena, California 91103

Attention:	Library	1 copy
	W. Hasbach	1 copy

NASA Scientific and Technical Information Facility
Box 7500
Bethesda, Maryland 20740

Attention:	NASA Representative	3 copies

General Dynamics, Convair Division
P. O. Box 1128
San Diego, California 92112

Attention:	F. J. Dore/Advanced Programs Laboratory	1 copy

Air Force - Aero Propulsion Laboratory
Wright-Patterson Air Force Base
Ohio 45433

Attention:	L. D. Massie (APIP-2)	1 copy

General Electric Company
Missile and Space Division
Valley Forge Space Technology Center
P. O. Box 8555
Philadelphia, Pennsylvania 19101

Attention:	S. Weinberger	3 copies

Federal Communications Commission
521 12th Street
Washington, D. C. 20554

Attention:	M. Fine	1 copy

DISTRIBUTION LIST (continued)

U. S. Information Agency
25 M Street, S.W.
Washington, D.C. 20547

Attention: IBS/EF/G. Jacobs — 1 copy

Naval Electronic Systems Command
PME 116
Washington, D.C. 20350

Attention: Lt. Commander L. Wardel — 1 copy

McDonnell Douglas Corporation
5301 Bolsa
Huntington Beach, California 92647

Attention: J. Chester (A-3-BBDO-830) — 2 copies

Poly Scientific Division
Litton Industries
1111 N. Main Street
Blacksburg, Virginia 24060

Attention: W. O'Brian — 2 copies

Spar Aerospace Products
825 Caladonia Road
Toronto, Ontario 315
Canada

Attention: T. Usher — 2 copies